UNIVERSITY OF OXFORD

Stochastic Model Predictive Control

by

Desmond Ng

A thesis submitted in partial fulfillment for the degree of Doctor of Philosophy

in the
Department of Engineering Science
Keble College

May 2011

Abstract

The work in this thesis focuses on the development of a Stochastic Model Predictive Control (SMPC) algorithm for linear systems with additive and multiplicative stochastic uncertainty subjected to linear input/state constraints. Constraints can be in the form of hard constraints, which must be satisfied at all times, or soft constraints, which can be violated up to a pre-defined limit on the frequency of violation or the expected number of violations in a given period.

When constraints are included in the SMPC algorithm, the difficulty arising from stochastic model parameters manifests itself in the online optimization in two ways. Namely, the difficulty lies in predicting the probability distribution of future states and imposing constraints on closed loop responses through constraints on predictions. This problem is overcome through the introduction of layered tubes around a centre trajectory. These tubes are optimized online in order to produce a systematic and less conservative approach of handling constraints. The layered tubes centered around a nominal trajectory achieve soft constraint satisfaction through the imposition of constraints on the probabilities of one-step-ahead transition of the predicted state between the layered tubes and constraints on the probability of one-step-ahead constraint violations. An application in the field of Sustainable Development policy is used as an example.

With some adaptation, the algorithm is extended the case where the uncertainty is not identically and independently distributed. Also, by including linearization errors, it is extended to non-linear systems with additive uncertainty.

Acknowledgements

First and foremost, I would like to express my sincerest gratitude to my supervisors, Dr. Mark Cannon and Prof. Basil Kouvaritakis for their enduring patience and guidance throughout my DPhil candidacy. Without them, it would have been an insurmountable task.

My thanks to present and past colleagues in the Oxford Control Group for their support and help all these years.

Thanks to the Oxford University Press (OUP) for funding my studies through the Clarendon Scholarships and Keble College through the Sloane Robinson Graduate Scholarship. Without these funds my DPhil in Oxford would still be a dream.

Finally, I would like to express my deepest love for my family, for without their emotional support and love, this thesis could not be done. Also, many thanks to friends and acquaintances in Oxford, where it would be too numerous to name here, for making my experience in the 'City of Dreaming Spires' truly a dream come true.

Contents

Abstract i

Acknowledgements ii

1 Introduction 1

2 Background 10
2.1 Deterministic MPC Review . . . 10
2.1.1 Stability . . . 15
2.1.2 Terminal Invariant Sets . . . 17
2.1.3 Reference Tracking . . . 22
2.2 Robust MPC Review . . . 23
2.2.1 Closed Loop Paradigm . . . 24
2.2.2 Augmented Autonomous State Space Formulation . . . 25
2.3 Nonlinear MPC Review . . . 28
2.4 Stochastic MPC Review . . . 31
2.5 Conclusion . . . 39

3 Tube Linear Stochastic Model Predictive Control 41
3.1 Introduction . . . 42
3.2 Preliminaries . . . 43
3.2.1 Problem Formulation . . . 43
3.2.2 Nested tubes . . . 48
3.3 Constraint Handling . . . 50
3.4 The Receding Horizon Algorithm . . . 59
3.4.1 Stage cost definition . . . 59
3.4.2 Receding horizon algorithm . . . 64
3.5 Numerical Example . . . 65
3.6 Conclusion . . . 70

4 A Fast Implementation of TSMPC 73
4.1 TSMPC Implementation . . . 73
4.1.1 Offline MPC . . . 74

4.1.2 Online MPC 77
4.2 Primal Barrier Interior-Point Method 85
4.2.1 Primal Barrier Method 86
4.2.2 Infeasible Start Newton Method 87
4.2.3 Phase 1 90
4.2.4 Warm Start 91
4.2.5 Fast Computation of Newton Step 92
4.3 Approximate Primal Barrier Method 96
4.3.1 Fixed t 96
4.3.2 Fixed Newton Iterations 97
4.4 Implementation Results 98
4.4.1 Second Order Example 98
4.4.2 Random Systems Example 103
4.5 Conclusion 103

5 TSMPC for Systems with Time Correlated Uncertainty 106
5.1 Problem Description 107
5.1.1 Time-correlated uncertainty 108
5.1.2 Confidence regions 110
5.1.3 Input and state constraints 112
5.2 Constraint Handling 114
5.3 The Receding Horizon Algorithm 117
5.4 Numerical Example 123
5.5 Conclusion 127

6 Application of TSMPC to Sustainable Development 130
6.1 Problem Description 130
6.1.1 The Sustainable Development Problem 130
6.1.2 Prometheus 132
6.2 Previous Work and Motivation 134
6.3 Using an ARX Model 138
6.3.1 Fitting the Model 139
6.3.2 State-space Form 143
6.3.3 State-space model with input shocks 148
6.4 Application of the TSMPC Algorithm 149
6.5 Numerical Results 151
6.6 Conclusion 155

7 Non-linear Stochastic MPC 158
7.1 Problem Formulation 158
7.2 Successive linearization MPC 160
7.3 Probabilistic Tubes 165
7.4 Probabilistic Tube Constraints 170
7.5 Cost Function 176
7.6 Receding Horizon NLSMPC 179

7.7 Numerical Example 181
7.8 Conclusion 187

8 Conclusion **190**

Bibliography **195**

Chapter 1

Introduction

Model Predictive Control (MPC) is a control methodology which is based around repeated online open loop optimizations to obtain an optimal input that governs the system to be controlled. As the name suggests, the predictions are based on a model which describes the dependence of the output on the current state and on the inputs. This model can be linear, non-linear and time-varying. To determine the best control action (or optimal input), a measure of performance of the system is needed over a time horizon. By minimizing this quantitative measure, the most desirable input can be calculated by optimizing the predicted performance. One of the main advantages of MPC is its systematic way of handling constraints. Constraints on the state, input, or output can be included and the optimization of the performance is performed subject to constraint satisfaction. The optimization is done in a receding horizon manner.This means that after each optimization, the first element of the input sequence is implemented. At the next step, this process is repeated in order to provide feedback and to compensate for the use of a finte number of optimization variables. The receding horizon control setting is illustrated in Figure 1.1.

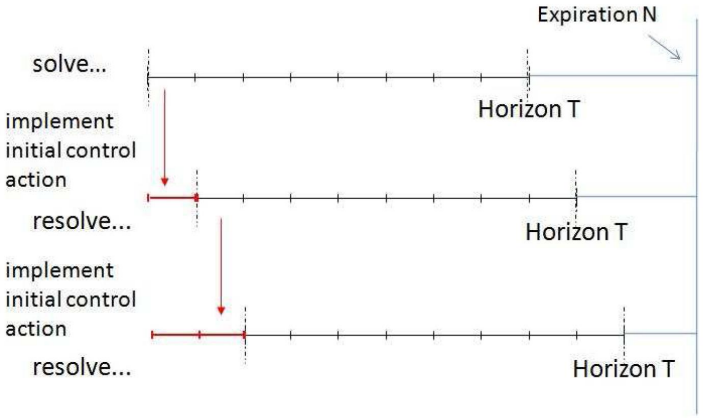

FIGURE 1.1: Receding horizon control. The optimization is solved at each step and only the first element of the input sequence is implemented.

To guarantee the efficacy of MPC, the properties of stability and recursive feasibility are of great importance. Given that the MPC controller produces inputs which are stabilizing, and feasible at current time, stability and feasibility has to be guaranteed at all future times. These two properties ensure that the control will drive the system to a desired reference and that all constraints will be satisfied in closed loop operation.

An intuitive illustration is the process of driving a car. The Model Predictive Controller is the driver, while the system being controlled is the car. The horizon is the view from the driver which is limited to a finite value. The control objective is to keep the car within a safe distance from the car in front and following the trajectory of the road. Therefore, at each step the driver needs to select a control action (accelerate, brake or do nothing) as new information becomes available. As the car is driving along the road, this forms the online receding horizon optimization.

Model Predictive Control was first implemented to process control by Richalet et al. [1]. The main focus within process control was on petro-chemical processes where economic considerations were emphasized. This required operating points situated on the boundary of the set of operating points feasible with respect to

constraints which is computed by solving linear programs on plants which were modeled using step and impulse models [1–3]. These were known as the first generation algorithms. These algorithm handles control and output constraints ad hoc and is very sensitive to even the slightest of disturbance. These shortcomings were addressed by second generation programs where quadratic programming is employed to solve the constrained open loop optimal control problem [4]. The third generation algorithms were introduced in the early 1990s distinguishes between several levels of constraints, provides recovery from infeasible solutions, real-time control and allows for a wide range of process dynamics and controller specifications [5]. This has led to a proliferation of MPC algorithms used in the industry. However, the stability was not addressed theoretically and the academic MPC community were focused on establishing the theoretical aspects of stability in MPC.

Largely independently of the developments in industry-led MPC, a similar methodology was developed within the adaptive control literature known as 'Generalized Predictive Control' [6, 7]. These algorithms are based on input-output models where the states are not accessible. It uses a finite horizon which does not guarantee stability. However, the use of a terminal constraint circumvents this problem and ensured stability for unconstrained linear systems [8, 9]. Hence the optimal controls can be computed algebraically with stability guarantees. Nonetheless, the inadequacy of Generalized Predictive Control (GPC) in handling control and state constraints hinders it progress and has since then paved the foundation for MPC algorithms. In current literature, the distinctive lines separating GPC, Receding Horizon Control, or Dynamic Matrix Control has faded and a unifying term of MPC is used.

Almost any real-world control problem involves systems which are inherently uncertain, have non-linear dynamics and are subjected to some form of constraint. Uncertainties to a system include random disturbances, and can be included in the

system model as additive or multiplicative stochastic variables. Therefore control methodologies, specifically MPC, have to ensure stability and feasibility subject to model uncertainty. This presents additional complexity in terms of computation and analysis. For the case of polytopic or bounded uncertainties, one method is to ensure that the MPC algorithm is both stable and feasible for worst-case uncertainties. If this holds true for the worst case, it would imply the algorithm is both stable and feasible for all uncertainty cases (as discussed in Section 2.2). This methodology is also known as Robust MPC which extends MPC 'robustness' to include uncertainties. The two main limitations of Robust MPC are that it leads to a conservative controller and heavy computation. The conservativeness is due to the fact that no information about the distribution of uncertainties is utilized; clearly the use of such information can lead to better performance if the distribution is non-uniform.

The shortcomings of Robust MPC motivated the development of Stochastic MPC (SMPC). Stochastic MPC takes uncertainty distributions into consideration and in particular uses information on a combination of mean and variance of the future outputs. This allows the output to be restricted to lie within a specified threshold with a given probability and enables upper bounds on the cost to be based on probabilistic bounds. Similarly, constraints which are violated with a frequency below a specified tolerance parameter can be reformulated as probabilistic constraints. The literature highlighted in this report is focused on linear state-space models. The properties of recursive feasibility and stability presented form the platform of SMPC for non-linear systems.

Research on SMPC to date has been focused on the stochastic formulation of constraints and objective function. Van Hessem and Bosgra [10] proposed stochastic constraints in which the system output was restricted to lie within specified bounds with a given probability. Batina et al. [11] formulated an objective function as the expected value of a quadratic cost defined on future predicted states and inputs.

Neither of these two papers gives a complete treatment of closed loop stability and feasibility. In [12], an SMPC algorithm is shown to have guaranteed closed loop stability. However, no consideration is given to constraints. In [13] and [14], probabilistic constraints are incorporated using the notions of a probabilistic invariant set and Markov chains.

One aim of this thesis is to extend the current work on SMPC in [13], which primarily focused on linear systems with constraints. This work extends the application of SMPC to a wider variety of problems by proposing a receding horizon control methodology for systems with additive and multiplicative bounded uncertainty and subjected to hard and soft constraints. These constraints are handled through the construction of a sequence of nested tubes and an associated Markov Chain model. The parameters defining the tubes are optimized simultaneously with the predicted future control trajectory online. The optimization is performed subject to linear constraints which ensures that both hard and soft constraints are satisfied. Through the definition of probabilistic tubes, constraint handling is improved by reducing conservativeness compared to the work in [13].

An important aspect of control algorithms is the computational efficiency. MPC algorithms essentially solve a constrained optimization problem at each time-step which has time constraints dictated by the sampling period of an application. Using a general purpose solver, typical computation times are in the order of seconds. Furthermore, without exploiting the inherent structure of the optimization the complexity increases as $O(N^3)$ where N is the prediction horizon. Therefore, for applications which require fast sampling (order of milliseconds), faster computation is required. One such method is to use an interior point method to solve the online optimization problem. For example in [15], by appropriate variable reordering, the interior-point search direction is computed by solving a tri-diagonal system of linear equations. The main advantage is that the computational complexity increases linearly $O(N)$ with the prediction horizon.

The survey paper [5] provides an extensive list and discussion of commercially available MPC algorithms in industry. MPC has been extensively used to control wide-scale industrial process systems ranging from chemical plants, oil and gas power plants to air traffic control applications. In addition, MPC has been used as a tool for sustainable development policy assessment [16]. This paper considers a problem of policy assessment of the allocation of public research and development budget between alternative power generation technologies. MPC also has applications in financial problems such as dynamic hedging and portfolio optimization [17, 18]. Dynamic hedging and portfolio optimization involves selecting optimal inputs in the form of various financial instruments such that risk (variance) is minimized and return (mean) is maximized. MPC has also been applied in [13] for the control of wind turbines in order to maximize power capture subject to constraints on fatigue damage. In another example, MPC has been applied by [19] to telecommunications network control whereby the goal is to provide fair allocation among links with minimal loss ratio and maximal utilization.This highlights the flexibility and efficacy of the MPC methodology as a tool for the solution to a diverse range of real-world problems involving stochastic models.

The Tube Stochastic Model Predictive Control (TSMPC) algorithm developed in this thesis is applied to a problem in a sustainable development (SD) context. The problem here is the quantitative comparison of possible SD policies in respect of public research and development (R&D)budget. An econometric model, Prometheus, models the relationship between R&D spending on 15 alternative power generation technologies, and 8 sustainable development indicators such as energy costs and carbon dioxide emission, over a timescale of 30 years. Prometheus is treated as a 'black-box' system to be modeled and controlled, in order to determine the best allocation of budget. The aim here is to demonstrate the applicability of the TSMPC algorithm to this problem and only 2 indicators(outputs) and 2 power generation technologies (inputs) are considered here.

Previous work by [16] has developed stochastic MPC algorithms with feasibility and stability guarantees, based on Moving Average (MA) models where the coefficients of the model are assumed to be random with a normal distribution. The MA model and normal distribution assumptions enables the definition and probabilistic constraints and the ability to convert these constraints into deterministic constraints in the optimization. The algorithm is divided into two parts. The first part computes an optimal set-point off-line which the controller needs to track. The second part involves solving the optimization problem online in a receding horizon manner. Work by [20] extended these algorithms to time-varying models, and non-linear models. The stability guarantee is established by imposing an equality constraint in the online optimization. Therefore, this results in a conservative controller. Furthermore, MA models take into account only previous inputs (not outputs) and therefore do not model accurately the dynamics of Prometheus. The aim here is to identify an Auto Regressive Model with External inputs (ARX) model which relates future outputs based on previous outputs and inputs. Furthermore, the random coefficients of the ARX model are assumed to be finitely supported random variables with distribution that can be identified from the input and output data. The TSMPC algorithm is then applied to control the ARX model.

This thesis is outlined as follows:

Chapter 2 describes the theoretical background to linear MPC. The discussion is extended to the case of nonlinear MPC. The exposition first considers deterministic MPC, where no uncertainties are included in the model. When disturbances are considered, deterministic MPC is extended to Robust MPC which is a methodology based on the worst-case scenarios. This leads to conservativeness and computationally demanding optimizations. The limitations of robust MPC motivate the development of the SMPC methodology

which utilizes information of the probabilistic distribution of uncertainties. Earlier contributions to the field of SMPC are highlighted.

Chapter 3 formulates a receding horizon control methodology (termed TSMPC) for systems with linear dynamics with additive and multiplicative bounded uncertainty and subject to hard and soft constraints. These constraints are handled through the construction of a sequence of nested polytopes and an associated Markov Chain model. The parameters defining the nested polytopes are optimized simultaneously with the predicted future control trajectory online. The optimization is performed subject to linear constraints which ensure that both hard and soft constraints are satisfied.

Chapter 4 aims to improve the computational efficiency of the TSMPC algorithm, which essentially consists of solving a series of Quadratic Programming (QP) optimization problems over time. By exploiting the inherent structure of the QP and using an approximate primal barrier interior point method, the computational efficiency is improved significantly as compared to using a generic solver. The computational efficiency improvements are highlighted using a numerical example.

Chapter 5 adapts the TSMPC algorithm applied to linear systems with hard and probabilistic constraints to handle the case where the model uncertainty is non stationary and not temporally independent.

Chapter 6 applies the TSMPC algorithm to a budget allocation problem in a Sustainable Development context. An econometric model is modeled using an ARX model and the TSMPC algorithm is used to compute the optimal budget allocation subject to probabilistic constraints on the indicators as well as hard constraints on the yearly budget allocations.

Chapter 7 formulates a receding horizon control methodology (termed NLSMPC) which is proposed for systems with nonlinear dynamics, additive stochastic

uncertainty, and both hard and soft (probabilistic) input/state constraints. Jacobian linearization about predicted trajectories is used to derive a sequence of convex optimization problems. Constraints are handled through the construction of a sequence of tubes and an associated Markov chain model. The parameters defining the tubes are optimized simultaneously with the predicted future control trajectory via online Linear Programming. An example illustrating the application the NLSMPC algorithm is given.

Chapter 8 provides a conclusion to the report and outlines future work.

Chapter 2

Background

In this section, the theory behind model predictive control for both the deterministic and stochastic case is presented. For the deterministic case, the Model Predictive Control (MPC) methodology for linear systems based on state space models is described. Concepts such as stability, feasibility and invariant sets which ensure the efficacy of MPC are outlined. In the stochastic case, uncertainties in the model in the form of disturbances, model mismatch, or imprecise knowledge of the model parameters add significant complexity to the problem. The earlier work leading to Stochastic MPC is outlined.

2.1 Deterministic MPC Review

The MPC review in this report will be focused on state-space models only. Consider the following linear state space system

$$x_{k+1} = Ax_k + Bu_k \tag{2.1}$$

$$y_k = Cu_k \tag{2.2}$$

where $x_k \in \mathbb{R}^n$,$u_k \in \mathbb{R}^m$ and $y_k \in \mathbb{R}^l$ denote the system state, input and output respectively at time k.

For simplicity, only the single input ($m = 1$) single output ($l = 1$) case (SISO) is considered in this Section. However, the extension of the relevant results to the multi-variable case is straightforward. The representation for the state predictions of (2.1) is given as

$$\mathbf{x} = M\mathbf{u} + v \tag{2.3}$$

$$M = \begin{bmatrix} B & 0 & \dots & 0 \\ AB & B & 0 & \dots \\ \vdots & \vdots & \dots & \vdots \\ A^{N-1}B & A^{N-2}B & \dots & B \end{bmatrix} \quad v = \begin{bmatrix} A \\ A^2 \\ \vdots \\ A^N \end{bmatrix} x_k \tag{2.4}$$

where $\mathbf{x} = [x^T_{k+1|k} \; x^T_{k+2|k} \; \dots \; x^T_{k+N|k}]^T$ and $\mathbf{u} = [u_{k|k} \; u_{k+1|k} \; \dots \; u_{k+N-1|k}]^T$. N is the prediction horizon and is assumed to be the same for both the input and outputs.

An objective function is used to give a quantitative measure of performance over the horizon N. The quadratic performance measure is widely used and is given by

$$J = \sum_{i=0}^{N} l_{k+i|k} \quad l_{k+i|k} = x^T_{k+i|k} Q x_{k+i|k} + u^T_{k+i|k} R u_{k+i|k}, \tag{2.5}$$

where $Q \geq 0$ and $R \geq 0$ are state and input weights. For the SISO case, R is a scalar. Also, Q is a positive semi-definite matrix

The objective function used in (2.5) is set up for a regulation problem where the controller is required to drive the state x_k to the origin in state space. Extensions

to tracking problems where the controller is set up to provide inputs that drive the states to a predefined set point are easy to derive and in essence constitute a reformulation of the tracking to a regulation problem (see Section 2.1.3).

The objective function can be rewritten in more compact form as

$$J = \mathbf{x}^T \tilde{Q} \mathbf{x} + \mathbf{u}^T \tilde{R} \mathbf{u} \tag{2.6}$$

where $\tilde{Q}$ is a block diagonal matrix with diagonal blocks Q, $\tilde{R}$ is a diagonal matrix with elements R. Substituting (2.3) into (2.6) yields

$$J = \mathbf{u}^T [M \tilde{Q}^T M + \tilde{R}] \mathbf{u} + 2\mathbf{u}^T M^T \tilde{Q} v + v^T \tilde{Q} v. \tag{2.7}$$

For the unconstrained case, the optimal input is chosen by minimizing the cost function, and is calculated by solving $\frac{dJ}{d\mathbf{u}} = 0$,thus obtaining

$$\mathbf{u} = -[M^T \tilde{Q} M + \tilde{R}]^{-1} M \tilde{Q} v \tag{2.8}$$

which leads to a simple linear feedback law of the form $u = Kx$. The first element of the input vector is implemented and the predicted trajectory at the next step (k+1) is re-calculated by repeating the optimization. Thus the predicted trajectory is updated repeatedly online. This forms the receding horizon strategy which is the essence of the MPC methodology.

Most practical applications deal with systems which are subject to constraints. The main advantage of MPC is that it can handle constraints in a systematic manner. Constraints on either the states and/or the inputs are specified in the form of

$$G\mathbf{x}_k + H\mathbf{u}_k \leq \mathbf{h}. \tag{2.9}$$

For example, given that the input is constrained within $-\bar{u} \leq u \leq \bar{u}$, this implies

$$G = 0, \quad H = \begin{bmatrix} I_N \\ -I_N \end{bmatrix}, \quad h = \bar{u} \begin{bmatrix} \mathbf{1} \\ \mathbf{1} \end{bmatrix} \tag{2.10}$$

where I_N is the N-dimensional identity matrix and $\mathbf{1}$ is a N-dimensional vector of ones.

In the presence of constraints, the optimization problem is cast as a Quadratic Program(QP) given by

$$\min_{\mathbf{u}} J \quad \text{s.t} \quad (2.9) \tag{2.11}$$

Since the optimization in (2.11) has only a finite horizon, there is no guarantee of closed-loop stability. In addition, the predicted and actual input and state trajectories may differ greatly even in the case where there are no constraints. These shortcomings are circumvented by using an infinite horizon:

$$J(k) = \sum_{i=0}^{\infty} [x^T(k+i|k)Qx(k+i|k) + u^T(k+i|k)Ru(k+i|k)] \tag{2.12}$$

This implies that the input vector $\mathbf{u}$ will be infinite dimensional and thus would render the optimization impracticable. However, the optimization of (2.12) generates a sequence of inputs which cause the state x_k to converge to zero. After some finite prediction horizon the optimal input sequence would have driven the state into a region where the constraints are no longer active. In effect, the infinite prediction horizon can be split into two parts, namely Mode 1 and Mode 2.

Mode 1 extends over a horizon $i = 0, \ldots, N$ where constraints may be active and the inputs are degrees of freedom. In Mode 2, $i = N+1, N+2, \ldots$ the inputs are dictated by the unconstrained optimal feedback law $u = Kx$. The infinite horizon

objective function is evaluated explicitly by rewriting the cost as

$$J(k) = \sum_{i=0}^{N-1} [x^T(k+i|k)Qx(k+i|k) + u^T(k+i|k)Ru(k+i|k)] \\ + x^T(k+N|k)\bar{Q}x(k+N|k) \tag{2.13}$$

where $\bar{Q}$ is a terminal weighting matrix. $\bar{Q}$ is chosen so the term $x^T(k+N|k)\bar{Q}x(k+N|k)$ equals the cost over the Mode 2 prediction horizon. Hence $\bar{Q}$ is calculated as the solution to the Lyapunov equation $\bar{Q} - (A+BK)^T\bar{Q}(A+BK) = Q + K^TRK$.

To prove this, the Lyapunov equation is pre- and post- multiplied with $x^T(i)$ and $x(i)$ respectively.

$$x^T(i)\bar{Q}x(i) - x^T(i)(A+BK)^T\bar{Q}(A+BK)x(i) = x^T(i)Qx(i) + x^T(i)K^TRKx(i)$$

Defining $x(i+1) = (A+BK)x(i)$ and $u(i) = Kx(i)$,

$$x^T(i)\bar{Q}x(i) - x^T(i+1)\bar{Q}x(i+1) = x^T(i)Qx(i) + u^T(i)Ru(i),$$

and summing this equation over $i = 0, 1, \ldots$ gives

$$x^T(0)\bar{Q}x(0) - \lim_{k\to\infty} x^T(k)\bar{Q}x(k) = \sum_{i=0}^{\infty} [x^T(i)Qx(i) + u^T(i)Ru(i)].$$

With the assumption that $(A+BK)$ is strictly stable, $\lim_{k\to\infty} x^T(k)\bar{Q}x(k) \to 0$ and therefore

$$x^T(0)\bar{Q}x(0) = \sum_{i=0}^{\infty} [x^T(i)Qx(i) + u^T(i)Ru(i)].$$

The main advantage of using this 'dual mode' prediction paradigm is that the infinite dimensional problem of minimizing $J(k)$ over $u(k+i|k)$, $i = 0, 1, \ldots$ is approximated by the minimization of (2.13) over the finite number of variables

$u(k+i|k)$, $i = 0, \ldots, N-1$.

2.1.1 Stability

Stability can be guaranteed if optimal value of the predicted cost is monotonically decreasing with time, in closed loop operation. This is ensured if the following conditions hold [21]

1. $(A, Q^{1/2})$ is observable.
2. The terminal weight $\bar{Q}$ is chosen so that J is equivalent to the infinite horizon predicted cost.
3. The optimal predicted input and state sequences at time k satisfy constraints over an infinite horizon.

Condition 1 above ensures that $J(k)$ is positive definite in $x(k)$. It is shown below that Conditions 2 and 3 ensure that the optimal predicted cost $J^*(k)$is non-increasing with k and satisfies

$$J^*(k+1) - J^*(k) \leq -[x^T(k)Qx(k) + u^T(k)Ru(k)] \tag{2.14}$$

along closed-loop trajectories.

The concept of the 'tail' of a sequence is used in the stability analysis. The 'tail' is the remainder of the sequence after removing the first term. For the (hypothetical) case of optimizing $J(k)$ over an infinite number of future input variables, stability and optimality follows from Bellman's principle of optimality, [22] according to which the tail of any optimal trajectory is itself the optimal trajectory from its starting point. However, for a practically implementable MPC law based on the

dual mode prediction paradigm, closed-loop stability follows from a Lyapunov analysis applied to (2.14).

To show that (2.14) is satisfied when the dual mode prediction paradigm is employed, first consider an input sequence at time k of length N given by

$$u^*(k) = [u^*(k|k)\ u^*(k+1|k)\ \ldots\ u^*(k+N-1|k)] \tag{2.15}$$

which has a corresponding infinite horizon cost of

$$J^*(k) = \sum_{i=0}^{N-1}[x^T(k+i|k)Qx(k+i|k) + u^{*T}(k+i|k)Ru^*(k+i|k)] \\ +x^T(k+N|k)\bar{Q}x(k+N|k)$$

At the next time step $k+1$, the tail of the input sequence corresponding to the optimal prediction at time k is denoted as

$$\tilde{u}(k+1) = [u^*(k+1|k)\ u^*(k+2|k)\ \ldots\ Kx^*(k+N|k)]. \tag{2.16}$$

The N^{th} element of the sequence $\tilde{u}(k+1)$ is equal to $u^*(k+N|k)$ which is defined as the linear feedback law $u = Kx$ employed over the mode 2 horizon.The corresponding cost of $\tilde{J}(k+1)$ associated with $\tilde{u}(k+1)$ is just $J^*(k)$ minus the first

element:

$$\begin{aligned}\tilde{J}(k+1) &= \sum_{i=1}^{N}[x^T(k+i|k)Qx(k+i|k) + u^{*T}(k+i|k)Ru^*(k+i|k)] \\ &\qquad + x^T(k+N+1|k)\bar{Q}x(k+N+1|k) \\ &= \sum_{i=1}^{\infty}[x^T(k+i|k)Qx(k+i|k) + u^{*T}(k+i|k)Ru^*(k+i|k)] \\ &= \sum_{i=0}^{\infty}[x^T(k+i|k)Qx(k+i|k) + u^{*T}(k+i|k)Ru^*(k+i|k)] \\ &\qquad - [x^T(k)Qx(k) + u^T(k)Ru(k)] \\ &= J^*(k) - [x^T(k)Qx(k) + u^T(k)Ru(k)].\end{aligned}$$

But if $\tilde{u}(k+1)$ satisfies the constraints of the MPC optimization at time $k+1$, then $\tilde{J}(k+1)$ is suboptimal at time $k+1$, so the optimal value satisfies

$$J^*(k+1) \leq \tilde{J}(k+1) = J^*(k) - [x^T(k)Qx(k) + u^T(k)Ru(k)] \tag{2.17}$$

implying that the optimal cost at current time must be at least as small as the cost evaluated for the tail of the optimal predicted input sequence computed at the previous sample satisfying (2.14). The four conditions for ensuring closed-loop asymptotic stability are summarized in [3].

2.1.2 Terminal Invariant Sets

The previous section establishes a guarantee of closed loop stability under the assumption that the predictions generated by the tail of input sequence $\tilde{u}(k)$ is feasible at all times $k = 1, 2, \ldots$. This section takes into account input and state constraints, and considers for simplicity (but without loss of generality) the case

of upper and lower bounds on the elements of the state and input vectors:

$$\underline{u} \leq u(k) \leq \overline{u}, \quad \underline{x} \leq x(k) \leq \overline{x} \tag{2.18}$$

The first $N-1$ elements of the $\tilde{u}(k+1)$ are feasible given that the optimal predicted input sequence at time k : $[u^*(k+1|k) \ \ldots \ Kx^*(k+N-1|k)]$ necessarily satisfies constraints. To ensure that $\tilde{u}(k+1)$ is feasible at time $k+1$, the N^{th} element, $u^*(k+N|k) = Kx^*(k+N|k)$ must also be feasible. Thus, additional constraints known as terminal constraints are introduced in the MPC optimization at time k to ensure feasibility of $\tilde{u}(k+1)$at the next time step.

Since the predicted inputs over Mode 2 are given by a pre-determined state feedback law, the constraints on $u(k+N|k)$ are equivalent to constraints on $x(k+N|k)$. Let Ω denote the region of state space where constraints on $x(k+N|k)$ are satisfied, then for the constraints (2.18) we require

$$x(k+N|k) \in \Omega \Rightarrow \begin{array}{c} \underline{u} \leq Kx(k+N|k) \leq \overline{u} \\ \underline{x} \leq x(k+N|k) \leq \overline{x} \end{array}. \tag{2.19}$$

The prediction generated by $\tilde{u}(k+1)$ must also satisfy the terminal constraint at time $k+1$, and this is equivalent to

$$x(k+N+1|k) \in \Omega. \tag{2.20}$$

Therefore the necessary and sufficient conditions for feasibility of the predictions generated by the tail $\tilde{u}(k+1)$, whenever the MPC optimization at time k is feasible, are listed below.

1. Constraints are satisfied at all points in Ω.

2. Ω is invariant in mode 2. $x(k+N|k) \in \Omega \Rightarrow (A+BK)x(k+N|k) \in \Omega$.

Invariant sets have been widely studied and a good survey is presented in [23]. There are several candidates for invariant sets but attention here is restricted to ellipsoidal and low-complexity polyhedral sets. An ellipsoidal set is defined as

$$E = \{x : x^T P x \leq 1\}, \quad P \geq 0 \tag{2.21}$$

Condition 2 above implies that $x^T \Phi^T P \Phi x \leq x^T P x \leq 1 \ \forall x \in E$ where $\Phi = A + BK$. Therefore, invariance is ensured if and only if $\Phi^T P \Phi \leq P$ which can equivalently be written as a Linear Matrix Inequality in P^{-1} using Schur complements as

$$\begin{bmatrix} P^{-1} & \Phi P^{-1} \\ P^{-1}\Phi^T & P^{-1} \end{bmatrix} \geq 0 \tag{2.22}$$

Feasibility must hold for all elements within the invariant set and this is ensured by the condition (stated here for a single input system for simplicity) that $\underline{u} \leq Kx \leq \overline{u}$. But for $x \in E$ we have

$$\begin{aligned} |Kx|^2 \leq |KP^{-\frac{1}{2}}P^{\frac{1}{2}}x| &\leq ||KP^{-\frac{1}{2}}||^2||P^{\frac{1}{2}}x||^2 \\ &\leq (KP^{-1}K^T)(x^T P x) \\ &\leq KP^{-1}K^T \end{aligned} \tag{2.23}$$

(And this inequality holds with equality for some $x \in E$). Thus feasibility can be rewritten as an LMI in P^{-1}. For example, if $-\underline{u} = \overline{u}$, then $|Kx| \leq \overline{u}$ for all $x \in E$ if and only if

$$\begin{bmatrix} P^{-1} & P^{-1}K \\ K^T P^{-1} & \bar{u}^2 \end{bmatrix} \geq 0 \tag{2.24}$$

It is noted that (2.24) is not only sufficient (as indicated by (2.23)) but also necessary for the feasibility of E under the control law $u = Kx$. By maximizing the size of the terminal invariant set, the set of feasible initial conditions is enlarged. The enlargement of E can be achieved by performing the convex optimization [24]

$$\max_{P^{-1}} \log det(P^{-1}) \quad \text{s.t}(2.22), (2.24) \tag{2.25}$$

As an alternative to ellipsoids, low complexity polyhedral invariant sets can be used. Firstly, the system in (2.1) is transformed to

$$z(k+1) = VAWz(k) + VBu(k) \tag{2.26}$$

where $V = W^{-1}$ and $z(k) = Vx(k)$. The mode 2 feedback law $u(k) = Kx(k)$ gives a state trajectory that is governed by the dynamics

$$z(k+1) = \Phi z(k) \tag{2.27}$$

where $\Phi = V(A + BK)W$

A polyhedral set is defined as

$$\Pi = \{x \in \mathbb{R}^n : |Vx| \leq \alpha\} \tag{2.28}$$

where α is a vector with positive elements. A simple low-complexity polyhedron with V as a full-rank square matrix is considered. The condition for invariance is that $|z(k+1)| \leq \alpha$ for $x(k+1) \in \Pi$ and this is satisfied if and only if $|\Phi Vx| \leq \alpha$ for all x such that $|Vx| \leq \alpha$, but

$$\begin{aligned} |\Phi Vx| &\leq |\Phi||Vx| \leq \alpha \\ &\Leftrightarrow |\Phi|\alpha \leq \alpha. \end{aligned} \tag{2.29}$$

This condition is necessary as well as sufficient for invariance of Π. Considering again the case of single input systems with $-\underline{u} = \overline{u}$, the condition for feasibility of Π under the control law $u(k) = Kx(k)$ is given by $|Kx| \leq \overline{u}$. But for all $x \in \Pi$ we have

$$\begin{aligned} |Kx| &\leq |KV^{-1}Vx| \\ &\leq |KW||Vx| \leq |KW|\alpha \leq \bar{u} \end{aligned} \tag{2.30}$$

(and this inequality holds with equality for some $x \in \Pi$). In the absence of uncertainties, and assuming $A + BK$ is to be strictly stable with real eigenvalues, it is convenient to chose the columns of V as the eigenvectors of $(A + BK)$ so that $\Phi = V(A + BK)W$ is a diagonal matrix of eigenvalues. In this case (2.29) is satisfied for any positive α since $|\phi_{ii}| = |\lambda_i|(< 1)$ and $|\phi_{ij}| = 0$ for $i \neq j$. Therefore the only condition on α is (2.30) [25]. This choice of V is suitable only for the case of $(A + BK)$ with real simple eigenvalues. Extension to the general case is possible, e.g in [26], but will not be discussed in this report. Alternatively, the choice of V can be computed by solving an optimization problem, specifically a non-linear program, which is more computationally demanding [27].

The maximization of the volume of the polyhedral set, Π, is given as the convex problem:

$$\max_{\alpha} det(diag(\alpha)) \quad \text{s.t}(2.30) \tag{2.31}$$

The dual mode MPC algorithm is given as follows

Algorithm 1. (Dual Model MPC)

1. (Off-line): Compute the maximum volume terminal invariant sets using either (2.25) or (2.31).

2. (Online): For $k = 0, 1, 2...$

$$\min_{\mathbf{u}} J \quad \text{s.t (2.9) and}$$
$$x_{k+N|k}^T P x_{k+N|k} \leq 1 \text{ or } \left|V x_{k+N|k}\right| \leq \alpha \tag{2.32}$$

3. Implement the first element of $\mathbf{u}$ and repeat the online optimization for next k

2.1.3 Reference Tracking

The MPC theory described so far has focussed on the regulation of state where the controller drives the states to converge to zero. The regulation problem can be extended to a reference tracking problem, where the controller drives the states to a predefined set-point.

Define x^{ss} and u^{ss} as the equilibrium states and inputs or predefined set-points,

$$x^{ss} = Ax^{ss} + Bu^{ss}. \tag{2.33}$$

Including these equilibrium states into the state-space formulation

$$x_{k+1} - x^{ss} = A(x_k - x^{ss}) + B(u_k - u^{ss}) \tag{2.34}$$

and setting $\tilde{x}_k = x_k - x^{ss}$ and $\tilde{u}_k = u_k - u^{ss}$ converts the tracking problem to a regulation problem.

2.2 Robust MPC Review

The theory so far has not considered uncertainty. Uncertainties can be of the form of disturbances or lack of precise knowledge of parameters inherent in the model. Feedback provides some robustness to uncertainties, but Robust MPC aims to provide robustness to a specific class of uncertainties. A strategy for dealing with uncertainties is to ensure that MPC is robust with respect to the worst-case disturbances within this class, and this holds for the worst-case, it would be robust for all cases.

Consider an extension of the model in (2.1) to include polytopic multiplicative uncertainty where the model is described by

$$x_{k+1} = A_k x_k + B_k u_k, \tag{2.35}$$

and where the state and input matrices lie inside a polytope Ω which is a convex hull of the vertices $(A^{(i)}, B^{(i)})$

$$(A_k, B_k) = \sum_{i=1}^{p} \eta_i (A^{(i)}, B^{(i)}), \quad \sum_{i=1}^{p} \eta_i = 1, \quad \eta_i \geq 0 \tag{2.36}$$

where (A_i, B_i) are known, and η_i are unknown, possibly time-varying parameters. Input and state constraints which need to be satisfied for all realizations of uncertainty and for all time k are imposed

$$x_k \in X, \quad u_k \in U. \tag{2.37}$$

The cost function which aims to minimize the worst case cost is given by

$$\min_{\mathbf{u}} \max_{(A,B)\in\Omega} J_k \tag{2.38}$$

$$\text{s.t (2.37) and } x_{k+N|k} \in X_f$$

As an alternative to minimizing the worst case cost, two algorithms are outlined here to explain how uncertainty can be dealt with robustly by the MPC methodology using a nominal cost instead.

2.2.1 Closed Loop Paradigm

Consider first the case of no uncertainty, for applications with open-loop unstable models, numerical problems will be encountered if long prediction horizons are used. The predictions of (2.3) and in particular the elements CA^jB of matrix M may assume large values if A has eigenvalues outside the unit circle. Then $M^T\tilde{Q}M+\tilde{R}$, which is to be inverted when calculating the unconstrained optimum, will be ill-conditioned. The closed loop paradigm is introduced to address this problem. The degrees of freedom in the optimization are re-parameterized as perturbations of a stabilizing feedback control law [28]

$$u_{k+i|k} = -Kx_{k+i|k} + c_i \quad i = 0, 1, \ldots, N-1 \tag{2.39}$$

$$u_{k+i|k} = -Kx_{k+i|k} \quad i = N, N+1, \ldots \tag{2.40}$$

In this formulation, the prediction models are no longer (A, B, C) but (Φ, B, C) where $\Phi = A - BK$. CA^jB is replaced by $C\Phi^jB$, thus avoiding ill-conditioning. Furthermore, the use of the perturbation c_i can be seen as a way of ensuring that constraints are respected whenever $c = 0$ is infeasible. However, the c_i is a perturbation of the unconstrained optimal and should be kept as small as possible. If K in (2.39) is the unconstrained optimal feedback gain for the nominal model (A_0, B_0), the minimization of cost J evaluated for the nominal model (A_0, B_0), can be shown to be equivalent to the minimization of [28]

$$J_c = \mathbf{c}^T W \mathbf{c}, \quad W = diag([B_0^T \Sigma B_0 + R, B_0^T \Sigma B_0 + R, \ldots, B_0^T \Sigma B_0 + R]) \tag{2.41}$$

where Σ is the solution to the Lyapunov equation $\Sigma - (A_0 + B_0 K)^T \Sigma (A_0 + B_0 K) = Q + K^T R K$.

In the online stage of the closed-loop paradigm MPC algorithm, the following optimization problem is solved at each time-step and the first element of the input vector is used as inputs.

Algorithm 2. (Closed-loop paradigm MPC)

$$\min_{c_{k+i|k}, i=0,1,\ldots,N-1} J_c$$

$$\text{s.t. } x_{k+i|k} \in X, \quad u_{k+i|k} \in U \tag{2.42}$$

$$\text{and } x_{k+N|k} \in X_f \tag{2.43}$$

If constraints (2.42) and (2.43) are invoked for all members in the uncertainty class, this may lead to excessive computation. Several works [29, 30] attempt to overcome this problem. This leads the discussion to an alternative that uses the closed-loop paradigm in conjunction with an augmented state space formulation.

2.2.2 Augmented Autonomous State Space Formulation

For a linear system with polytopic uncertainty, the constraints (2.42) and (2.43) are invoked for all members of the uncertainty class and this leads to an exponential explosion in the online computation rendering the approach impracticable. For the algorithm defined in the previous section, constraints need to be checked along the prediction horizon thereby necessitating the propagation of the effects of uncertainty. The constraints are invoked explicitly over Mode 1 and implicitly over Mode 2 through the stability (terminal) constraint. By utilizing an augmented autonomous state space formulation, the stability constraint from N steps ahead into the future can be transferred to current time. This avoids the problem

of propagation of uncertainty. This is achieved by transferring most of the online computations off-line, leaving only a trivial optimization online.

An augmented state vector is defined as [31]:

$$z_k = [x_k^T \ c_0^T \ \dots \ c_{N-1}^T]^T. \tag{2.44}$$

Consequently, the prediction dynamics are given by

$$z_{k+1} = \Psi_k z_k, \quad u_k = \tilde{K} z_k, \Psi_k = \begin{bmatrix} \Phi_k & [B_k \ 0 \ \dots \ 0] \\ 0 & M \end{bmatrix}, \tilde{K} = [K \ e_1] \tag{2.45}$$

where Φ_k lies within the polytope with vertices given by $\Phi_i = A_i + B_i K, i = 1, \dots, L$ and

$$M = \begin{bmatrix} 0 & I & 0 & \dots & 0 \\ 0 & 0 & I & \dots & 0 \\ \vdots & \vdots & & & \vdots \\ 0 & 0 & 0 & \dots & 0 \end{bmatrix}, \quad e_1 = [I \ 0 \ \dots \ 0], \tag{2.46}$$

where I is the $m \times m$ identity matrix. The evolution of state vector along the prediction horizon N is as follows

$$z_k = \begin{bmatrix} x_k \\ c_0 \\ \vdots \\ c_{N-2} \\ c_{N-1} \end{bmatrix}, z_{k+1} = \begin{bmatrix} x_{k+1} \\ c_1 \\ \vdots \\ c_{N-1} \\ 0 \end{bmatrix}, \dots, z_{k+N} = \begin{bmatrix} x_{k+N} \\ 0 \\ \vdots \\ 0 \\ 0 \end{bmatrix}, \dots \tag{2.47}$$

An augmented ellipsoid is defined by

$$E_z = \{z | z^T P_z z \leq 1 \}, \quad P_z > 0 \tag{2.48}$$

The ellipsoid is required to be invariant with respect to the dynamics of (2.45) and this is achieved if, and only if $\Psi^T P_z \Psi \leq P_z$, or equivalently:

$$\begin{bmatrix} P_z^{-1} & \Psi P_z^{-1} \\ P_z^{-1}\Psi^T & P_z^{-1} \end{bmatrix} \geq 0 \tag{2.49}$$

In addition, the invariant ellipsoid is required to be feasible. For the case of only input constraints, for all $z_k \in E_z$, the control law $u = \tilde{K}z$ will be feasible over the entire prediction horizon if and only if $|\tilde{K}^T P_z^{-1} \tilde{K}| \leq \bar{u}^2$, or equivalently

$$\begin{bmatrix} P_z^{-1} & P_z^{-1}\tilde{K} \\ \tilde{K}^T P_z^{-1} & \bar{u}^2 \end{bmatrix} \geq 0 \tag{2.50}$$

As a consequence of invariance and feasibility, if $\mathbf{c}$ is found at current time such that $z_k \in E_z$, then the predicted augmented states would all lie in E_z and would thus ensure feasibility of the entire input trajectory. Feasibility at all future times and closed loop stability is guaranteed [31].

The Efficient MPC algorithm is outlined as follows:

Algorithm 3. (Efficient MPC algorithm)

1. (Off-line): Maximize the volume of the projection of E_z onto the x-subspace by maximizing $\log(det[I\ 0]P_z^{-1}[I\ 0]^T)$ subject to (2.49) and (2.50).

2. (Online) For $k = 0, 1, 2...$, solve

$$\min_{\mathbf{c}} J_c$$
$$\text{s.t } z_k \in E_z \tag{2.51}$$

3. Implement the first element of $\mathbf{c}$ and repeat online optimization for next k.

The required minimization of the convex cost subject to the convex quadratic constraint can be solved efficiently using a technique discussed in [32].

2.3 Nonlinear MPC Review

In most real-life applications, linear models are insufficient to model dynamics with nonlinear behaviour. Nonlinearities that arise in modeling physical systems include saturation (common in practical electronic or magnetic amplifiers), relays, hysteresis, and quantization [33]. In this section, MPC applied to nonlinear systems (NMPC) is discussed [34].

A nonlinear model with state variables ($x \in \mathbf{R}^n$) and inputs ($u \in \mathbf{R}^m$) is given by

$$x_{k+1} = f(x_k, u_k) \tag{2.52}$$

where f is twice continuously differentiable with respect to x and u and the constraints on the system states and inputs are $x_k \in X$, $u_k \in U$ where X, U are polytopic sets defined by linear inequalities. It can be assumed that the equilibrium is always at the origin, $f(0, 0) = 0$ [35]. This assumption is valid because a change of coordinates $z_k = x_k - x_{ss}$,$v_k = u_k - u_{ss}$ can always be introduced so

that the equilibrium is at the origin in the new coordinates:

$$\begin{aligned} z_{k+1} = x_{k+1} - x_{ss} &= f(z_k + x_{ss}, v_k + u_{ss}) - f(x_{ss}, u_{ss}) \\ &= g(z_k, v_k) \\ 0 &= g(0, 0). \end{aligned}$$

The objective function is a quadratic form given by

$$J(\mathbf{x}_k, \mathbf{u}_k) = \sum_{i=0}^{N-1} \left(x_{k+i|k}^T Q x_{k+i|k} + u_{k+i|k}^T R u_{k+i|k} \right) + x_{k+N|k}^T Q_f x_{k+N|k}. \tag{2.53}$$

where Q, R are positive definite matrices and Q_f is a suitable terminal weight and $\mathbf{x}_k$ and $\mathbf{u}_k$ are vectors of predicted state $\mathbf{x}_k = [x_{k+1|k}^T, \ldots, x_{k+N|k}^T]^T$ and input sequences $\mathbf{u}_k = [u_{k|k}^T, \ldots, u_{k+N-1|k}^T]^T$. The NMPC algorithm is therefore defined by

Algorithm 4. (NMPC algorithm)

$$\min_{\mathbf{u}_k, \mathbf{x}_k} \; J(\mathbf{x}_k, \mathbf{u}_k) \tag{2.54a}$$

$$\text{s.t} \quad x_{k+i|k} \in X, \; u_{k+i|k} \in U \tag{2.54b}$$

$$x_{k+i+1|k} = f(x_{k+i|k}, u_{k+i|k}) \tag{2.54c}$$

$$x_{k+N|k} \in \Omega_T \tag{2.54d}$$

for $i = 0, \ldots, N-1$ and where $x_{k+N|k} \in \Omega_T$ is a terminal stability constraint for some suitable ellipsoidal or polytopic set Ω_T.

The optimization (2.54) is a nonconvex problem due to the non-linear predictions (2.54c). This has two main implications. Firstly, a particular solution must be computed online within strict time constraints, whereas the number of iterations required to reach a given solution accuracy is unknown. Secondly, convergence to a globally optimal solution cannot be guaranteed. Without this guarantee, the

closed-loop stability of the NMPC strategy in turn, cannot be guaranteed, as this is dependent on a sufficient decrease in the value of the receding horizon objective. As the NMPC optimization may converge to several locally optimal solutions with different associated predicted cost, there is no guarantee of sufficient decrease in the objective value.

A viable approach is to compute an optimal control sequence of convex QP problems, which are solved to generate a sequence of iterates converging to an optimal solution. By rewriting (2.54) in the form

$$\min_{z} \; J(z) \tag{2.55a}$$

$$\text{s.t. } c_E(z) = 0, \quad c_I(z) \leq 0 \tag{2.55b}$$

where $z = [\mathbf{x}^T \; \mathbf{u}^T]^T$ with $\mathbf{x}$ and $\mathbf{u}$ defined as vectors of state and input predictions at current time where $c_E = 0$ and $c_I \leq 0$ invoke the equality and inequality constraints implied by (2.54c) and (2.54b),(2.54d) respectively. An optimal solution for (2.55) satisfies the first order necessary KKT conditions. By application of Newton's method to the problem of determining a stationary point of the Lagrangian function which satisfies the KKT conditions yield the equivalent QP subproblem:

$$\min_{d^{(k)}} \nabla_z J(z^{(k)})^T d^{(k)} + \frac{1}{2} d^{(k)T} \nabla_z^2 J(z) d^{(k)} \tag{2.56a}$$

$$\text{s.t.} \nabla_z c_E(z^{(k)})^T d^{(k)} + c_E(z^{(k)}) = 0 \tag{2.56b}$$

$$\nabla_z c_I(z^{(k)})^T d^{(k)} + c_I(z^{(k)}) \leq 0. \tag{2.56c}$$

where the solution $d^{(k)}$ determines a search direction which is used to determine the next iterate $z^{(k+1)}$ via a line search. This is a successive linearization strategy, where the nonlinear model dynamics are linearized at each iteration about the predicted trajectories for the state and control variables obtained from the previous

iteration. The resulting linear time varying system is used in place of (2.54c).

Without limits on the step size $\|d^{(k)}\|$, the successive linearization method may not converge, or require many iterations of the Sequential Quadratic Programming (SQP) subproblem before the linearization errors in the approximate cost becomes sufficiently small, thus requiring the solution of a large number of QP problems at each sampling interval. A method proposed in [36] overcomes this problem by adding polytopic bounds on predicted states and inputs. Using local Lipschitz bounds on the nonlinear model, the additional bounds are used to formulate an upper bound on the cost (2.54a) for the nonlinear model, which is minimized instead. This allows guarantees of closed loop stability to be obtained on the basis of the SQP subproblem cost regardless of the magnitude of linearization errors. These bounds are retained as optimization variables to be minimized.

2.4 Stochastic MPC Review

MPC research to date has been extended to include stochastic disturbances without constraints. MPC can be extended to handle stochastic uncertainty in the presence of constraints via the method of robustness as explained in the previous section. The method of robustness ensures stability and feasibility for the worst-case uncertainty and therefore would hold for all realizations of uncertainty. However, this approach disregards any a priori information about the probability distribution of uncertainty. By incorporating information about the distribution of uncertainty, a less sub-optimal controller can be obtained. This has recently led to the development of Stochastic MPC which aims to achieve a systematic, non-conservative and computationally efficient method for propagating the effects of uncertainty over a prediction horizon.

In this section, the advantages and limitations of available key results in Stochastic MPC by [13, 37, 38] are outlined.

In [37], a formulation to handle probabilistic constraint is proposed. The process dynamics are modeled using a discrete time linear model:

$$x(k+1) = Ax(k) + Bu(k) + Gw(k) \tag{2.57a}$$

$$z(k) = C_z x(k) + E_z u(k) \tag{2.57b}$$

$$y(k) = Cx(k) + Fw(k) \tag{2.57c}$$

where $y(k)$ is the measured output vector, $z(k)$ is the performance channel on which the objective as well as the constraints are imposed, and $w(k)$ is vector of exogenous stochastic disturbances with a Gaussian distribution. The objective function chosen to be minimized is $\mathbb{E}(c^T z)$ which is a linear function of z where $\mathbb{E}(.)$ denotes the expectation operator. The control law is given by $u - u^r = K(y - y^r)$, where K is a pre-stabilizing controller and u^r, y^r are references. The probabilistic constraint considered here is a polytope

$$P(z_t \in \mathcal{P}) \geq \alpha, \quad \text{where } \mathcal{P} = \{\zeta : H^T \zeta \leq g\}, \tag{2.58}$$

where $\alpha \in [0, 1]$. The Gaussian processes z_k can be fully defined by the mean $\bar{z}$ and its covariance matrix Z. The constraint $P(z_t \in \mathcal{P})$ is equivalent to

$$\frac{1}{\sqrt{(2\pi)^n \det(Z)}} \int_{\mathcal{P}} \exp^{-0.5(\zeta - \bar{z})^T Z^{-1} (\zeta - \bar{z})} \, d\zeta \geq \alpha, \tag{2.59}$$

which is a difficult constraint to incorporate in an optimization problem. By defining an ellipsoid $\epsilon_r = \{\zeta : \zeta^T Z^{-1} \zeta \leq r^2\}$ and by ensuring that

$$P(z_t \in \epsilon_r) \geq \alpha, \quad \bar{z} + \epsilon_r \subset \mathcal{P}, \tag{2.60}$$

then the constraint will be satisfied. The first condition can be converted into a one-dimensional integration while the latter is easily shown to be equivalent to

$$h_j^T \bar{z} + r\sqrt{h_j^T Z h_j} \leq g_j \quad \forall j, \tag{2.61}$$

where h_j, g_j denoted the jth row of matrix H and the jth element of vector g respectively. An open-loop solution and efficient method of computing the solution is derived in [37], but no consideration is given to closed-loop stability and feasibility. This method was further investigated in [39],[10], which extended the case to include bounded disturbances and exploited the state and innovations feedback. However, both did not analyze the closed-loop properties either.

In [38], the linear discrete time stochastic dynamical system considered is

$$x(k+1) = Ax(k) + Bu(k) + \sum_{j=1}^{q}(C_j x(k) + D_j u(k))w_j(k) \tag{2.62}$$

with $w(k) = [w_1(k) \ \ldots \ w_q(k)]^T$ and the control aim is to regulate the system to the origin while respecting quadratic constraints of the form

$$\begin{bmatrix} x(k) \\ u(k) \end{bmatrix}^T H_l \begin{bmatrix} x(k) \\ u(k) \end{bmatrix} + f_l^T \begin{bmatrix} x(k) \\ u(k) \end{bmatrix} \leq \beta_l, \quad l = 1, \ldots L_1 \tag{2.63}$$

$$x^T(k) H_l^X x(k) + (f_l^X)^T x(k) \leq \beta_l^X, \quad l = 1, \ldots, L_2 \tag{2.64}$$

with $H_l \geq 0$ and $H_l^X \geq 0$. By choosing $H_l = H_l^X = 0$, the constraints are linear.

The receding horizon control policy proposed is based on solutions of finite horizon optimizations that uses open-loop plus linear feedback, satisfies (2.63) and (2.64)

in expectation, and use a terminal cost and terminal constraint given as

$$\min_{\bar{u}_N(.|k),K(.|k)} \mathbb{E}\left(\sum_{i=0}^{N-1}\begin{bmatrix} x_N(i|k) \\ u_N(i|k)\end{bmatrix}^T M \begin{bmatrix} x_N(i|k) \\ u_N(i|k)\end{bmatrix} + x_N^T(N|k)\Phi x_N(N|k)\right) \tag{2.65a}$$

$$\text{s.t. } x_N(0|k) = x(k), \quad u_N(0|k) = \bar{u}_N(0|k) \tag{2.65b}$$

$$u_N(i|k) = \bar{u}_N(i|k) + K(i|k)\left(x_N(i|k) - \mathbb{E}_k(x_N(i|k)\right), \ i = 1, \ldots, N-1 \tag{2.65c}$$

$$\mathbb{E}_k\left(x_N^T(N|k)\Phi x_N(N|k)\right) \leq \alpha, (u_N(.|k), x_N(.|k)) \in \mathcal{C}(x(k), N) \tag{2.65d}$$

where $\mathbb{E}_k(.)$ denotes the expectation operator condition on information available at time k, N is the horizon length and $x_N(i|k), i = 0, \ldots, N$ and $u_N(i|k), i = 0, \ldots, N-1$ are the predicted state and control sequences respectively. The constraint set $\mathcal{C}$ is defined as

$$\mathcal{C}(x(k), N) = \mathbb{E}_k\left(\begin{bmatrix} x_N(i|k) \\ u_N(i|k)\end{bmatrix}^T H_l \begin{bmatrix} x_N(i|k) \\ u_N(i|k)\end{bmatrix} + f_l^T \begin{bmatrix} x_N(i|k) \\ u_N(i|k)\end{bmatrix}\right) \leq \beta_l \tag{2.66}$$

$$i = 0, \ldots, N-1, l = 1, \ldots, L_1$$

as well as

$$\mathcal{C}(x(k), N) = \mathbb{E}_k\left(x_N^T(i|k)H_l^X x_N(i|k) + (f_l^X)^T x_N(i|k)\right) \leq \beta_l^X \tag{2.67}$$

$$i = 1, \ldots, N, l = 1, \ldots, L_2.$$

The work in [38] showed that the optimization problem can be converted to a convex semi-definite program by utilizing the convex characterization of the mean and covariance processes of the dynamical system.

Define matrix variables $P(i), i = 1, \ldots, N-1$ which satisfy the following inequality

$$\begin{aligned} P(i) &\geq \mathbb{E}_k \left(\begin{bmatrix} x(k) \\ u(k) \end{bmatrix} \begin{bmatrix} x(k) \\ u(k) \end{bmatrix}^T \right) \\ &= \begin{bmatrix} \bar{x}(i) \\ \bar{u}(i) \end{bmatrix} \begin{bmatrix} \bar{x}(i) \\ \bar{u}(i) \end{bmatrix}^T + \begin{bmatrix} \Sigma(i) \\ U(i) \end{bmatrix} \Sigma^{-1}(i) \begin{bmatrix} \Sigma(i) \\ U(i) \end{bmatrix}^T . \end{aligned} \tag{2.68}$$

This in turn can be expressed as a Linear Matrix Inequality using Schur complements as

$$\begin{bmatrix} P(i) & \begin{bmatrix} \Sigma(i) \\ U(i) \end{bmatrix} & \begin{bmatrix} \bar{x}(i) \\ \bar{u}(i) \end{bmatrix} \\ \begin{bmatrix} \Sigma(i) & U^T(i) \end{bmatrix} & \Sigma(i) & 0 \\ \begin{bmatrix} \bar{x}^T(i) & \bar{u}^T(i) \end{bmatrix} & 0 & 1 \end{bmatrix} \geq 0. \tag{2.69}$$

The objective function, terminal constraint and constraint sets can all be rewritten in LMI form in terms of $P(i)$, and the problem is recast as an SDP problem given by

$$\min_{\bar{u}(i), \bar{x}(i), P(i), \Sigma(i), U(i)} \sum_{i=0}^{N-1} Tr(MP(i)) + Tr(\Phi P^X(N)) \tag{2.70a}$$

$$\text{s.t. } Tr(H_l P(i)) + f_l^T \begin{bmatrix} \bar{x}(i) \\ \bar{u}(i) \end{bmatrix} + g \leq \beta_l \tag{2.70b}$$

$$Tr(H_l^X P^X(i)) + (f_l^X)^T \bar{x}(i) \leq \beta_l^X \tag{2.70c}$$

$$Tr(\Phi P(N)) \leq \alpha. \tag{2.70d}$$

where $Tr(x)$ denotes the trace of x. Primbs [38] also analyzed closed loop stability and feasibility in detail. The advantage of solving an SDP in a receding horizon manner makes the computation tractable and allows real time implementation of a controller for stochastic systems. However, the computational burden may be

prohibitive for a longer horizon or large system due to the constraints in LMI form and the number of matrix variables to be determined online. Furthermore, the assumption that constraints are met in expectation is simplistic and therefore limits the applicability of this method.

An alternative SMPC algorithm proposed by [13] guarantees close-loop stability and feasibility of probabilistic constraints through the use of probabilistic invariance. The paper considers an uncertain linear system given by the model

$$x_{k+1} = A_k x_k + B_k u_k + d_k \tag{2.71}$$

where the elements of A_k,B_k and d_k are random Gaussian variables independently and identically distributed at each time k. The uncertainty description can be written as

$$[A_k \ B_k \ d_k] = [\bar{A} \ \bar{B} \ 0] + \sum_{j=1}^{m} [\tilde{A}_j \ \tilde{B}_j \ \tilde{g}_j] q_{k,j} \tag{2.72}$$

with $q_k = [q_{k,1} \dots q_{k,m}]^T \sim N(0, I)$.

The control sequence is defined by perturbations on a feedback law $u_{k+i} = Kx_{k+i} + c_{i|k}$ for $i = 0, \dots, N$ and $u_{k+i} = Kx_{k+i}$ $i = N, N+1, \dots$, where the feedback gain K is optimal for the case of no constraints with respect to the cost function defined in equation (2.81) below.

The system output is also subject to additive and multiplicative uncertainty:

$$\psi_k = C_k x_k + D_k u_k + \eta_k \tag{2.73}$$

$$[C_k \ D_k \ \eta_k] = [\bar{C} \ \bar{D} \ 0] + \sum_{j=1}^{m} [\tilde{C}_j \ \tilde{D}_j \ \tilde{\eta}_j] q_{k,j} \tag{2.74}$$

with $q_k = [q_{k,1} \dots q_{k,m}]^T \sim N(0, I)$.

The system in (2.71) is rewritten in an augmented autonomous form

$$z_{i+1|k} = \Psi_{k+i} z_{i|k} + \delta_{k+i}, \quad i = 0, 1, \ldots \tag{2.75}$$

$$z_{0|k} = [x_k^T \; c_{0|k}^T \; \ldots \; c_{N-1|k}^T]^T \tag{2.76}$$

and consequently, the uncertainty description is written as

$$[\Psi_k \; d_k] = [\bar{\Psi} \; 0] + \sum_{j=1}^{m} [\tilde{\Psi}^{(j)} \; \tilde{\gamma}^{(j)}] q_{k,j} \tag{2.77}$$

$$\bar{\Psi} = \begin{bmatrix} \bar{\Phi} & \bar{B}E \\ 0 & M \end{bmatrix}, \tilde{\Psi}^{(j)} = \begin{bmatrix} \tilde{\Phi}^{(j)} & \tilde{B}^{(j)}E \\ 0 & 0 \end{bmatrix}, \tilde{\gamma}^{(j)} = \begin{bmatrix} \tilde{g}^{(j)} \\ 0 \end{bmatrix}. \tag{2.78}$$

where $\Phi = A + BK$ and

$$M = \begin{bmatrix} 0 & I & 0 & \ldots & 0 \\ 0 & 0 & I & \ldots & 0 \\ \vdots & \vdots & & & \vdots \\ 0 & 0 & 0 & \ldots & 0 \end{bmatrix}, \quad E = [I \; 0 \; \ldots \; 0] \tag{2.79}$$

where I is the identity matrix with dimensions equal to the size of u_k.

The constraints in this algorithm were defined to be soft constraints which means that constraint violations may occur, but the frequency of constraint violations, averaged over a horizon N_c, must be no greater than a predefined limit. If constraints are such that $\psi_k \in I_\psi$ where $I_\psi = [\psi_L, \psi_U]$, then requiring the average rate of violation to be less than $\frac{N_{max}}{N_c}$ is equivalent to

$$\frac{1}{N_c} \sum_{i=0}^{N_c-1} Pr\{\psi_{k+i} \notin I_\psi\} \leq \frac{N_{max}}{N_c}. \tag{2.80}$$

The predicted cost is defined as the expected value of a quadratic cost

$$J_k = \sum_{i=0}^{\infty} \mathbb{E}_k(L_i), \quad L_i = z_i^T \tilde{Q} z_i - Tr(\Theta \tilde{Q}) \tag{2.81}$$

where Θ is the solution of the Lyapunov equation $\Theta - \bar{\Psi}\Theta\bar{\Psi}^T - \sum_{j=1}^{m} \tilde{\Psi}_j \Theta \tilde{\Psi}_j^T = \sum_{j=1}^{m} \tilde{\gamma}_j \tilde{\gamma}_j{}^T$ and $\tilde{Q} = \begin{bmatrix} Q + K^T R K & K^T R E \\ E^T R K & E^T R E \end{bmatrix}$.

The soft constraint on the system output can be written as a probabilistic constraint using a sequence of nested sets. For the case of two nested sets, $\epsilon_1 \subset \epsilon_2$ defined in the space of z, let $S_1 = \epsilon_1$ and $S_2 = \epsilon_2 - \epsilon_1$. Conditional probabilities are defined as $Pr(\psi \notin I_\psi | x_k \in S_j) = p_j \quad j = 1, 2$. The assumption that p_1 is small is made, which implies S_1 is the 'safe region'. Consequently, p_2 is approximately 1 implying that S_2 is the 'unsafe region'. A matrix of transition probabilities is defined as

$$\Pi = \begin{bmatrix} p_{11} & p_{12} \\ p_{21} & p_{22} \end{bmatrix} \tag{2.82}$$

where p_{ij} is the probability that the state of (2.75) is steered from S_j to S_i in one step.

The probability of constraint violation at time $k + i$ is then given by

$$Pr(\psi_{i|k} \notin I_\psi) = [p_1 \; p_2] \Pi^i \begin{bmatrix} Pr(x_k \in S_1) \\ Pr(x_k \in S_2) \end{bmatrix} \tag{2.83}$$

Due to the special structure of Π, the rate at which constraint violations accumulate given $x_k \in S_j$ tends to

$$R_j = [p_1 \; p_2] w_1 v_1^T e_j, \quad j = 1, 2 \tag{2.84}$$

where e_1 and e_2 denote the first and second columns of the identity matrix and w_1 and v_1 are the right and left eigenvectors of Π. If R_1 and R_2 are less than $\frac{N_{max}}{N_c}$, then there exists finite i^* such that for all $i \geq i^*$, the total expected number of constraint violations over i steps will be less than $i\frac{N_{max}}{N_c}$. This ensures that the soft constraints on Ψ are satisfied provided $i^* \leq N_c$.

The algorithm involves off-line and online stages. In the off-line stage, the nested sets defined above are computed subject to bounds p_j on constraint violation probability and p_{ij} on transition probability maximized. In the online stage, the controller has two aims depending on the current state. The cost (2.81) is minimized whenever the current state, x_k is in the 'safe region' (i.e. the projection of S_1 onto the x-subspace). If not, the state is returned as quickly as possible to the 'safe region' by driving the expected value of the next state x_{k+1} as far inside the 'safe region' as possible.

2.5 Conclusion

Robust model predictive control do not consider distribution of stochastic model uncertainty. However, this becomes necessary when soft probabilistic constraints are present, and the capability for handling such constraints becomes more important when unknown disturbances are large. It avoids the trade-off between computation and optimality of robust MPC. This is achieved by replacing the requirement in robust MPC that constraints are satisfies for all realizations of uncertainty with a guarantee that constraints are satisfied with specified probabilities instead.

Problems which consider only additive disturbances and probabilistic constraints were considered in [10], [40], and [19]. Each of these approaches proposed a receding horizon control law, but none considered recursive feasibility or stability

of the control strategy in closed loop operation. The same objection applies to works in [41] and [42]. Therefore the work in this thesis aims to solve these issues. Furthermore, the works in [10] and [19] considered only normally distributed disturbances and did not guarantee closed loop feasibility and the work in this thesis does not place any restriction on the uncertainty distribution except that it is finitely distributed and ensures feasibility recursively.

Chapter 3

Tube Linear Stochastic Model Predictive Control

[1]This chapter considers constrained control of linear systems with additive and multiplicative stochastic uncertainty and linear input/state constraints. Both hard and soft constraints are considered, and bounds are imposed on the probability of soft constraint violation. Assuming the plant parameter to be finitely supported, a method of constraint handling is proposed in which a sequence of tubes, corresponding to a sequence of confidence levels on the predicted future plant state, is constructed online around nominal state trajectories. A set of linear constraints is derived by imposing bounds on the probability of constraint violations at each point on an infinite predicting horizon through constraints on one-step-ahead predictions. A guarantee of the recursive feasibility of the online optimization ensures that the closed loop system trajectories satisfy both the hard and probabilistic soft constraints. The approach is illustrated by a numerical example.

[1]The work in this Chapter has been published in [43].

3.1 Introduction

When constraints are included in a Stochastic Model Predictive Control algorithm, the difficulty caused by stochastic parameters manifests itself in the online optimization. In this chapter, this problem is overcome through the introduction of layered tubes centered on a nominal model trajectory. These tubes are adjusted online in order to derive a systematic and non-conservative MPC law for linear systems with bounded additive and multiplicative uncertainty subject to hard and soft constraints. The soft constraints are assumed to be constraints which can be violated with an average frequency less than a predefined limit [11, 19, 40]. More importantly, the issue of feasibility guarantees [12–14, 44] where the closed loop system is guaranteed to satisfy constraints on the predicted trajectories is addressed in this chapter. The use of layered tubes centred around a nominal trajectory enables soft constraint satisfaction through the imposition of constraints on the probabilities of transition of the predicted state between the layered tubes and constraints on the probability of one-step-ahead constraint violations within each tube. This approach was employed in [25, 30], for the case of linear systems subject to multiplicative uncertainty, or subject to and additive disturbance which accounts for the linearization error of nonlinear dynamics about a seed trajectory [36]. The idea of tube MPC has been used subsequently in robust MPC for systems with additive disturbances [45, 46], however these approaches use fixed sets of states that are computed offline to define the tube, whereas the work here employs tubes that are optimized online, thus ensuring a greater degree of flexibility in predictions. The results of this algorithm are illustrated by a numerical example.

3.2 Preliminaries

Notation: For clarity, throughout this chapter as well as the rest of the thesis, superscripts j denote vertices of the uncertainty class, superscripts s will denote vertices associated with polytopic confidence regions, superscripts l, m will identify particular tube layers, subscripts r will be used to identify the vertices of the polytopes that define the tubes, subscripts k will denote instants of time whereas subscripts i will identify prediction instants.

3.2.1 Problem Formulation

Consider the discrete-time model and uncertainty description of the form:

$$x_{k+1} = \hat{A}_k x_k + \hat{B}_k u_k + \hat{d}_k \tag{3.1}$$

$$[\hat{A}_k \ \hat{B}_k \ \hat{d}_k] = [\hat{A}^0 \ \hat{B}^0 \ \hat{d}^0] + \sum_{j=1}^{\rho} [\hat{A}^{(j)} \ \hat{B}^{(j)} \ \hat{d}^{(j)}] q_{jk} \tag{3.2}$$

where $x \in \mathbb{R}^n$,$u \in \mathbb{R}^m$,$\hat{d} \in \mathbb{R}^n$ denote the state, input and additive disturbance vectors, and q_{jk} denotes a random variable with a finitely supported distribution that is identical and temporally independent for all k. Let $\mathbf{q}_k = [q_{1k}, \ldots, q_{\rho k}]^T$, then, with an appropriate choice of state variables, it can be assumed without loss of generality that the mean and covariance of $\mathbf{q}_k$ are given by

$$\mathbb{E}(\mathbf{q}_k) = 0, \quad \mathbb{E}(\mathbf{q}_k \mathbf{q}_k^T) = I. \tag{3.3}$$

Use will be made of the dual mode prediction paradigm, described in the previous chapter and in [3], according to which the first N predicted control moves (Mode 1) are free whereas the remainder (Mode 2) are dictated by a pre-determined state feedback. In addition, use will also be made of the closed loop paradigm (also described in Chapter 2 and in [28]), and thus the predicted control moves will be

given by:

$$u_{k+i|k} = \hat{K}x_{k+i|k} + c_{i|k} \quad i = 0, 1, \ldots, N-1 \quad Mode\ 1 \tag{3.4}$$
$$c_{i|k} = 0, \quad i = N, N+1, \ldots \quad Mode\ 2$$

where $c_{i|k}$, $i = 0, \ldots, N-1$ are free optimization variables.

Then, (3.4) combined with the transformation $z = Vx$ (the definition of matrix V is discussed below), allows the reformulation of (3.1):

$$z_{k+i+1} = \Phi_{k+i} z_{k+i|k} + B_{k+i} c_{i|k} + d_{k+i} \tag{3.5}$$

for which, after some rearrangement of (3.2) we have

$$[\Phi_{k+i}\ B_{k+i}\ d_{k+i}] = [\Phi^0\ B^0\ 0] + \sum_{j=1}^{\rho} [\Phi^{(j)}\ B^{(j)}\ d^{(j)}] q_{jk} \tag{3.6}$$

where Φ^0,B^0 and $\Phi^{(j)}$,$B^{(j)}$,$d^{(j)}$ are defined by

$$\Phi = V(\hat{A} + \hat{B}\hat{K})W, \quad W = V^{-1} \tag{3.7}$$
$$B = V\hat{B} \quad d = V\hat{d}$$

The performance objective defined below is the expected value of an infinite horizon quadratic cost. In Mode 1, the choice of $\hat{K}$ does not affect performance due to perturbations $c_{i|k}$. However, since the perturbations are zero in Mode 2, $\hat{K}$ should be computed such that the system (3.1) is mean square stable. If the system is mean square stable under the Mode 2 control law, then $\mathbb{E}(x_{k+i}x_{k+i}^T) \to 0$ and $x_{k+i} \to 0$ as $k \to \infty$ almost surely, irrespective of the initial condition x_0. Mean square stability is ensured by the following condition [24]:

$$P - \mathbb{E}((\hat{A} + \hat{B}\hat{K})^T P(\hat{A} + \hat{B}\hat{K})) \geq Q + \hat{K}^T R\hat{K}, \quad P > 0. \tag{3.8}$$

It can be shown that if the mean square stability condition is satisfied for a given P then the cost function J_k under the Mode 2 control law is bounded by

$$J_k = \mathbb{E}_k \left(\sum_{i=0}^{\infty} x_{k+i}^T (Q + \hat{K}^T R \hat{K}) x_{k+i} \right) \leq x_k^T P x_k. \tag{3.9}$$

Substituting (3.2) into (3.8) and expanding the equation yields

$$\begin{aligned} P - (\hat{A}^0 + \hat{B}^0 \hat{K})^T P (\hat{A}^0 + \hat{B}^0 \hat{K})) - \sigma_i^2 \sum_{j=1}^{\rho} (\hat{A}^{(j)} + \hat{B}^{(j)} \hat{K})^T P (\hat{A}^{(j)} + \hat{B}^{(j)} \hat{K}) \\ \geq Q + \hat{K}^T R \hat{K} \end{aligned} \tag{3.10}$$

where σ_j^2 is $\mathbb{E}(\mathbf{q}_k^T \mathbf{q}_k) = \text{diag}(\sigma_1^2, \ldots, \sigma_\rho^2)$ and as stated in (3.3) it is assumed that $\mathbb{E}(\mathbf{q}_k^T \mathbf{q}_k) = I$. Pre and post multiplying by $S = P^{-1}$ gives

$$\begin{aligned} S - (S\hat{A}^0 S + \hat{B}^0 \hat{K} S)^T P (\hat{A}^0 S + \hat{B}^0 \hat{K}) S) \\ - \sum_{j=1}^{\rho} (\hat{A}^{(j)} S + \hat{B}^{(j)} \hat{K} S)^T P (\hat{A}^{(j)} S + \hat{B}^{(j)} \hat{K} S) \geq SQS + S\hat{K}^T R \hat{K} S. \end{aligned} \tag{3.11}$$

Using Schur complements, and substituting $Y = \hat{K}S$ the inequality (3.11) can be rewritten as an LMI in S and Y

$$\begin{bmatrix} S & D^{0T} & D^{(1)T} & \ldots & D^{(\rho)T} & S & Y^T \\ D^0 & S & & & & & \\ D^{(1)} & & S & & & & \\ \vdots & & & \ddots & & & \\ D^{(\rho)} & & & & S & & \\ S & & & & & Q^{-1} & \\ Y & & & & & & R^{-1} \end{bmatrix} > 0 \tag{3.12}$$

where $D^0 = \hat{A}^0 S + \hat{B}^0 \hat{K} S$ and $D^{(j)} = \hat{A}^{(j)} S + \hat{B}^{(j)} \hat{K} S, j = 1, \ldots, \rho$. Therefore

a mean square stabilizing feedback gain $\hat{K}$ can be computed by minimizing the upper bound of the cost function in Mode 2 $x_k^T P x_k$ (or equivalently maximizing its inverse) subject to the mean square stability condition.

$$\max_{S,Y} \quad tr(S) \quad s.t.(3.12) \tag{3.13}$$

Although the computation of the state feedback law $\hat{K}$ ensures that that $u = \hat{K}x$ is mean-square stabilizing in the absence of constraints, this does not guarantee the feasibility of the invariance condition over the entire uncertainty class of (3.6). To ensure the invariance condition is satisfied, the feedback $\hat{K}$ can be de-tuned (by changing R) and/or the parameter V can be adjusted. The matrix V can be chosen for convenience to be the inverse of the eigenvector matrix of $\hat{A}^0 + \hat{B}^0\hat{K}$ so that Φ^0 is the eigenvalue matrix, which is diagonal and (because $\hat{K}$ is mean square stabilizing) has elements within the unit circle centred at the origin of the complex plane. This ensures that the invariance condition is satisfied at the centre of the uncertainty class [25], and hence facilitates the definition of robustly invariant polytopic sets.

In this setting the control law of (3.4) can be rewritten as

$$u_{k+i|k} = K z_{k+i|k} + c_{i|k} \quad K = \hat{K}V^{-1}. \tag{3.14}$$

The system of (3.1) is assumed to be subjected to hard and soft constraints in x and u which, for the transformed model of (3.5) and (3.14) are of the form:

$$\psi_k^H = F_H z_k + G_H c_k \leq h_H \tag{3.15}$$

$$\psi_k^S = F_s z_k + G_s c_k \leq h_S. \tag{3.16}$$

Constraints (3.15) are hard (inviolable), whereas (3.16) are soft (may be violated at any given k), but the average rate of violation of (3.16) over a fixed horizon N_c

must not exceed a specified bound $\frac{N_{max}}{N_c}$:

$$\frac{1}{N_c}\left\{\sum_{i=1}^{N_c} Pr\{F_s z_{k+i} + G_s c_{k+i} > h_S\}\right\} \leq \frac{N_{max}}{N_c}. \tag{3.17}$$

Given any distribution for q_k, it is possible to define polytopic confidence regions, $Q(p)$ in q-space, with vertices $q^{(s)}(p), s = 1, \ldots, v$, with the property:

$$Pr\{q \in Q(p)\} \geq p. \tag{3.18}$$

Lemma 1. Let $q_j^{(s)}(p), j = 1, \ldots, \rho$ denote the elements of $q^{(s)}(p)$ and let

$$[\Phi(q^{(s)}(p))\ B(q^{(s)}(p))\ d(q^{(s)}(p))] = [\Phi^0\ B^0\ 0] + \sum_{j=1}^{\rho}[\Phi^{(j)}\ B^{(j)}\ d^{(j)}]q_j^{(s)}(p) \tag{3.19}$$

Then the following statements are true

$$\begin{aligned} Pr\left\{\Phi \in \left(\Phi^0 + L[\Phi(q^{(1)}(p))\ \ldots\ \Phi(q^{(v)}(p))]\right)\right\} \geq p \\ Pr\left\{B \in \left(B^0 + L[B(q^{(1)}(p))\ \ldots\ B(q^{(v)}(p))]\right)\right\} \geq p \\ Pr\left\{d \in \left(d^0 + L[d(q^{(1)}(p))\ \ldots\ d(q^{(v)}(p))]\right)\right\} \geq p \end{aligned} \tag{3.20}$$

where $L[.]$ denotes the linear span.

Proof. This result follows directly from (3.18). □

This result can be used to express sufficient conditions for satisfaction of probabilistic constraints (which are required to hold with a given probability) in the form of deterministic linear constraints defined on the basis of the vertices $q^{(s)}, s-1, \ldots, v$, of Q.

Consider for example a triangular distribution supported on [-a,a] shown in Figure 3.1. Given a probability of p, the confidence region is defined by[-b,b]. Then

a polytope in q-space can be taken to be square with four vertices as shown in Figure 3.2 to ensure that (3.18) is satisfied.

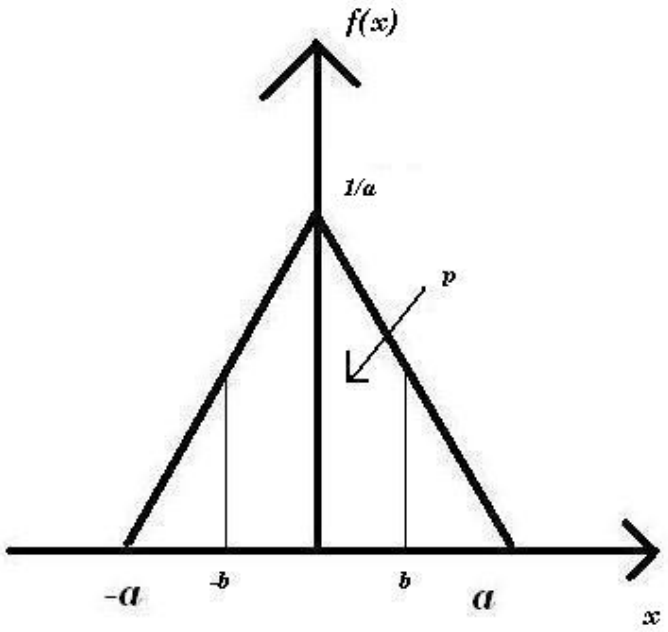

FIGURE 3.1: A triangular distribution which is finitely supported on [-a,a]. For a given probability p the confidence region lies in [-b,b].

3.2.2 Nested tubes

To handle constraints on the distributions of predicted states and inputs in a computationally efficient manner, we construct a sequence of μ tubes comprising polytopes $Z_{i|k}^{(l)}$ which are centred on a nominal model trajectory $z_{k+i|k}^{c}$, in Mode 1, and polytopes $Z_{T}^{(l)}$ centered around the origin in Mode 2:

$$Z_{i|k}^{(l)} = \{z : |z - z_{k+i|k}^{c}| \leq \overline{z}_{i|k}^{(l)}\}, \quad l = 1, \ldots, \mu \quad in\ Mode\ 1 \tag{3.21a}$$

$$Z_{T}^{(l)} = \{z : |z| \leq \overline{z}_{T}^{(l)}\}, \quad l = 1, \ldots, \mu \quad in\ Mode\ 2. \tag{3.21b}$$

As a result of using a finite number of probabilistic tubes and imposing a fixed geometry on their cross-section, the approach is subject to a degree of conservativeness. Therefore, the use of multiple nested tubes reduces the conservativeness.

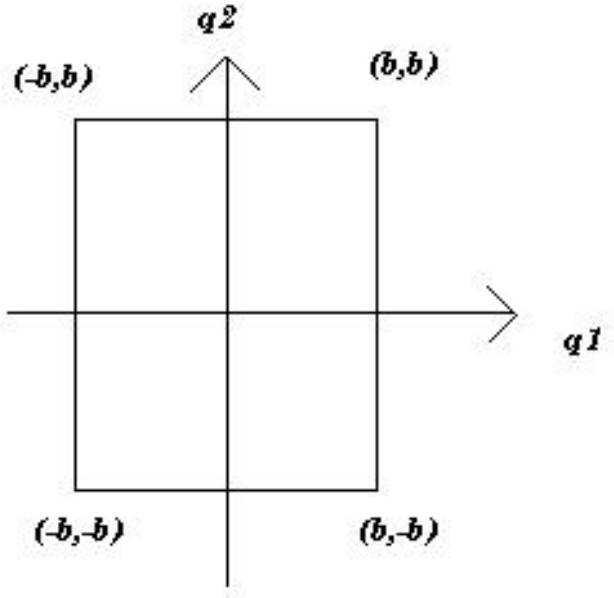

FIGURE 3.2: From the triangular distribution, the confidence polytopic region has vertices defined by b.

Here the nominal trajectory $z^c_{k+i|k}$ is obtained from a recursion of the nominal dynamics of (3.5) (namely for $\Phi_{k+i} = \Phi^0$,$B_{k+i} = B^0$,$d_{k+i} = 0$) as:

$$z^c_{k+i|k} = [\Phi^0]^i z_{k|k} + \sum_{j=1}^{N} [\Phi^0]^{i-j} B^0(c_{j|k}) = [\Phi^0]^i z_{k|k} + M^0_i \mathbf{c} \tag{3.22}$$

for $i = 1, \ldots, N$, where

$$M^0_i = \left[[\Phi^0]^{i-1}\ B^0\ \ldots\ B^0\ 0 \ldots\ 0 \right], \quad \mathbf{c}_k = [c_{0|k}\ \ldots\ c_{N-1|k}]^T. \tag{3.23}$$

To ensure that the tubes are nested in the sense that

$$Z^{\mu}_{i|k} \supseteq Z^{\mu-1}_{i|k} \supseteq \ldots \supseteq Z^1_{i|k}$$
$$Z^{\mu}_{T} \supseteq Z^{\mu-1}_{T} \supseteq \ldots \supseteq Z^1_{T}$$

the following constraints are imposed for $i = 1, \ldots, N$:

$$\overline{z}^{\mu}_{i|k} \geq \overline{z}^{\mu-1}_{i|k} \geq \ldots \geq \overline{z}^{1}_{i|k} > 0 \tag{3.25a}$$

$$\overline{z}^{\mu}_{T} \geq \overline{z}^{\mu-1}_{T} \geq \ldots \geq \overline{z}^{1}_{T} > 0. \tag{3.25b}$$

The state at time k is assumed to be known, so we set $Z^{(l)}_{0|k} = z_k$, $l = 1, \ldots, \mu$. In addition the terminal constraint

$$Z^{(l)}_{k+N|k} \subseteq Z^{(l)}_{T} \quad l = 1, \ldots, \mu \tag{3.26}$$

is imposed. Note that the above polytopes are orthotopes in z-space and hence have vertices, $D_r\overline{z}^{(l)}_{i|k}$,$D_r\overline{z}^{(l)}_{t}$, respectively, where $\{D_r,\ r = 1, \ldots, 2^n\}$ are the diagonal matrices whose elements are ± 1. A hypothetical sequence of polytopes is shown in Figure 3.3.

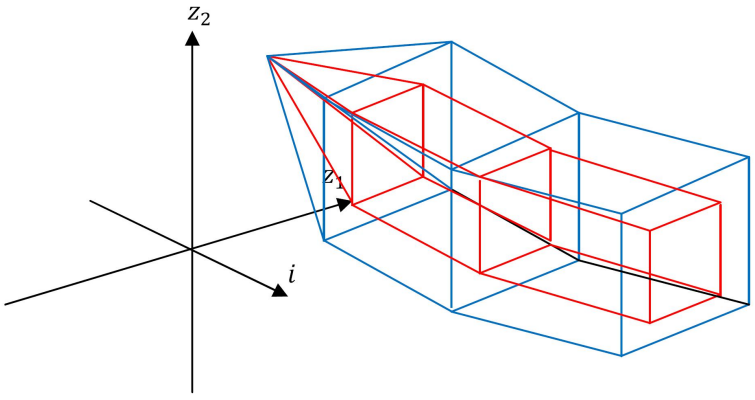

FIGURE 3.3: Evolution of tubes along the prediction horizon.Two nested tubes $\mu = 2$ are shown centered around the nominal trajectory.

3.3 Constraint Handling

This section considers how to impose constraints on predicted inputs and states, and shows that satisfaction of both the hard constraint (3.15), and the probabilistic bound (3.17) on violations of the soft constraint (3.16), can be ensured through

constraints on one-step-ahead predictions. The strategy is to constrain the probability that, for each i, the i-step-ahead predicted state lies in any particular set $Z_{i|k}^{(l)}$(or $Z_t^{(l)}$ for $i > N$) by constraining the probabilities of transition from $Z_{h|k}^{(m)}$ to $Z_{h+1|k}^{(l)}$, for $h = 0, 1, \ldots, N-1$ and from $Z_t^{(m)}$ to $Z_t^{(l)}$, to be no less than p_{lm} for $l, m = 1, \ldots, \mu$. Further constraints are imposed in order to ensure that the probability of violating system constraints at prediction time $i+1$ does not exceed p_l for $l = 1, \ldots, \mu$ whenever the i-step-ahead predicted state lies within $Z_{i|k}^{(l)}$(or $Z_t^{(l)}$ for $i > N$).

The approach is based on the following condition (note that the notation $Pr(X|Y)$ denotes the *maximum* probability of X given Y):

(1) One-step-ahead transitional probability constraints:

$$Pr\{z_{k+i+1|k} \in Z_{i+1|k}^{(m)} | z_{k+i|k} \in Z_{i|k}^{(l)}\} \geq p_{ml} \quad in\ Mode\ 1 \tag{3.27a}$$

$$Pr\{z_{k+i+1|k} \in Z_T^{(m)} | z_{k+i|k} \in Z_T^{(l)}\} \geq p_{ml} \quad in\ Mode\ 2. \tag{3.27b}$$

(2) Universality constraint on outer polytope:

$$Pr\{z_{k+i+1|k} \in Z_{i+1|k}^{(\mu)} | z_{k+i|k} \in Z_{i|k}^{(l)}\} = 1 \quad in\ Mode\ 1 \tag{3.28a}$$

$$Pr\{z_{k+i+1|k} \in Z_T^{(\mu)} | z_{k+i|k} \in Z_T^{(l)}\} = 1 \quad in\ Mode\ 2. \tag{3.28b}$$

(3) One-step-ahead constraint violation probability:

$$Pr\{\psi_{k+i+1|k}^S > h_S | z_{k+i|k} \in Z_{i|k}^{(l)}\} \leq p_l \quad in\ Mode\ 1 \tag{3.29a}$$

$$Pr\{\psi_{k+i+1|k}^S > h_S | z_{k+i|k} \in Z_T^{(l)}\} \leq p_l \quad in\ Mode\ 2. \tag{3.29b}$$

(4) Feasibility of outer polytope with respect to hard constraint:

$$Pr\{\psi^H_{k+i|k} > h_H | z_{k+i|k} \in Z^{(\mu)}_{i|k}\} = 1 \quad in\ Mode\ 1 \tag{3.30a}$$

$$Pr\{\psi^H_{k+i|k} > h_H | z_{k+i|k} \in Z^{(\mu)}_{T}\} = 1 \quad in\ Mode\ 2. \tag{3.30b}$$

Thus (1) constraints the probability of transition between tubes, while (3) bounds the probability of one-step-ahead constraint violation given that ith predicted state lies in a particular tube. Furthermore (2) ensures that the outer tube is universal in the sense that it contains the predicted state at each time-step, and condition (4) ensures that this outer tube (and hence also the inner tubes) is feasible with respect to the hard constraint.

The probabilities p_{lm}, p_l for $l, m = 1, \ldots, \mu$ appearing in condition 1-4 are design parameters that are free to be chosen by the designer of the MPC strategy. Conditions on these probabilities that ensure satisfaction of the probabilistic constraint (3.17) are given in Assumption 2 below. In order to facilitate invoking conditions (1)-(4) via a set of linear constraints, we also make the following assumptions on the values of p_{lm} and p_l.

Assumption 1. The probabilities p_{lm} and p_l for $l, m = 1, \ldots, \mu$ are chosen so that

$$p_{lm+1} \leq p_{lm} \quad l, m = 1, \ldots, \mu - 1 \tag{3.31a}$$

$$p_{\mu l} = 1 \quad l = 1, \ldots, \mu \tag{3.31b}$$

$$p_{l+1} \geq p_l \quad l = 1, \ldots, \mu - 1. \tag{3.31c}$$

Conditions (3.31a) and (3.31b) are consistent with the nested property implied by (3.25a) and (3.25b) and the universality property implied by (3.28a) and (3.28b), and will therefore be satisfied by any chosen set of transition probabilities p_{lm}.

Similarly, condition (3.31c) corresponds to the natural requirement that the probability of one-step-ahead violation of soft constraints should be greater at points that are further from the center of the tube.

Clearly the constraints of (3.28a) and (3.28b) and (3.30a) and (3.30b) ensure that predicted trajectories satisfy the hard constraints (3.15). The following result provides a means of ensuring satisfaction of probabilistic bounds on the predicted number of violations of the soft constraint (3.16).

Lemma 2. Under constraints (3.26)-(3.29) and (3.31), the probability of violation of the soft constraint (3.16) at the i^{th}-step-ahead is bounded from above as:

$$Pr\{\psi^S_{k+i+1|k} > h_S\} \leq [p_1 \ \dots \ p_\mu]^T (T^{-1}\Pi)^i e_1 \tag{3.32}$$

where Π is a matrix of transition probabilities:

$$\Pi = \begin{bmatrix} p_{11} & \cdots & p_{1\mu} \\ \vdots & \ddots & \vdots \\ p_{\mu 1} & \cdots & p_{\mu\mu} \end{bmatrix},$$

and T is a lower-triangular matrix:

$$T = \begin{bmatrix} 1 & 0 & \dots & 0 \\ 1 & 1 & & 0 \\ \vdots & \vdots & \ddots & \\ 1 & 1 & \dots & 1 \end{bmatrix}, \quad T^{-1} = \begin{bmatrix} 1 & 0 & \dots & 0 \\ -1 & 1 & & 0 \\ \vdots & \vdots & \ddots & \\ 0 & \dots & -1 & 1 \end{bmatrix}$$

and where $e_1 = [1 \ 0 \ \dots \ 0]^T$.

Proof. On account of the terminal constraint (3.26) and the fact that the probabilities p_{lm} and p_l are the same for both Mode 1 and Mode 2, there is no need to distinguish between the two modes, so the proof applies to a general prediction

time i, (which may be greater than N). If $Z^{(l)}_{i|k}$ for $l = 1, \ldots, \mu$ were disjoint, then

$$\sum_{l=1}^{\mu} p_l Pr\{z_{k+i|k} \in Z^{(l)}_{k+i|k}\} \tag{3.33}$$

would give an upper bound for the probability of violation of (3.16) at the ith step. However, since these sets are nested, a tight bound is given by:

$$\begin{aligned} Pr\{\psi^S_{k+i+1|k} > h_S\} \leq & p_1\{z_{k+i|k} \in Z^{(1)}_{k+i|k}\} + \\ & \sum_{l=2}^{\mu} p_l[Pr\{z_{k+i|k} \in Z^{(l)}_{k+i|k}\} - Pr\{z_{k+i|k} \in Z^{(l-1)}_{k+i|k}\}] \\ & = [p_1 \ \ldots \ p_\mu] T^{-1} v_{k+i|k} \end{aligned} \tag{3.34}$$

where $v_{k+i|k}$ is defined by:

$$v_{k+i|k} = \left[Pr\{z_{k+i|k} \in Z^{(1)}_{k+i|k}\}, \ldots, Pr\{z_{k+i|k} \in Z^{(\mu)}_{k+i|k}\} \right]^T. \tag{3.35}$$

By the same argument it follows that $v_{k+i|k} \geq \Pi T^{-1} v_{k+i-1|k}$, and, since (3.31a) and (3.31b) imply that ΠT^{-1} has non-negative elements, with $[0 \ \ldots \ 0 \ 1]$ in the last row, it can be shown by induction that:

1. $v_{k+i|k} \geq (\Pi T^{-1})^i v_k$ where $v_k = [1 \ \ldots \ 1]^T$,
2. all elements of $(\Pi T^{-1})^i v_k$ are non-negative and the last is equal to 1.

Furthermore from (3.31c), the first $\mu - 1$ elements of $[p_1 \ \ldots \ p_\mu] T^{-1}$ are non-positive, and the last it p_μ. Combining this observation with 1. and 2., it follows that

$$Pr\{\psi^S_{k+i+1|k} > h_S\} \leq [p_1 \ \ldots \ p_\mu] T^{-1} (\Pi T^{-1})^i v_k$$

and the proof is completed by noting $T^{-1}(\Pi T^{-1})^i v_k = (T^{-1}\Pi)^i T^{-1} v_k = (T^{-1}\Pi)^i e_1$ and $T^{-1}v_k = e_1$ follows from the fact that $z_{k|k} = z^c_{k|k} \in Z^{(1)}_{k|k} \in Z^{(2)}_{k|k} \in \dots Z^{(\mu)}_{k|k}$ so that v_k is the vector of 1's. □

The transition probability matrix with elements p_{ml} defines the transition probability of the current state, given that it lies within set $Z^{(m)}_T$, to the next state, which lies within the set $Z^{(l)}_T$, as illustrated in Figure 3.4 for Mode 2.

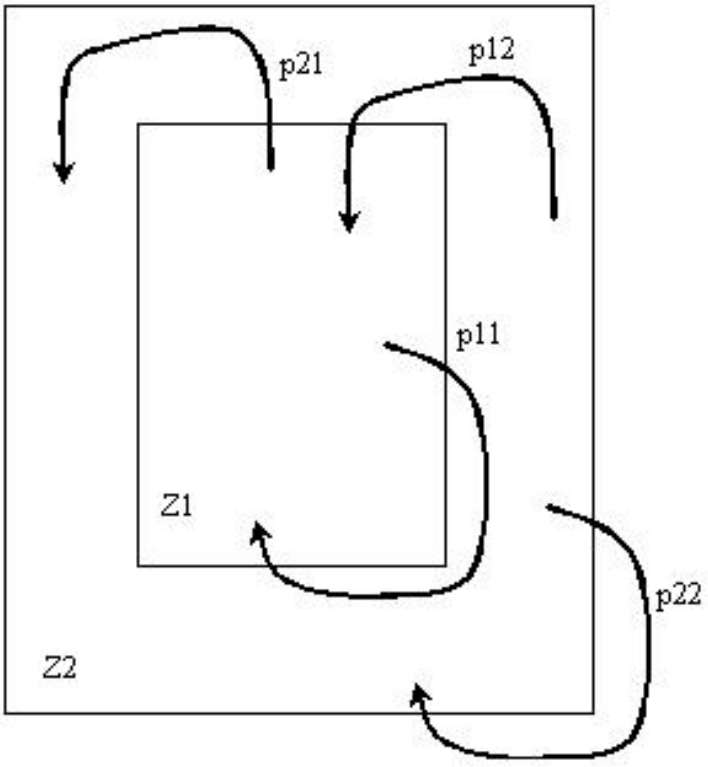

FIGURE 3.4: For the case of $\mu = 2$ tubes with transition probabilities p_{lm} in Mode 2. Note that probabilities p_{22} and p_{21} are equal to 1.

The probabilities p_{lm} and p_l appearing in conditions 1-4 are design parameters that are free to be chosen by the designer of the MPC strategy. Conditions on these probabilities that ensure satisfaction of the probabilistic constraint (3.17) are given below.

Assumption 2. The probabilities p_{lm},p_l for $l, m = 1, \ldots, \mu$ are chosen so that

$$\frac{1}{N_c} \sum_{i=0}^{N_c-1} [p_1 \ \ldots \ p_\mu](T^{-1}\Pi)^i e_l \leq \frac{N_{max}}{N_c} \quad l = 1, \ldots, \mu. \tag{3.36}$$

A direct consequence of Lemma 2 is that the probabilistic bound (3.17) on soft constraint violation is necessarily satisfied under (3.26)-(3.29) and (3.31) if p_{lm} and p_l are chosen according to the Assumption (1) and Assumption (2).

We next show that, on account of Lemma 1, conditions (3.27)-(3.30) can be ensured by invoking the following set of inequalities involving the vertices of the polytopes defining the tubes and the vertices of the polytopic confidence region $Q(p)$.

$$\Big|\Phi(q^{(s)}(p_{lm}))[z^c_{k+i|k} + D_r \overline{z}^{(l)}_{k+i|k}] + B(q^{(s)}(p_{lm}))c_{i|k} + d(q^{(s)}(p_{lm})) - z^c_{k+i+1|k}\Big| \leq \overline{z}^{(m)}_{k+i+1|k} \tag{3.37a}$$

$$\Big|\Phi(q^{(s)}(p_{lm}))D_r \overline{z}^{(l)}_T + d(q^{(s)}(p_{lm}))\Big| \leq \overline{z}^{(m)}_T \tag{3.37b}$$

$$\Big|\Phi(q^{(s)}(1))[z^c_{k+i|k} + D_r \overline{z}^{(\mu)}_{k+i|k}] + B(q^{(s)}(1))c_{i|k} + d(q^{(s)}(1)) - z^c_{k+i+1|k}\Big| \leq \overline{z}^{(\mu)}_{k+i+1|k} \tag{3.38a}$$

$$\Big|\Phi(q^{(s)}(1))D_r \overline{z}^{(\mu)}_T + d(q^{(s)}(1))\Big| \leq \overline{z}^{(\mu)}_T \tag{3.38b}$$

$$F_S \left\{ \Phi(q^{(s)}(1-p_l))[z^c_{k+i|k} + D_r \overline{z}^{(l)}_{k+i|k}] + B(q^{(s)}(1-p_l))c_{i|k} + d(q^{(s)}(1-p_l)) \right\} + G_S c_{i+1|k} \leq h_S \tag{3.39a}$$

$$F_S \left\{ \Phi(q^{(s)}(1-p_l)) D_r \overline{z}^{(l)}_T + d(q^{(s)}(1-p_l)) \right\} \leq h_S \tag{3.39b}$$

$$F_H[z^c_{k+i|k} + D_r \overline{z}^{(\mu)}_{k+i|k}] + G_H c_{i|k} \leq h_H \tag{3.40a}$$

$$F_H D_r \overline{z}^{(\mu)}_T \leq h_H \tag{3.40b}$$

$$\left| z^c_{k+N|k} + D_r \overline{z}^{(l)}_{k+N|k} \right| \leq \overline{z}^{(l)}_T \tag{3.41}$$

Theorem 1. Conditions (3.37)-(3.40) and (3.41) are sufficient for (3.27)-(3.30) and (3.26) respectively.

Proof. Invoking (3.37a) for $s = 1, \ldots, v$ gives

$$-\overline{z}^{(l)}_{k+i+1|k} \leq \Phi(q)[z^c_{k+i|k} + D_r \overline{z}^{(m)}_{k+i|k}] + B(q)c_{i|k} + d(q) - z^c_{k+i+1|k} \leq \overline{z}^{(l)}_{k+i+1|k}$$

for all $q \in Q(p_{lm})$. From the model (3.5) and the definition (3.21a) of $Z^{(l)}_{i|k}$ it therefore follows that invoking (3.37a) for $r = 1, \ldots, 2^n$ gives $z_{k+i+1|k} \in Z^{(l)}_{i+1|k}$ with probability p_{lm} for all $z_{k+i|k} \in Z^{(m)}_{i|k}$, and hence (3.37a) implies (3.27a).

By the same argument, (3.38a) imposes a probability of transition from $Z^{(\mu)}_{k+i|k}$ to $Z^{(\mu)}_{k+i+1|k}$ of $p_{\mu\mu} = 1$. Enforcing the transition between outer polytopes to hold with probability 1 ensures (by linearity) that the transition probability from $Z^{(l)}_{k+i|k}$ to

$Z^{(\mu)}_{k+i+1|k}$ is also $p_{\mu l} = 1$, for all $l = 1, \ldots, \mu$, which is in accordance with (3.31b), and therefore (3.38a) implies (3.28a).

Similarly, condition (3.39a) implies (3.29a) by ensuring that the soft constraint (3.16) holds with probability $1 - p_l$ at prediction time-step $i+1$ whenever $z_{k+i|k} \in Z^{(l)}_{i|k}$. Furthermore, (3.40a) ensures that the hard constraints (3.15) are satisfied for all $z \in Z^{(\mu)}_{k+i|k}$, and by linearity therefore, (3.15) also holds for all $z \in Z^{(l)}_{k+i|k}$ $l = 1, \ldots, \mu$.

Conditions (3.37b)-(3.40b) are analogous to (3.37a)-(3.40a), but apply to Mode 2 (rather than Mode 1), and thus can be proved in a similar manner. Finally, note that (3.42) implies that the vertices of $Z^{(l)}_{k+N|k}$ lie in $Z^{(l)}_T$ and thus ensures that the terminal condition (3.26) is satisfied. □

The receding horizon optimization of predicted input and state trajectories is performed over the free variables $\mathbf{c}_k$, implying that the bounds $\overline{z}^{(l)}_{k+i|k}$ can also be treated as degrees of freedom which can be used in the online optimization. However there is little advantage in retaining the terminal set parameters $\{\overline{z}^{(l)}_T, l = 1, \ldots, \mu\}$ as variables in the online optimization. Instead we propose to determine these bounds off-line by solving the following maximization:

$$\max_{\overline{z}^{(l)}_T, l=1\ldots,\mu} \prod_{l=1}^{\mu} \mathrm{prod}(\overline{z}^{(l)}_T) \quad \text{s.t. (3.37b), (3.38b), (3.39b), (3.40b)} \tag{3.42}$$

where $\mathrm{prod}(\overline{z})$ denotes the product of the elements of $\overline{z}$. The rationale behind (3.42) is that it is a convex problem, and that it maximizes the products of the volumes of $Z^{(l)}_T$, $l = 1, \ldots, \mu$ thereby making the terminal constraints (3.26) less stringent and thus enlarging the region of attraction of the proposed method.

3.4 The Receding Horizon Algorithm

3.4.1 Stage cost definition

The predictions governed by (3.1)-(3.4) can be written in an augmented autonomous state-space form [31, 32] where the model is given by

$$\chi_{k+i+1|k} = \hat{\Psi}_{k+i}\chi_{k+i|k} + \tilde{d}_{k+i} \tag{3.43a}$$

$$\chi_{k|k} = \begin{bmatrix} x_k \\ f_k \end{bmatrix}, \quad f_k = \begin{bmatrix} c_{0|k} \\ \vdots \\ c_{N-1|k} \end{bmatrix} \tag{3.43b}$$

and its uncertainty description given by

$$[\hat{\Psi}_k \ \tilde{d}_k] = [\hat{\Psi}^{(0)} \ 0] + \sum_{j=1}^{\rho} [\Psi^{(j)} \ \tilde{d}^{(j)}] q_{jk} \tag{3.44}$$

where

$$\hat{\Psi}^{(0)} = \begin{bmatrix} \hat{\Phi}^{(0)} & \hat{B}^{(0)}E \\ 0 & M \end{bmatrix}, \quad \Psi^{(j)} = \begin{bmatrix} \hat{\Phi}^{(j)} & \hat{B}^{(j)}E \\ 0 & 0 \end{bmatrix}, \quad \tilde{d}^{(j)} = \begin{bmatrix} \hat{d}^{(j)} \\ 0 \end{bmatrix}, \tag{3.45}$$

$$M = \begin{bmatrix} 0 & I & 0 & \dots & 0 \\ 0 & 0 & I & \dots & 0 \\ \vdots & \vdots & & & \vdots \\ 0 & 0 & 0 & \dots & 0 \end{bmatrix}, \quad E = [I \ 0 \ \dots \ 0], \tag{3.46}$$

where I is the $m \times m$ identity matrix.

Under the assumption that (3.43) is mean square stable, it is shown in [47] that the covariance matrix $E_k(\chi_i \chi_i^T)$ converges to a finite limit as $i \to \infty$ along the

predicted trajectories of (3.43), provided that $\hat{\Psi}_{k+i}$ and $\tilde{d}_{k+i}$ are independent.

Lemma 3. [13]. The sequence generated in (3.43) satisfies $\lim_{i\to\infty} E_k(\chi_i) = 0$ and $\lim_{i\to\infty} E_k(\chi_i\chi_i^T) = \Theta$, where Θ is the solution of the Lyapunov equation

$$\Theta - \hat{\Psi}^{(0)}\Theta[\hat{\Psi}^{(0)}]^T - \sum_{s=1}^{\rho} \hat{\Psi}^{(s)}\Theta[\hat{\Psi}^{(s)}]^T = \sum_{s=1}^{\rho} \tilde{d}^{(s)}[\tilde{d}^{(s)}]^T \tag{3.47}$$

if and only if there exists $P > 0$ satisfying

$$P - \hat{\Psi}^{(0)T}P\hat{\Psi}^{(0)} - \sum_{s=1}^{\rho} \hat{\Psi}^{(s)T}P\hat{\Psi}^{(s)} > 0. \tag{3.48}$$

Proof. Given the linearity of (3.43), the sequence χ_i is the sum of the sequences, ζ and ξ generated by the following two systems

$$\zeta_{i+1} = \hat{\Psi}_{k+i}\zeta_i \quad \zeta_0 = \chi_0 \tag{3.49}$$

$$\xi_{i+1} = \hat{\Psi}_{k+i}\xi_i + \tilde{d}_{k+i}, \quad \xi_0 = 0 \tag{3.50}$$

Condition (3.48) is necessary and sufficient for mean square stability of (3.49) and therefore ensures that $\mathbb{E}_k(\zeta_i\zeta_i^T) \to 0$ and hence $\zeta_i \to 0$ almost surely, as $i \to \infty$. From (3.50) we have $\mathbb{E}_k(\xi_i) = 0$ for all i, and it follows that $\mathbb{E}_k(\chi_i) \to 0$ as $i \to \infty$. Since ξ_i is independent of $\hat{\Psi}_{k+i}$, (3.50) also gives

$$\begin{aligned}
\mathbb{E}_k(\xi_{i+1}\xi_{i+1}^T) &= \mathbb{E}_k\{(\hat{\Psi}_{k+i}\xi_i + \tilde{d}_{k+i})(\hat{\Psi}_{k+i}\xi_i + \tilde{d}_{k+i})^T\} \\
&= \mathbb{E}_k(\hat{\Psi}_{k+i}\xi_i\xi_i^T\hat{\Psi}_{k+i}^T) + \mathbb{E}_k(\tilde{d}_{k+i}\tilde{d}_{k+i}^T) \\
= \hat{\Psi}^{(0)}\mathbb{E}_k(\xi_i\xi_i^T)\hat{\Psi}^{(0)T} &+ \sum_{s=1}^{\rho} \hat{\Psi}_j^{(s)}\mathbb{E}_k(\xi_i\xi_i^T)\hat{\Psi}_j^{(s)T} + \sum_{s=1}^{\rho} \tilde{d}^{(s)}\tilde{d}^{(s)T}
\end{aligned} \tag{3.51}$$

Let $\hat{\Theta}_i = \mathbb{E}_k(\xi_i\xi_i^T) - \Theta$, then from (3.47) and (3.51) we have

$$\hat{\Theta}_{i+1} = \Phi^{(0)}\hat{\Theta}_i\Phi^{(0)T} + \sum_{s=1}^{\rho} \Phi^{(s)}\hat{\Theta}_i\Phi^{(s)T}. \tag{3.52}$$

From the mean square stability condition of (3.48), it follows that $\hat{\Theta} \to 0$, so that $\mathbb{E}_k(\xi_i \xi_i^T) \to \Theta$ as $i \to \infty$. Finally, note that $\mathbb{E}_k(\chi_i \chi_i^T) \to \mathbb{E}_k(\xi_i \xi_i^T)$ since $\zeta_i \to 0$ as $i \to \infty$. □

To develop the overall MPC receding horizon algorithm we need to first define the predicted cost which is to be optimized online. For the case with no additive uncertainty, the existence of P satisfying (3.48) implies that $\mathbb{E}_k(\chi_i \chi_i^T) = 0$ as $i \to \infty$. In this case, the predicted cost is defined by

$$\begin{aligned} J_k &= \sum_{i=0}^{\infty} \mathbb{E}_k(x_{k+i}^T Q x_{k+i} + u_{k+i}^T R u_{k+i}) \\ &= \sum_{i=0}^{\infty} \mathbb{E}_k(\chi_i^T \tilde{Q} \chi_i) \end{aligned} \tag{3.53}$$

where

$$\tilde{Q} = \begin{bmatrix} Q + \hat{K}^T R \hat{K} & \hat{K}^T R E \\ E^T R \hat{K} & E^T R E \end{bmatrix}. \tag{3.54}$$

Such a cost is well-defined and hence is suitable for a predicted performance cost to be minimized online by a receding horizon control law. However, in the case of persistent non-zero additive uncertainty, it follows from Lemma 3 that the stage cost converges to a nonzero limit.

Theorem 2. Under the assumption that $u = \hat{K}x$ is mean square stabilizing, then

$$\lim_{i \to \infty} \mathbb{E}_k(\chi_i^T \tilde{Q} \chi_i) = tr(\Theta \tilde{Q}) \tag{3.55}$$

where $tr(\tilde{Q})$ denotes the trace of matrix $\tilde{Q}$.

This implies that the cost is infinite in the case of persistent non-zero additive uncertainty and therefore to obtain a finite cost, the predicted cost must be modified

to

$$J_k = \sum_{i=0}^{\infty} \mathbb{E}_k(\chi_i^T \tilde{Q} \chi_i - tr(\Theta \tilde{Q})). \tag{3.56}$$

Theorem 3. [13] The cost J_k of (3.56) is a known quadratic function of $\mathbf{c}_k$ which is given as

$$J_k = \begin{bmatrix} Wz_{0|k} \\ \mathbf{c}_k \\ 1 \end{bmatrix}^T P \begin{bmatrix} Wz_{0|k} \\ \mathbf{c}_k \\ 1 \end{bmatrix} \tag{3.57a}$$

$$P = \begin{bmatrix} P_\chi & P_{\chi 1} \\ P_{1\chi} & P_1 \end{bmatrix} \quad P_{\chi 1} = P_{1\chi}^T \tag{3.57b}$$

$$P_\chi - \hat{\Psi}^{(0)T} P_\chi \hat{\Psi}^{(0)} - \sum_{s=1}^{m} \hat{\Psi}^{(s)T} P_\chi \hat{\Psi}^{(s)} = \tilde{Q} \tag{3.57c}$$

$$P_{1\chi} = \sum_{s=1}^{m} \tilde{d}^{(s)T} P_\chi \hat{\Psi}^{(s)} (I - \hat{\Psi}^{(0)})^{-1} \tag{3.57d}$$

$$P_1 = -tr(\Theta P_\chi). \tag{3.57e}$$

Proof. Define $V_i = \chi_i^T P_\chi \chi_i + \chi_i^T P_{\chi 1} + P_{1\chi} \chi_i + P_1$, then from $\chi_{i+1} = \hat{\Psi}_{k+i} \chi_i + \tilde{d}_{k+i}$ we have

$$\begin{aligned} \mathbb{E}_k(V_i) - \mathbb{E}_k(V_{i+1}) &= \mathbb{E}_k(\chi_i^T [P_\chi - \mathbb{E}(\hat{\Psi}_{k+i}^T P_\chi \hat{\Psi}_{k+i})] \chi_i) \\ +2[P_{1\chi}(I - \hat{\Psi}^{(0)}) - \mathbb{E}(\tilde{d}_{k+i}^T P_\chi \hat{\Psi}_{k+i})] \mathbb{E}_k(\chi_i) &- \mathbb{E}(\tilde{d}_{k+i}^T P_\chi \tilde{d}_{k+i}) \end{aligned} \tag{3.58}$$

The first term of the right hand side from (3.57c) can be written as

$$\mathbb{E}_k(\chi_i^T [P_\chi - \mathbb{E}(\hat{\Psi}_{k+i}^T P_\chi \hat{\Psi}_{k+i})] \chi_i) = \mathbb{E}_k(\chi_i^t \tilde{Q} \chi_i). \tag{3.59}$$

By post-multiplying (3.47) by P_χ and extracting the trace gives

$$tr(\Theta P_\chi - \hat{\Psi}^{(0)}\Theta\hat{\Psi}^{(0)T}P_\chi - \sum_{s=1}^{m}\hat{\Psi}^{(s)}\Theta\hat{\Psi}^{(s)T}P_\chi) =$$
$$tr(\Theta[P_\chi - \hat{\Psi}^{(0)}P_\chi\hat{\Psi}^{(0)T} - \sum_{s=1}^{m}\hat{\Psi}^{(s)}P_\chi\hat{\Psi}^{(s)T}]) = \sum_{s=1}^{m} tr(\tilde{d}^{(s)}\tilde{d}^{(s)T}P_\chi) \tag{3.60}$$

and (3.57c) therefore implies

$$tr(\Theta\tilde{Q}) = \sum_{s=1}^{m}\tilde{d}^{(s)T}P_\chi\tilde{d}^{(s)} = \mathbb{E}(\tilde{d}_{k+i}^{T}P_\chi\tilde{d}_{k+i}). \tag{3.61}$$

Substituting (3.59) and (3.61) into (3.58), and using (3.57d) gives

$$\mathbb{E}_k(V_i) - \mathbb{E}_k(V_{i+1}) = \mathbb{E}_k(\chi_i^T\tilde{Q}\chi_i) - tr(\Theta\tilde{Q}), \tag{3.62}$$

and if the equation is summed for all $i \geq 0$ we obtain

$$V_0 - \lim_{i\to\infty}\mathbb{E}_k(V_i) = \sum_{i=0}^{\infty}\mathbb{E}_k(\chi_i^T\tilde{Q}\chi_i - tr(\Theta\tilde{Q})) = J_k. \tag{3.63}$$

The proof is completed by showing that $E_k(V_i) \to 0$ as $i \to \infty$. This follows from the definition of V_i and (3.57e), which give

$$\mathbb{E}_k(V_i) = \mathbb{E}_k(\chi_i^T P_\chi\chi_i) + 2P_{1\chi}\mathbb{E}_k(\chi_i) - tr(\Theta P_\chi) \tag{3.64}$$

and therefore

$$\lim_{i\to\infty}\mathbb{E}_k(V_i) = \lim_{i\to\infty}\mathbb{E}_k(\chi_i^T P_\chi\chi_i) - tr(\Theta P_\chi) \tag{3.65}$$
$$= \lim_{i\to\infty} tr[\mathbb{E}_k(\chi_i\chi_i^T)P_\chi] - tr(\Theta P_\chi) = 0 \tag{3.66}$$

where $\lim_{i\to\infty}\mathbb{E}_k(\chi_i) = 0$ and $\lim_{i\to\infty}\mathbb{E}_k(\chi_i\chi_i^T) = \Theta$. □

3.4.2 Receding horizon algorithm

The exact stage cost defined above is minimized in the following a receding horizon manner.

Algorithm 5. (Tube Stochastic MPC)

1. (OFF-LINE): Determine $\overline{z}_T^{(l)}, l = 1, \ldots, \mu$ by performing maximization in (3.42).

2. (ONLINE): At each time instant $k = 0, 1, \ldots$ perform the optimization:

$$\min_{\overline{z}_{k+i|k}^{(l)}, \mathbf{c}_k} J_k \quad \text{s.t } (3.25a), (3.37a), (3.38a), (3.39a), (3.40a), (3.41) \tag{3.67}$$

3. Implement $u_k = Kz_k + c_{0|k}$ where $\mathbf{c}_k^*$ is optimal for (3.67).

The ability to adjust the size, shape and centres of the polytopes $Z^{(l)}$ introduces into the problem useful degrees of freedom but it also increases computational complexity. Should this be a concern, it is possible to allow only the centres and scaling of the polytopes to be adjusted online by replacing the vector of upper bounds $\overline{z}_{k+i|k}^{(l)}$ with $\overline{z}_{k+i|k}^{(l)}\mathbf{1}$ where $\overline{z}_{k+i|k}^{(l)}$ is now a scalar and $\mathbf{1}$ is a vector of ones.

Theorem 4. If the online optimization (3.67) is feasible at $k = 0$, then (3.67) remains feasible at all times $k = 1, 2, \ldots$ and the closed loop system of (3.1) and (3.2) under the TSLMPC algorithm satisfies the hard constraints (3.15) and the probabilistic bound (3.17) on soft constraints (3.16). Furthermore the closed loop system is stable in the sense that $L_k = x_k^T Q x_k + u_k^T R u_k$ satisfies

$$\lim_{n\to\infty} \frac{1}{n} \sum_{k=0}^{n} \mathbb{E}_0(L_k) \leq tr(\Theta \tilde{Q}). \tag{3.68}$$

Proof. For all $k > 0$, the assumption that (3.67) is feasible at time $k-1$ implies that feasible values for the optimization variables at time k are given by

$$\mathbf{c}_k = \mathbf{c}^*_{k-1}, \quad \overline{z}^{(l)}_{i|k} = \begin{cases} \overline{z}^{(l)}_{i+1|k-1} & i = 1, \ldots, N-1 \\ \overline{z}^{(l)}_t & i = N. \end{cases}$$

Hence feasibility is guaranteed at all $k > 0$ given feasibility at $k = 0$. It follows that the trajectories of the closed loop system under receding horizon application of the TSLMPC algorithm necessarily satisfy hard constraints and follow the prescribed one-step-ahead transition probabilities p_{lm}, together with the probabilities p_l of soft constraint violation. It follows that (3.36) and therefore (3.17) are satisfied in closed loop. Given feasibility, the proof of the property (3.68) is the same as the proof of Theorem 5 in [13]. □

3.5 Numerical Example

The SLMPC algorithm is illustrated by an example which demonstrates the efficacy of the SLMPC algorithm in respecting both hard and soft constraints in comparison with the unconstrained optimal case. Consider the system with the following parameters:

$$\hat{A}^0 = \begin{bmatrix} 1.2 & 0.1 \\ 0.1 & 1.26 \end{bmatrix}$$

$$\hat{A}^{(1)} = \frac{10^{-2}}{a} \begin{bmatrix} -1 & -0.5 \\ -1 & 0.2 \end{bmatrix} \quad \hat{A}^{(2)} = \frac{10^{-2}}{a} \begin{bmatrix} -0.6 & 0.7 \\ -0.3 & 0.3 \end{bmatrix}$$

$$\hat{B}^0 = \begin{bmatrix} 0.5 \\ 0.21 \end{bmatrix} \quad \hat{B}^{(1)} = \frac{10^{-3}}{a} \begin{bmatrix} -1 \\ -2 \end{bmatrix} \quad \hat{B}^{(2)} = \frac{10^{-3}}{a} \begin{bmatrix} 2 \\ -9 \end{bmatrix}$$

$$\hat{d}^0 = \begin{bmatrix} 0 \\ 0 \end{bmatrix} \quad \hat{d}^{(1)} = \frac{1}{a} \begin{bmatrix} 0.1 \\ 0.01 \end{bmatrix} \quad \hat{d}^{(2)} = \frac{1}{a} \begin{bmatrix} 0.5 \\ 0.12 \end{bmatrix}$$

$$Q = \begin{bmatrix} 1 & 0 \\ 0 & 1 \end{bmatrix} \qquad R = 1 \quad \hat{K} = [-0.12 \ \ -4.66]$$

The parameters $\hat{A}^{(i)}$, $\hat{B}^{(i)}$, and $\hat{d}^{(i)}$ is chosen arbitrary for the sake of example. However, for a real-life application the model parameters is identified from measurements and the variance of these random parameters will determine the value of parameters $\hat{A}^{(i)}$, $\hat{B}^{(i)}$, and $\hat{d}^{(i)}$.

The uncertainty class considered in the example is drawn from a finitely supported triangular distribution over [-a, a] where a=$\sqrt{6}$ which gives a variance of $\mathbb{E}(q_k q_k^T) = I$. We take $\mu = 2$, and the transition probabilities between tubes over one time step, and the probability of constraint violation in a given tube are chosen respectively to be

$$\Pi = \begin{bmatrix} 0.3 & 0.1 \\ 1 & 1 \end{bmatrix} \quad p = [0.1 \ 0.3]^T$$

Matrix V is chosen to be the eigenvector matrix of $\Phi = (\hat{A} + \hat{B}\hat{K})$ which transform the states in to z-space. These values are computed to be

$$K = [-0.74 \ \ -1.24] \quad V = \begin{bmatrix} 2.20 & -8.80 \\ -1.22 & 9.00 \end{bmatrix} \quad W = \begin{bmatrix} 0.99 & 0.97 \\ 0.14 & 0.24 \end{bmatrix}$$

$$\Phi^0 = \begin{bmatrix} 0.84 & 0 \\ 0 & 0.58 \end{bmatrix} \quad \Phi^{(1)} = \begin{bmatrix} -0.01 & -0.01 \\ -0.01 & 0.01 \end{bmatrix} \quad \Phi^{(2)} = \begin{bmatrix} -0.01 & 0 \\ 0 & 0.05 \end{bmatrix}$$

The system is subjected to hard constraints and soft constraints. The parameters which defines the hard and soft constraints on the system are in the form of

$$F_H = \begin{bmatrix} 1 & 0 \\ 0 & 1 \end{bmatrix}, \quad G_H = 0, \quad h_H = \begin{bmatrix} 15 \\ 15 \end{bmatrix}$$

$$F_S = \begin{bmatrix} 1 & 0 \\ 0 & 1 \end{bmatrix}, \quad G_S = 0, \quad h_S = \begin{bmatrix} 0.8 \\ 3 \end{bmatrix}$$

The maximum allowable number of soft constraint violations is N_{max} over a horizon of $N_c = 5$ steps. The choice of Π and p above are chosen so that the following assumption (refer to (3.36)) is satisfied

$$\frac{1}{5}\sum_{i=0}^{4}[p_1 \ p_2](T^{-1}\Pi)^i e_1 = 0.24 \leq \frac{N_{max}}{N_c} \tag{3.69}$$

The algorithm consists of an off-line stage and an online stage. The off-line stage involves setting up parameters as shown above and optimizing the area of the terminal invariant set in Mode 2. The maximized invariant terminal sets are computed to be the sets defined by $|z^{(1)}| < [0.89 \ 2.72]^T$ and $|z^{(2)}| < [0.93 \ 2.90]^T$. The off-line parameters in the stage cost J_k (3.57a), namely P, are calculated to

be

$$P_1 = -1.03, \quad P_\chi = \begin{bmatrix} 11.1 & -29.6 & 0 & 0 & 0 & 0 & 0 \\ -29.6 & 125.2 & 0 & 0 & 0 & 0 & 0 \\ 0 & 0 & 3.1 & 0 & 0 & 0 & 0 \\ 0 & 0 & 0 & 9.3 & 0 & 0 & 0 \\ 0 & 0 & 0 & 0 & 27.9 & 0 & 0 \\ 0 & 0 & 0 & 0 & 0 & 83.6 & 0 \\ 0 & 0 & 0 & 0 & 0 & 0 & 250.8 \end{bmatrix}$$

$$P_{\chi 1}^T = P_{1\chi} = \begin{bmatrix} -0.07 & 0.25 & 0.01 & 0.01 & 0.01 & 0.01 & 0.01 \end{bmatrix}$$

The choice of initial condition has significant effect on the performance of the SLMPC algorithm when comparing with the LQG case. A set of initial points chosen from a grid of $z_1 \in [-2, 2]$ and $z_2 \in [-2, 2]$. It can be seen that for initial points which starts inside the feasible set (does not violated any constraints at time $k = 0$) the performance of LQG and the SLMPC algorithm as measured by the sum of stage costs is the same. Therefore, there is no clear advantage of using the SLMPC algorithm for points inside the feasible set. For points outside the feasible set, as an example if f $z_0 = [2\ 2]^T$ is chosen, the advantage of SLMPC over LQG can be seen more clearly.

The SLMPC algorithm is simulated for $k = 20$ steps with one time-varying realization of uncertainty in the model. At the first step $k = 0$, Figure 3.5 and Figure 3.6 shows the evolution of polytopic bounds of $Z^{(1)}$ and $Z^{(2)}$ along the prediction horizon of $N = 5$ for the first and second elements of z_k respectively. It can be seen that these polytopic bounds grow as uncertainty is propagated along the horizon.

Due to uncertainty, the SLMPC algorithm has to be simulated for a wide range of possible realizations of uncertainties, (again 50 realizations were deemed to be

sufficient). Figure 3.7 and Figure 3.8 show the mean closed loop state trajectories for the first and second element of z_k respectively as compared to the case with only linear feedback law (Mode 2). It can be seen from Figure 3.7 that over 50 realizations the first element of z_k violates soft constraints with a maximum average of 5 violations per 5 consecutive time instants which is more than the maximum allowable violations of 2. On the contrary, the SLMPC algorithm has a maximum average of only 1 constraint violations per 5 consecutive time instants.

Figure 3.10 shows the mean cumulative sum closed loop stage cost for the SLMPC algorithm compared to the LQG case which is the optimal cost without constraints. It can be seen that the algorithm ensures feasibility of both hard and soft constraints at the expense of a slightly higher stage cost. The SLMPC algorithm achieved a cumulative cost sum of 70.9, while retaining feasibility while the LQG case achieved a lower sum of 67.6 but is infeasible.

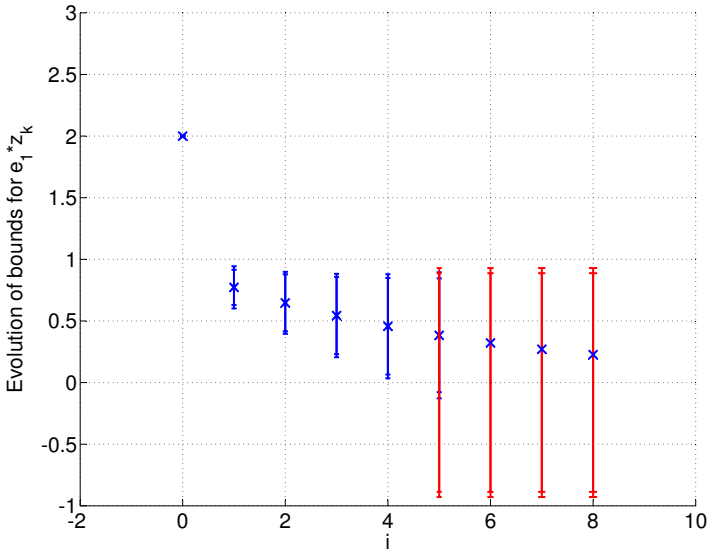

FIGURE 3.5: The evolution of the polytopes along a prediction horizon of 5 for the first element of $z_{k+i|k}$ is shown (in blue). The polytope at $i = 5$ lies within the terminal regions (in red). The polytopes are centred around the nominal trajectory $z^c_{k+i|k}$ (shown as x).

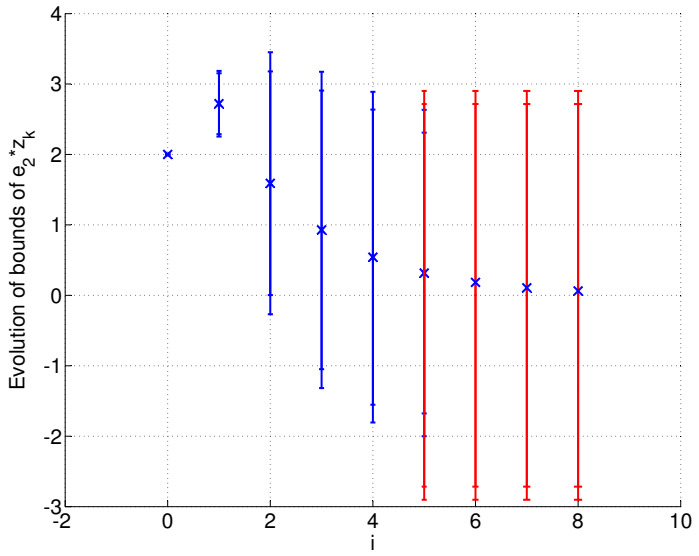

FIGURE 3.6: The evolution of the polytopes along a prediction horizon of 5 for the second element of $z_{k+i|k}$ is shown (in blue). The polytope at $i = 5$ lies within the terminal regions (in red). The polytopes are centred around the nominal trajectory $z^c_{k+i|k}$ (shown as x).

3.6 Conclusion

Despite the potential advantages of stochastic MPC as a methodology that can account for combined statistical and hard constraints in optimal control problems, there are very few results addressing the issue of closed loop feasibility guarantees for constrained stochastic systems. This chapter discusses a means of handling such constraints and proposes a receding horizon algorithm with feasibility and stability guarantees, illustrated by means of a numerical example. As a result of using a finite number of probabilistic tubes and imposing a fixed geometry on their cross-section, the approach is subject to a degree of conservativeness. Future work will therefore focus on ways to reduce this while keeping computational complexity within acceptable bounds.

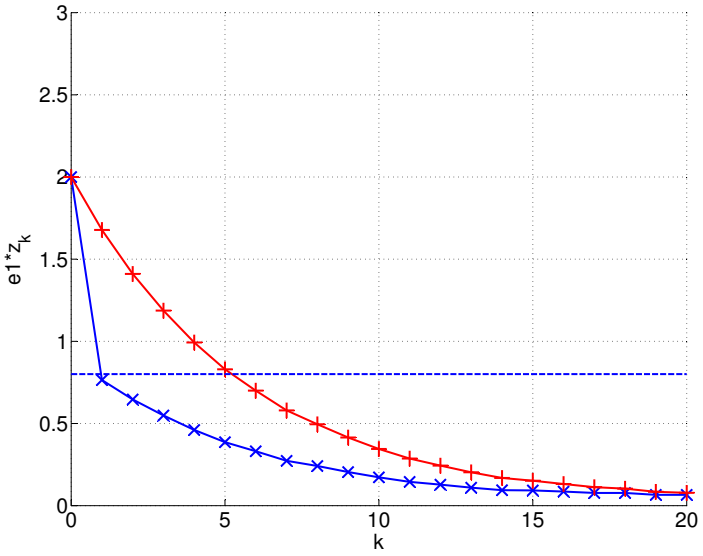

FIGURE 3.7: The first element of the closed-loop state trajectory, z_k for the SLMPC algorithm(x markers) as compared to the LQG case(+ markers). The soft constraint is shown as the dotted line.

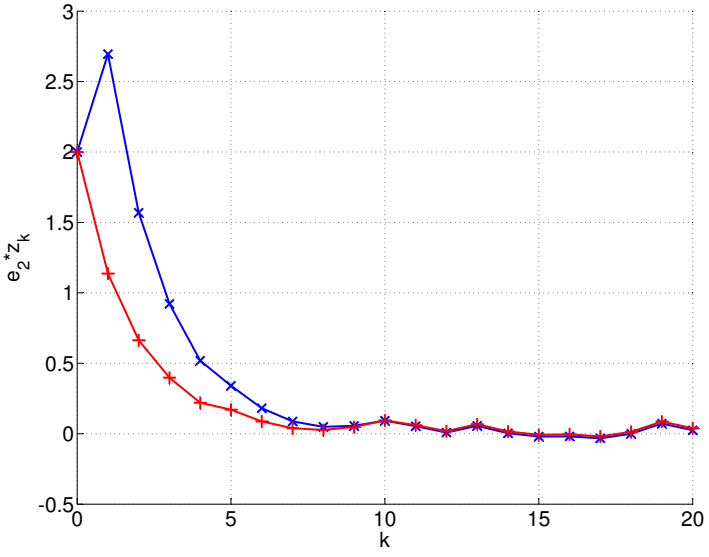

FIGURE 3.8: The second element of the closed-loop state trajectory, z_k for the SLMPC algorithm(x markers) as compared to the LQG case(+ markers).

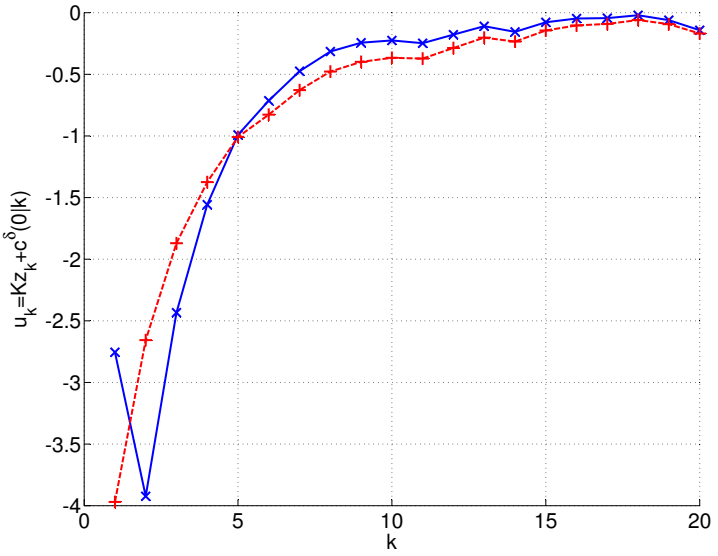

FIGURE 3.9: Ensemble mean of input trajectories for the SLMPC algorithm(x markers) as compared to the LQG case(+ markers).

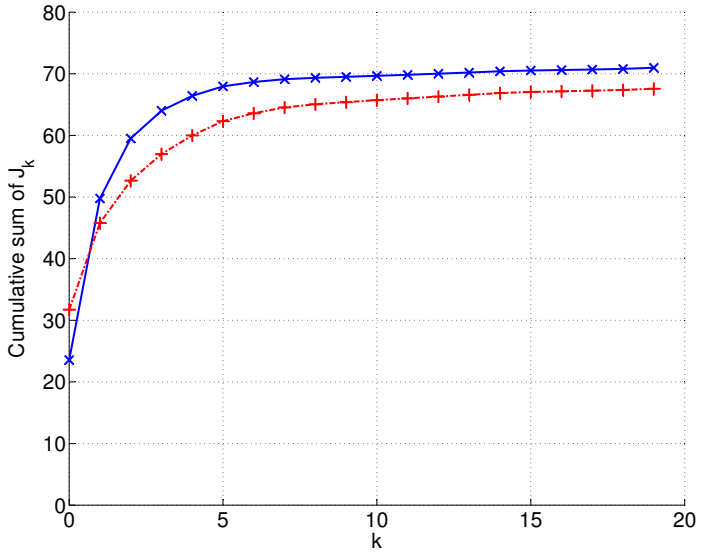

FIGURE 3.10: The cumulative sum of ensemble mean of closed-loop stage costs for the SLMPC algorithm(x markers) as compared to the LQG case(+ markers).

Chapter 4

A Fast Implementation of TSMPC

4.1 TSMPC Implementation

In the previous chapter, an MPC algorithm for linear systems with finitely supported additive and multiplicative stochastic uncertainties (TSMPC) was developed. Both hard and soft constraints are considered, and bounds are imposed on the probability of soft constraint violation. The constraints are handled using a sequence of tubes which corresponds to a sequence of confidence levels on the predicted future plant state constructed online and centred around nominal state trajectories. A set of linear constraints is derived by imposing bounds on the probability of constraint violation at each point on an infinite prediction horizon through constraints on one-step-ahead predictions and on the probabilities of transition of the predicted state between the layered tubes. The intractable infinite prediction horizon is cast as a tractable finite horizon problem through the imposition of a terminal constraint whereby the layered tube at the end of the

finite prediction horizon is restricted to lie within this terminal set in the online optimization. This terminal set is computed offline.

This chapter aims to improve the computational efficiency of the TSMPC algorithm by solving the QP during online optimization using a primal barrier interior point method. The computational speed can be improved by using an approximate primal barrier method whereby the barrier parameter and number of Newton iterations are fixed. The set of linear constraints have considerable structure which is exploited to yield further considerable improvements in computational complexity. Two numerical examples are given to highlight the improvements.

4.1.1 Offline MPC

Following from the previous chapter, the off-line optimization entails finding a maximum volume for the terminal sets $(\bar{z}_t^{(l)}, l = 1, \ldots, \mu)$ under a predetermined state feedback law (Mode 2). The offline optimization is given by

$$\begin{aligned}
\max_{\bar{z}_t^{(l)},\ l=1,\ldots,\mu} & \prod_{l=1}^{\mu} \mathrm{prod}(\bar{z}_t^{(l)}) \\
\text{s.t.} & \left|\Phi(q^{(s)}(p_{ml}))D_r\bar{z}_T^{(l)} + d(q^{(s)}(p_{ml}))\right| \leq \bar{z}_t^{(m)} \\
& \left|\Phi(q^{(s)}(1))D_r\bar{z}_T^{(\mu)} + d(q^{(s)}(1))\right| \leq \bar{z}_t^{(\mu)} \\
& F_S\left\{\Phi(q^{(s)}(1-p_l))D_r\bar{z}_T^{(l)} + d(q^{(s)}(1-p_l)\right\} \leq h_S \\
& F_H D_r \bar{z}_T^{(\mu)} \leq h_H \\
& 0 \leq \bar{z}_T^{(1)} \leq \ldots \leq \bar{z}_T^{(\mu)}
\end{aligned}$$

By defining the offline optimization variable as

$$z_{off} = \left[\bar{z}_t^{(1)}, \bar{z}_t^{(2)}, \ldots, \bar{z}_t^{(\mu)}\right]^T \tag{4.1}$$

the linear constraints in the offline optimization can be written in matrix form.

The one-step-ahead transition probability constraints (3.37b) and universality constraint on the outer polytope (3.38b) respectively are

$$\begin{aligned}
&\left|\Phi(q^{(s)}(p_{ml}))D_r\bar{z}_T^{(l)} + d(q^{(s)}(p_{ml}))\right| \leq \bar{z}_t^{(m)} \\
\Leftrightarrow\ & F_A\left\{\Phi(q^{(s)}(p_{ml}))D_r\bar{z}_T^{(l)} + d(q^{(s)}(p_{ml}))\right\} \leq F_B\bar{z}_t^{(m)} \\
&\left|\Phi(q^{(s)}(1))D_r\bar{z}_T^{(\mu)} + d(q^{(s)}(1))\right| \leq \bar{z}_t^{(\mu)} \\
\Leftrightarrow\ & F_A\left\{\Phi(q^{(s)}(1))D_r\bar{z}_T^{(\mu)} + d(q^{(s)}(1))\right\} \leq F_B\bar{z}_t^{(\mu)}
\end{aligned}$$

where $F_A = [I_n,\ -I_n]^T$ and $F_B = [I_n,\ I_n]^T$,$I_n \in \mathbb{R}^{n\times n}$, which is rewritten as

$$\begin{bmatrix} \widetilde{\Phi}_1 \\ \widetilde{\Phi}_2 \\ \vdots \\ \widetilde{\Phi}_\mu \end{bmatrix} z_{off} \leq \begin{bmatrix} d_1 \\ d_2 \\ \vdots \\ d_\mu \end{bmatrix} \tag{4.2}$$

where $d_i = \left[-F_A d(q^{(s)}(p_{i1})), \ldots, -F_A d(q^{(s)}(p_{i\mu}))\right]^T$.

$$\widetilde{\Phi}_1 = \begin{bmatrix} F_A\Phi(q^{(s)}(p_{11}))D_r - F_B & 0 & \ldots & 0 \\ F_A\Phi(q^{(s)}(p_{21}))D_r & -F_B & \ldots & 0 \\ \vdots & 0 & \ddots & 0 \\ F_A\Phi(q^{(s)}(p_{\mu 1}))D_r & 0 & \ldots & -F_B \end{bmatrix}$$

$$\widetilde{\Phi}_2 = \begin{bmatrix} -F_B & F_A\Phi(q^{(s)}(p_{12}))D_r & \dots & 0 \\ 0 & F_A\Phi(q^{(s)}(p_{22}))D_r - F_B & \dots & 0 \\ \vdots & \vdots & \ddots & 0 \\ 0 & F_A\Phi(q^{(s)}(p_{\mu 2}))D_r & \dots & -F_B \end{bmatrix}$$

$$\widetilde{\Phi}_\mu = \begin{bmatrix} -F_B & 0 & \dots & F_A\Phi(q^{(s)}(p_{1\mu}))D_r \\ 0 & -F_B & \dots & F_A\Phi(q^{(s)}(p_{2\mu}))D_r \\ \vdots & 0 & \ddots & \vdots \\ 0 & 0 & \dots & F_A\Phi(q^{(s)}(p_{\mu\mu}))D_r - F_B \end{bmatrix}$$

The one-step-ahead soft constraint violation probability constraints is

$$F_S \left\{ \Phi(q^{(s)}(1-p_l))D_r\bar{z}_T^{(l)} + d(q^{(s)}(1-p_l) \right\} \leq h_S$$

which can be rewritten as ($h_i = h_S - F_S d(q^{(s)}(1-p_i))$)

$$\begin{bmatrix} F_S\Phi(q^{(s)}(1-p_1))D_r & \dots & 0 \\ \vdots & \ddots & 0 \\ 0 & \dots & F_S\Phi(q^{(s)}(1-p_\mu))D_r \end{bmatrix} z_{off} \leq \begin{bmatrix} h_1 \\ \vdots \\ h_\mu \end{bmatrix} \tag{4.3}$$

The hard constraints is

$$F_H D_r \bar{z}_T^{(\mu)} \leq h_H$$

which is rewritten as

$$\begin{bmatrix} 0 & \dots & F_H D_r \end{bmatrix} z_{off} \leq \begin{bmatrix} h_H \end{bmatrix} \tag{4.4}$$

The nestedness constraint is

$$0 \leq \bar{z}_T^{(1)} \leq \ldots \leq \bar{z}_T^{(\mu)}$$

which is rewritten as

$$\begin{bmatrix} -I_n & \ldots & 0 & 0 \\ I_n & -I_n & 0 & 0 \\ 0 & \ddots & \ddots & 0 \\ 0 & \ldots & I_n & -I_n \end{bmatrix} z_{off} \leq \begin{bmatrix} 0 \\ 0 \\ \vdots \\ 0 \end{bmatrix} \tag{4.5}$$

4.1.2 Online MPC

For the sake of brevity, the constraints are written only for the case of $\mu = 2$, and is easily extendable to $\mu > 2$. Define the overall optimization variable as $z \in \mathbb{R}^{Nn_z}$, where $n_z = m + n(\mu + 1)$ for time k as

$$z = \begin{bmatrix} c_{0|k}, & \bar{z}_{1|k}^{(1)}, & \bar{z}_{1|k}^{(2)} \; z_{1|k}^{c}, & \ldots \; c_{N-1|k}, & \bar{z}_{N|k}^{(1)}, & \bar{z}_{N|k}^{(2)} \; z_{N|k}^{c} \end{bmatrix}^T. \tag{4.6}$$

Equality Constraints

A predicted trajectory of the nominal model, that is without any disturbances and with model parameters given by their mean values, satisfies

$$z_{k+i+1|k}^{c} = \Phi^0 z_{k+i|k}^{c} + B^0 c_{i|k}.$$

and predictions over the horizon N are obtained by recursion and encoded as equality constraints, written as

$$\begin{bmatrix} -B^0 & 0 & 0 & I_n & & & & & & & & \\ 0 & 0 & 0 & -\Phi^0 & -B^0 & 0 & 0 & I_n & & & & \\ & & & & & \ddots & & & & & & \\ & & & & 0 & 0 & 0 & -\Phi^0 & -B^0 & 0 & 0 & I_n \end{bmatrix} z = \begin{bmatrix} \Phi^0 z_{0|k} \\ 0 \\ \vdots \\ 0 \end{bmatrix} \tag{4.7}$$

where $I_n \in \mathbb{R}^{n\times n}$ is the identity matrix.

Transitional Constraints

The one-step-ahead transition probability constraints (3.37a) and universality constraint on the outer polytope (3.38a) respectively are

$$\begin{aligned} &\left|\{\Phi(q^{(s)}(p_{ml}))[z^c_{k+i|k} + D_r \bar{z}^{(l)}_{k+i|k}] + B(q^{(s)}(p_{ml}))c_{i|k} + d(q^{(s)}(p_{ml}))\} - z^c_{k+i+1|k}\right| \\ &\qquad \leq \bar{z}^{(m)}_{k+i+1|k} \\ \Leftrightarrow\ &F_A\left\{\Phi(q^{(s)}(p_{ml}))[z^c_{k+i|k} + D_r \bar{z}^{(l)}_{k+i|k}] + B(q^{(s)}(p_{ml}))c_{i|k} + d(q^{(s)}(p_{ml})) - z^c_{k+i+1|k}\right\} \\ &\qquad \leq F_B \bar{z}^{(m)}_{k+i+1|k} \end{aligned}$$

$$\begin{aligned} &\left|\{\Phi(q^{(s)}(1))[z^c_{k+i|k} + D_r \bar{z}^{(\mu)}_{k+i|k}] + B(q^{(s)}(1))c_{i|k} + d(q^{(s)}(1))\} - z^c_{k+i+1|k}\right| \leq \bar{z}^{(\mu)}_{k+i+1|k} \\ &\quad \Leftrightarrow F_A\left\{\{\Phi(q^{(s)}(1))[z^c_{k+i|k} + D_r \bar{z}^{(\mu)}_{k+i|k}] + B(q^{(s)}(1))c_{i|k} + d(q^{(s)}(1))\} - z^c_{k+i+1|k}\right\} \\ &\qquad \leq F_B \bar{z}^{\mu}_{k+i+1|k} \end{aligned}$$

where $F_A = [I_n, \ -I_n]^T$ and $F_B = [I_n, \ I_n]^T$, which is written as

$$\begin{bmatrix} F_1 & 0 & 0 & 0 & \dots & 0 \\ E_1 & F_1 & 0 & 0 & \dots & 0 \\ 0 & \ddots & \ddots & \ddots & & \\ \vdots & \dots & & E_1 & F_1 & 0 \\ 0 & \dots & 0 & 0 & E_1 & F_1 \end{bmatrix} z \leq \begin{bmatrix} H_1^0 \\ H_1 \\ \vdots \\ \\ H_1 \end{bmatrix} \tag{4.8}$$

where $E_1, F_1 \in \mathbb{R}^{(2n\mu^2 2^{2n}) \times n_z}$ and $H_1^0, H_1 \in \mathbb{R}^{(2n\mu^2 2^{2n}) \times 1}$

$$E_1 = \begin{bmatrix} 0 & F_A\Phi(q^{(s)}(p_{ml}))D_r & 0 & F_A\Phi(q^{(s)}(p_{ml})) \\ 0 & F_A\Phi(q^{(s)}(p_{ml}))D_r & 0 & F_A\Phi(q^{(s)}(p_{ml})) \\ 0 & 0 & F_A\Phi(q^{(s)}(p_{ml}))D_r & F_A\Phi(q^{(s)}(p_{ml})) \\ 0 & 0 & F_A\Phi(q^{(s)}(p_{ml}))D_r & F_A\Phi(q^{(s)}(p_{ml})) \end{bmatrix}$$

$$F_1 = \begin{bmatrix} F_AB(q^{(s)}(p_{ml})) & -F_B & 0 & -F_A \\ F_AB(q^{(s)}(p_{ml})) & 0 & -F_B & -F_A \\ F_AB(q^{(s)}(p_{ml})) & -F_B & 0 & -F_A \\ F_AB(q^{(s)}(p_{ml})) & 0 & -F_B & -F_A \end{bmatrix}$$

$$H_1^0 = \begin{bmatrix} -F_Ad(q^{(s)}(p_{ml})) - F_A\Phi(q^{(s)}(p_{ml}))z_{0|k} \\ -F_Ad(q^{(s)}(p_{ml})) - F_A\Phi(q^{(s)}(p_{ml}))z_{0|k} \\ -F_Ad(q^{(s)}(p_{ml})) - F_A\Phi(q^{(s)}(p_{ml}))z_{0|k} \\ -F_Ad(q^{(s)}(p_{ml})) - F_A\Phi(q^{(s)}(p_{ml}))z_{0|k} \end{bmatrix} \quad H_1 = \begin{bmatrix} -F_Ad(q^{(s)}(p_{ml})) \\ -F_Ad(q^{(s)}(p_{ml})) \\ -F_Ad(q^{(s)}(p_{ml})) \\ -F_Ad(q^{(s)}(p_{ml})) \end{bmatrix}$$

Soft Constraints

The soft constraint violation probability constraints of (3.39a)

$$F_S\left\{\Phi(q^{(s)}(1-p_l))[z^c_{k+i|k}+D_r\bar{z}^{(l)}_{k+i|k}]+B(q^{(s)}(1-p_l))c_{i|k}+d(q^{(s)}(1-p_l))\right\}+ G_S c_{i+1|k}\leq h_S$$

can be rewritten as

$$\begin{bmatrix} F_2 & G_2 & 0 & 0 & \dots & 0 \\ E_2 & F_2 & G_2 & 0 & \dots & 0 \\ 0 & \ddots & \ddots & \ddots & & \\ \vdots & \dots & & E_2 & F_2 & G_2 \\ 0 & \dots & 0 & 0 & E_2 & F_2 \end{bmatrix} z \leq \begin{bmatrix} H_2^0 \\ H_2 \\ \vdots \\ \\ H_2 \end{bmatrix} \tag{4.9}$$

where $E_2, F_2, G_2 \in \mathbb{R}^{(n_s\mu 2^{2n})\times n_z}$ and $H_2^0, H_2 \in \mathbb{R}^{(n\mu 2^{2n})\times 1}$

$$E_2 = \begin{bmatrix} 0 & F_S\Phi(q^{(s)}(1-p_l))D_r & 0 & F_S\Phi(q^{(s)}(1-p_l)) \\ 0 & 0 & F_S\Phi(q^{(s)}(1-p_l))D_r & F_S\Phi(q^{(s)}(1-p_l)) \end{bmatrix}$$

$$F_2 = \begin{bmatrix} F_S B(q^{(s)}(1-p_l)) & 0 & 0 & 0 \\ F_S B(q^{(s)}(1-p_l)) & 0 & 0 & 0 \end{bmatrix} \quad G_2 = \begin{bmatrix} G_S & 0 & 0 & 0 \\ G_S & 0 & 0 & 0 \end{bmatrix}$$

$$H_2^0 = \begin{bmatrix} H_S - F_S d(q^{(s)}(1-p_l)) - F_S\Phi(q^{(s)}(1-p_l))z_{0|k} \\ H_S - F_S d(q^{(s)}(1-p_l)) - F_S\Phi(q^{(s)}(1-p_l))z_{0|k} \end{bmatrix}$$

$$H_2 = \begin{bmatrix} H_S - F_S d(q^{(s)}(1-p_l)) \\ H_S - F_S d(q^{(s)}(1-p_l)) \end{bmatrix}$$

Terminal Constraints

The terminal constraint is given by

$$\begin{aligned} \left| z^c_{k+N|k} + D_r \bar{z}^{(l)}_{k+N|k} \right| &\leq \bar{z}^{(l)}_T \\ \Leftrightarrow F_A \left\{ z^c_{k+N|k} + D_r \bar{z}^{(l)}_{k+N|k} \right\} &\leq F_B \bar{z}^{(l)}_T \end{aligned}$$

which is equivalent to

$$\begin{bmatrix} 0 & 0 & \dots & F_3 \end{bmatrix} z \leq H_3 \tag{4.10}$$

where $F_3 \in \mathbb{R}^{(2n\mu 2^n)\times n_z}$ and $H_3 \in \mathbb{R}^{(2n\mu 2^n)\times 1}$

$$F_3 = \begin{bmatrix} 0 & F_A D_r & 0 & F_A I \\ 0 & 0 & F_A D_r & F_A I \end{bmatrix}$$

$$H_3 = \begin{bmatrix} F_B \bar{z}^{(1)}_T \\ F_B \bar{z}^{(2)}_T \end{bmatrix}$$

Nestedness Constraints

The nestedness constraint of (3.25a) given by

$$\bar{z}^{\mu}_{i|k} \geq \bar{z}^{\mu-1}_{i|k} \geq \dots \geq \bar{z}^{1}_{i|k} > 0$$

can be rewritten as

$$\begin{bmatrix} F_4 & 0 & 0 & \dots & 0 \\ 0 & F_4 & 0 & \dots & 0 \\ 0 & \vdots & \ddots & & \\ \vdots & \dots & & F_4 & 0 \\ 0 & \dots & 0 & 0 & F_4 \end{bmatrix} z \leq \begin{bmatrix} 0 \\ 0 \\ \vdots \\ \\ 0 \end{bmatrix} \tag{4.11}$$

where $F_4 \in \mathbb{R}^{(n\mu)\times n_z}$

$$F_4 = \begin{bmatrix} 0 & -I_n & 0 & 0 \\ 0 & I_n & -I_n & 0 \end{bmatrix}$$

Hard Constraints

The hard constraints of (3.40a)

$$F_H \left\{ z^c_{k+i|k} + D_r \bar{z}^{(\mu)}_{k+i|k} \right\} + G_H c_{i|k} \leq h_H$$

can bes rewritten as

$$\begin{bmatrix} F_5 & 0 & 0 & 0 & \dots & 0 \\ E_5 & F_5 & 0 & 0 & \dots & 0 \\ 0 & \ddots & \ddots & \ddots & & \\ \vdots & \dots & & E_5 & F_5 & 0 \\ 0 & \dots & 0 & 0 & E_5 & F_5 \end{bmatrix} z \leq \begin{bmatrix} h_H \\ h_H \\ \vdots \\ \\ h_H \end{bmatrix} \tag{4.12}$$

where $F_5 \in \mathbb{R}^{(n_h 2^n)\times n_z}$ and $H_5 \in \mathbb{R}^{(n_h 2^n)\times 1}$

$$E_5 = \begin{bmatrix} 0 & 0 & F_H D_r & F_H \end{bmatrix}$$
$$F_5 = \begin{bmatrix} G_H & 0 & 0 & 0 \end{bmatrix}$$

To summarize, inequalities (4.8), (4.9), (4.10), (4.11),and (4.12) which form the inequality constraints, can be written compactly as $P_{ts}z \leq h_{ts}$, $P_{tm}z \leq h_{tm}$, $P_s z \leq h_s$, $P_h z \leq h_h$,and $P_n z \leq h_n$; similarly the equality constraint of (4.7) can be written compactly as $Cz = b$.

Predicted Cost

Following from the previous chapter, the predicted cost to be optimized online is given as

$$J_k = \sum_{i=0}^{\infty} \left\{ \mathbb{E}_k (x_{k+i|k}^T Q x_{k+i|k} + u_{k+i|k}^T R u_{k+i|k}) - L_{ss} \right\}$$

where $L_{ss} = \lim_{i\to\infty} \mathbb{E}_k (x_{k+i|k}^T Q x_{k+i|k} + u_{k+i|k}^T R u_{k+i|k})$. This cost can be obtained as a quadratic function of $c_k = [c_{0|k}^T, \ldots, c_{N-1|k}^T]^T$ which is expressed as

$$J_k = \begin{bmatrix} x_k \\ c_k \end{bmatrix}^T P_\chi \begin{bmatrix} x_k \\ c_k \end{bmatrix} + 2P_{\chi 1} \begin{bmatrix} x_k \\ c_k \end{bmatrix} + P_1 \tag{4.13}$$

where P_χ, $P_{\chi 1}$,and P_1 are the same as in the previous chapter. P_χ and $P_{\chi 1}$ have a block structure of the form

$$P_\chi = \begin{bmatrix} P_\chi^x & 0 \\ 0 & P_\chi^c \end{bmatrix} \quad P_{\chi 1} = \begin{bmatrix} P_{\chi 1}^x \\ P_{\chi 1}^c \end{bmatrix}.$$

where $P_{\chi}^{x} \in \mathbb{R}^{n \times n}$ and $P_{\chi}^{c} \in \mathbb{R}^{Nm \times Nm}$ has block diagonal structure and $P_{\chi 1}^{x} \in \mathbb{R}^{n \times n}$ and $P_{\chi 1}^{c} \in \mathbb{R}^{Nm \times n}$.

Equation (4.13) is expanded yielding and ignoring constant terms

$$J_k = x_k^T P_{\chi}^{x} x_k + 2P_{\chi 1}^{x} x_k + P_1 + c_k^T P_{\chi}^{c} c_k + 2P_{\chi 1}^{c} c_k$$

This is re-written in terms of the optimization variable z by applying the transformation $c_k = H_o z$ and ignoring the first three constant terms, which are independent of z

$$J_k = z^T H z + g^T z \tag{4.14}$$

where $H = H_o^T P_{\chi}^{c} H_o$ and $g^T = 2P_{\chi 1}^{c} H_o$ and $H_o \in \mathbb{R}^{Nm \times T n_z}$

$$H_o = \begin{bmatrix} I_m & 0 & 0 & 0 & & & \\ & & & & \ddots & & \\ & & & & & I_m & 0 & 0 & 0 \end{bmatrix}$$

where $I_m \in \mathbb{R}^{m \times m}$ is the identity matrix.

The online optimization, which is a Quadratic Programming (QP) is written in compact form as

$$\min_{z} \; z^T H z + g^T z \tag{4.15a}$$

$$\text{s.t } P_{ts} z \leq h_{ts}, \; P_{tm} z \leq h_{tm}, \; P_n z \leq h_n \tag{4.15b}$$

$$P_h z \leq h_h, \; P_s z \leq h_s \tag{4.15c}$$

$$Cz = b \tag{4.15d}$$

Note that the inequalities are concatenated into a single matrix and vector respectively as $Pz \leq h$ with $P \in \mathbb{R}^{w \times n_z}$ and $h \in \mathbb{R}^w$ where

$$P = \begin{bmatrix} P_{ts} \\ P_{tm} \\ P_n \\ P_h \\ P_s \end{bmatrix} \quad h = \begin{bmatrix} h_{ts} \\ h_{tm} \\ h_n \\ h_h \\ h_s \end{bmatrix}$$

and where w is the total number of inequalities. It can be seen that the QP has considerable structure. For example, (4.7), (4.8),and (4.12) has a lower bi-diagonal structure, and (4.9) has block tri-diagonal structure. These structures are exploited in a generic optimization solver and can be solved efficiently.

The QP is solved exactly using MATLAB© with a generic optimization solver SDPT3 [48] and coded with the aid of modeling software YALMIP [49] on a Pentium© 4 2.8GHz, 1GB RAM computer running WINDOWS© XP. From this point onwards, the QP solved in this manner is given the term 'Exact SMPC'.

4.2 Primal Barrier Interior-Point Method

The QP problem can be solved reliably using a variety of methods and one such method is the Primal Barrier Interior-Point method. The main advantage of this method is that it exploits the structure of the problem. Evidently, the QP problem has considerable structure. Both the inequality and equality constraints have block tridiagonal and block-diagonal structure which can be exploited to solve the QP efficiently. In this section, the basic Primal Barrier Interior-Point Method [50] is described. A variation of this method, which is given in [51], is also implemented

here to give significant improvements in efficiency. Interior Point methods, specifically Primal-Dual Interior-Point methods have been utilized in an MPC context in recent years [15, 52, 53] and have proven to be an efficient method to solve optimization problems arising from MPC for large systems. However, much of this work has been limited to deterministic and robust cases. In recent years, the use of Interior-point methods in MPC for stochastic systems has been explored in [51, 54].

4.2.1 Primal Barrier Method

A particular interior-point method is the barrier method [50, §11]. This method, like any interior point method, solves an optimization problem with linear equality and inequality constraints by reducing it to a sequence of linear equality constrained problems, which is solved using Newton's methods.

The problem (4.15) is approximated by

$$\min_{z} \; f(z) = t(z^T H z + g^T z) + \phi(z) \tag{4.16a}$$

$$\text{s.t } Cz = b \tag{4.16b}$$

where $t > 0$ is the barrier parameter and ϕ is the log barrier associated with the inequality constraints, defined as

$$\phi(z) = \sum_{i=1}^{w} -\ln(h_i - p_i^T z) \tag{4.17}$$

where p_i^T is the i^{th} row of P. $\phi(z)$ is known as the logarithmic barrier and its domain is all set of points z which satisfy the inequality constraints strictly. This problem is convex and has a unique solution for all $t > 0$. Define the solution to (4.16) as $z^*(t)$ which is optimal for a given barrier parameter t. It is shown in [50,

§11] that the solution obtained using this method is no more than $\frac{w}{t}$ suboptimal, that is, $|f(z) - f(z^*)| < \frac{w}{t}$. As $t \to \infty$, $z^*(t)$ converges to an optimal point.

The gradient and Hessian of the logarithmic barrier function is given by

$$\nabla\phi(z) = \sum_{i=1}^{w} \frac{1}{(-p_i^T z + h_i)} p_i \tag{4.18}$$

$$\nabla^2\phi(z) = P^T \mathbf{diag}\left(\frac{1}{(p_i^T z - h_i)}\right)^2 P \tag{4.19}$$

where **diag**(.) forms the diagonal matrix.

The basic primal barrier method is summarized as follows

1. Given a strictly feasible z, an initial $t^{(0)} > 0$, $\mu > 1$ and specified tolerance $\epsilon > 0$, solve (4.16) to obtain $z^*(t)$.
2. Update the current step $z = z^*(t)$.
3. Increase t by $t = \mu t$ and repeat Step 1 until the sub-optimality is below ϵ.

4.2.2 Infeasible Start Newton Method

The equality constrained problem (4.16) can be solved using Newton's method [50, §9] given a strictly feasible initial trajectory z, that is $z \in \mathbf{dom}\phi$ and $Cz = b$. This requirement can be relaxed by using an infeasible start Newton method [50, §10.3]. This section shows how the equality constrained minimization problem is reduced to an unconstrained problem, in particular, reduced to a system of linear equations (also known as KKT equations in [50]) and describes the infeasible start Newton method.

The first order optimality conditions for a given point z in the domain of $f(z)$ to be optimal is

$$Cz^* = b \tag{4.20}$$

$$\nabla f(z^*) + C^T \nu^* = 0. \tag{4.21}$$

which is also known as the primal and dual feasibility equations and $\nu \in \mathbb{R}^{Nn}$. If the current point is not be feasible, the goal is to find a step Δz so that $z+\Delta z \approx z^*$ and in turn satisfies the optimality conditions.

Alternatively, the optimality conditions (4.20) and (4.21) are rewritten in terms of primal and dual residuals defined by

$$r_{pri}(z^*, \nu^*) = Cz^* - b = 0 \tag{4.22}$$

$$r_{dual}(z^*, \nu^*) = \nabla f(z^*) + C^T \nu^* = 0. \tag{4.23}$$

Given current estimates z and ν, the goal is now to find a primal and dual step Δz,$\Delta\nu$ so that $r(z+\Delta z, \nu+\Delta\nu) = (r_{pri}(z+\Delta z, \nu+\Delta\nu), r_{dual}(z+\Delta z, \nu+\Delta\nu)) = (0, 0)$. The first-order Taylor approximation of r near the current estimates is

$$r_{pri} = C(z + \Delta z) - b = 0 \tag{4.24}$$

$$r_{dual} \approx \hat{r}_{dual} = \nabla f(z) + \nabla^2 f(z)\Delta z + C^T(\nu + \Delta\nu) = 0 \tag{4.25}$$

which yields

$$\begin{bmatrix} \nabla^2 f(z) & C^T \\ C & 0 \end{bmatrix} \begin{bmatrix} \Delta z \\ \Delta\nu \end{bmatrix} = - \begin{bmatrix} r_{dual}(z, \nu) \\ r_{pri}(z, \nu) \end{bmatrix} \tag{4.26}$$

Using (4.18) and (4.19), the gradient and Hessian of the objective function $f(z)$ is

$$\nabla f(z) = 2tHz + tg + P^T d \tag{4.27}$$

$$\nabla^2 f(z) = 2tH + P^T \mathbf{diag}\,(d)^2\, P \tag{4.28}$$

where $d \in \mathbb{R}^w$ with elements $d_i = \frac{1}{(p_i^T z - h_i)}$.

Substituting (4.27) and (4.28) into (4.26) yields

$$\begin{bmatrix} 2tH + P^T \mathbf{diag}\left(\frac{1}{(p_i^T z - h_i)}\right)^2 P & C^T \\ C & 0 \end{bmatrix} \begin{bmatrix} \Delta z \\ \Delta \nu \end{bmatrix} = - \begin{bmatrix} r_{dual}(z,\nu) \\ r_{pri}(z,\nu) \end{bmatrix} \tag{4.29}$$

where

$$r_{pri} = Cz - b$$

$$r_{dual} = 2tHz + tg + P^T d + C^T \nu.$$

Therefore, the equality constrained problem is shown here to be equivalent to solving a KKT system.

The Infeasible Start Newton method algorithm is outlined as follows

Algorithm 6. (Infeasible start Newton Method)

1. Given that z is in the domain of $\phi(z)$, ν, $\epsilon > 0$,$\alpha \in (0, 0.5)$, $\beta \in (0, 1)$.

2. Compute the primal and dual Newton steps Δz, $\Delta \nu$ by solving (4.29).

3. Backtracking line search on $\|r\|_2$:

   a) Set $z = z + s\Delta z$ where $s = 1$. The step direction must satisfy $P(z + s\Delta z) < h$ strictly (or $z + s\Delta z \in \mathbf{dom}\phi(z)$). Expanding this yields $Pz + sP\Delta z < h$. Only strictly positive elements of the vector $sP\Delta z > 0$

might violate the inequality and therefore only these elements are of concern. Assume that there are n such elements. Hence, domain satisfaction is ensured if $s_i p_i^T \Delta z < h_i - p_i^T z$ for all $i = 1, \dots n$. Rearranging this yields $s_i < \frac{h_i - p_i^T z}{p_i^T \Delta z}$. The maximum step length s_{max} such that domain satisfaction is guaranteed is computed by $s_{max} = min(s_i)$. Strict domain satisfaction is ensured by scaling down the maximum step length, $s_{max} = 0.99 s_{max}$.

b) Start with $s = \max(1, s_{max})$

c) While $\|r(z + s\Delta z, \nu + s\Delta\nu)\|_2 > (1 - \alpha s)\|r(z, \nu)\|_2$, keep updating $s = \beta s$.

4. Update the steps, that is $z = z + s\Delta z$, $\nu = \nu + s\Delta\nu$

5. Repeat Step 2, until $Cz = b$ and $\|r(z, \nu)\|_2 \leq \epsilon$.

When a full step length ($s = 1$) is taken, all future iterates are primal feasible. That is, once $r_{pri} = 0$ it will stay at 0 for all future iterates and z and ν converges to an optimal point.

4.2.3 Phase 1

The Infeasible Start Newton method requires a strictly feasible starting point z^0 that satisfies $Pz < h$ strictly (or z in the domain of the barrier function) but need not satisfy the equality constraints $Cz = b$. Furthermore, the number of Newton iterates depends on z_0. If this starting point is not known, an off-line computation, known as the sum of infeasibilities method, is performed by solving

$$\min_s \ 1^T s \tag{4.30a}$$

$$\text{s.t } p_i^T z - h_i < s_i \tag{4.30b}$$

$$s \geq 0 \tag{4.30c}$$

where $s \in \mathbb{R}^w$. The optimal value of $s_i, i = 1, \ldots, w$ is zero and achieved if and only if the inequalities are feasible.

Alternatively, a simpler basic method is used if the number of inequalities, w is big

$$\min_s \; s \tag{4.31a}$$

$$\text{s.t } p_i^T z - h_i < s \tag{4.31b}$$

where $s \in \mathbb{R}$ which results in the less degrees of freedom for s. If $s < 0$, then (4.31a) has a strictly feasible solution. Furthermore, if (z, s) are feasible with $s < 0$ then $p_i^T z - h_i < 0$ and therefore, the optimization problem does not need to be solved to a high accuracy and can be terminated whenever $s < 0$.

4.2.4 Warm Start

The idea of warm starting is that a previously computed trajectory can be used as a good starting point for the next optimization.

If at time $k-1$, a feasible trajectory computed is given by

$$\tilde{z}_{k-1} = \begin{bmatrix} \tilde{c}_{0|k-1}, & \tilde{\bar{z}}^{(1)}_{1|k-1}, & \tilde{\bar{z}}^{(2)}_{1|k-1} & \tilde{z}^{c}_{1|k-1}, & \ldots & \tilde{c}_{N-1|k-1}, & \tilde{\bar{z}}^{(1)}_{N|k-1}, & \tilde{\bar{z}}^{(2)}_{N|k-1} & \tilde{z}^{c}_{N|k-1} \end{bmatrix}^T, \tag{4.32}$$

the primal barrier method can be initialized at time k by using the previously computed trajectory that is shifted by one time step. At time step k the following initial trajectory is used

$$z_k = \begin{bmatrix} \tilde{c}_{1|k}, & \tilde{\bar{z}}^{(1)}_{2|k}, & \tilde{\bar{z}}^{(2)}_{2|k} & \tilde{z}^{c}_{2|k}, & \ldots 0, & 0.99\bar{z}^{(1)}_t, & 0.99\bar{z}^{(2)}_t & 0 \end{bmatrix}^T. \tag{4.33}$$

The trajectory is just the trajectory at $k-1$ shifted by one time step and concatenated with $c_{N|k}=0$ and $z^c_{N+1|k}=0$. This is by definition of the Mode 2. The terminal sets is used because once the terminal constraint $P_{tm}z \leq h_{tm}$ is satisfied, all future sets will be in the terminal sets with probability 1. The reason a scaling factor of 0.99 is used because the primal barrier requires strict feasibility ($P_{tm}z < h_{tm}$) and this is achieved using the scaling factor.

One of the main advantages of the TSMPC algorithm is the guarantee of stability and feasibility in the online optimization assuming feasibility at time $k=0$. That is, if feasibility is achieved at $k=0$, the algorithm is guaranteed to be feasible for all $k>0$. This advantage is still valid even if the online optimization problem is solved using the primal barrier method. However, both the primal and dual residual needs to be strictly feasible, that is the absolute value of the residuals must be lower than a specified tolerance parameter.

4.2.5 Fast Computation of Newton Step

The number of inequalities w grows exponentially with the system order n and therefore, the computational complexity is dominated by multiplication of big matrices. In particular, in the computation of $H_p = P^T\mathbf{diag}(d)P$ or equivalently $H_p = P_{ts}^T\mathbf{diag}(d_{ts})P_{ts} + P_{tm}^T\mathbf{diag}(d_{tm})P_{tm} + P_n^T\mathbf{diag}(d_n)P_n + P_h^T\mathbf{diag}(d_h)P_h + P_s^T\mathbf{diag}(d_s)P_s$. However, P has considerable structure which can be exploited to reduce the computational burden. Take for example the computation of $H_{ts} =$

$P_{ts}^T \mathbf{diag}(d_{ts}) P_{ts}$ which yields a block tri-diagonal structure

$$H_{ts} = \begin{bmatrix} P_{11} & P_{12} & 0 & \dots & 0 & 0 \\ P_{21} & P_{22} & P_{23} & \dots & 0 & 0 \\ 0 & P_{32} & P_{33} & \dots & 0 & 0 \\ \vdots & \vdots & \vdots & \ddots & \vdots & \vdots \\ 0 & 0 & 0 & \dots & P_{N-1,N-1} & P_{N-1,N} \\ 0 & 0 & 0 & \dots & P_{N,N-1} & P_{N,N} \end{bmatrix} \tag{4.34}$$

where each corresponding blocks can be formed by

$$P_{ii} = F_1^T d_i F_1 + E_1^T d_{i+1} E_1, \quad i = 1, \dots, N-1$$
$$P_{i,i+1} = P_{i+1,i}^T = E_1^T d_{i+1} F_1 \quad i = 1 \dots, N-1$$

$$P_{N,N} = F_1^T d_N F_1$$

where

$$d_1 = \mathbf{diag}\left(\frac{1}{(H^0 - Fz_1)_j^2}\right)$$
$$d_i = \mathbf{diag}\left(\frac{1}{(H^0 - Ez_{i-1}Fz_i)_j^2}\right) \quad i = 2, \dots, N$$

What essentially is a multiplication of a big matrix can be decomposed into a smaller set of multiplications. The flop count for matrix multiplication without exploiting structure is $N^3 n_w^2$, keeping only the leading terms. n_w is the number of rows of E and F corresponding to only transitional constraints (ie. $n_w = 2n\mu^2 2^{2n}$). In contrast, exploiting matrix structure above yields a flop count of Nn_w^2 which grows only linearly with N. Since P_{tm}, P_n, P_s, P_h has the same structure, the same method is applied when forming the remaining additional terms in H_p. The formation of $\Phi = 2tH + H_p$ also yields a block tri-diagonal matrix since H is a

block diagonal matrix.

Solving (4.29) using block elimination consists of

1. Form the Schur complement $Y = C\Phi^{-1}C^T$.
2. Determine $\Delta\nu$ by solving $Y\Delta\nu = \beta, \quad \beta = r_{pri} - C\Phi^{-1}r_{dual}$.
3. Determine Δz by solving $\Phi\Delta z = -r_{dual} - C^T\Delta\nu$.

For Step 1, Φ can be factored using Cholesky factorization $\Phi = LL^T$ where L has a lower bi-diagonal structure

$$L = \begin{bmatrix} L_{11} & 0 & 0 & \dots & 0 & 0 \\ L_{21} & L_{22} & 0 & \dots & 0 & 0 \\ 0 & L_{32} & L_{33} & \dots & 0 & 0 \\ \vdots & \vdots & \vdots & \ddots & \vdots & \vdots \\ 0 & 0 & 0 & \dots & L_{N-1,N-1} & 0 \\ 0 & 0 & 0 & \dots & L_{N,N-1} & L_{N,N}. \end{bmatrix} \tag{4.35}$$

where L_{ii} are lower triangular matrices with positive diagonal elements and $L_{i+1,i}$ are general square matrices of order n_z, where each can be formed by

$$\begin{aligned} L_{11}L_{11}^T &= P_{11} \\ L_{ii}L_{i+1,i}^T &= P_{i,i+1}, \quad i = 1, \dots, N-1 \\ L_{ii}L_{ii}^T &= P_{ii} - L_{i,i-1}L_{i,i-1}^T, \quad i = 2, \dots, N. \end{aligned}$$

The computation of the inverse of Φ is then obtained by backward and forward substitution. These steps take about n_z^3 flops and grows linearly with horizon N. Therefore, the overall complexity in Step 1 is order Nn_z^3 plus the additional flops corresponding multiplication with the corresponding sub-blocks of C^T and

C. This factorization method is widely used in Interior Point MPC methods as described in [15, 51, 53].

Since Φ^{-1} can be factored efficiently and it has already been computed in Step 1, Step 3 involves only back substitution followed by forward substitution. In Step 2 however, the factorization of Y is approximately order $N^3 n_z^3$ and therefore grows cubicly with the prediction horizon. This is a big disadvantage which is caused by the lost of structure in Y. However, the entire QP can be reformulated to form a structured Y by using redundant optimization variables.

By defining $z_i = [c_{i-1|k}, \ \bar{z}^{(1)}_{i|k}, \ \bar{z}^{(2)}_{i|k} \ z^c_{i|k}]$, for $i = 1, \ldots, N$, the optimization variable z can be arranged as

$$z = [z_1, z_1, z_2, z_2, \ldots, z_{N-1}, z_{N-1}, z_N]^T . \tag{4.36}$$

Correspondingly, all the inequality constraints yield a block diagonal structure. For example, whereas the transitional constraints are shown here, previously had a block bi-diagonal structure, now they have a block diagonal structure.

$$\begin{bmatrix} F_1 & 0 & 0 & 0 & \ldots & & 0 \\ 0 & E_1 & F_1 & 0 & \ldots & & 0 \\ 0 & \ddots & \ddots & \ddots & & & \\ \vdots & \ldots & & E_1 & F_1 & & 0 \\ 0 & \ldots & 0 & 0 & 0 & E_1 & F_1 \end{bmatrix} z \leq \begin{bmatrix} H_1^0 \\ H_1 \\ \vdots \\ \\ H_1 \end{bmatrix} . \tag{4.37}$$

$$\Phi^{-1} = \begin{bmatrix} P_{11}^{-1} & 0 & 0 & \dots & 0 & 0 \\ 0 & P_{22}^{-1} & 0 & \dots & 0 & 0 \\ 0 & 0 & P_{33}^{-1} & \dots & 0 & 0 \\ \vdots & \vdots & \vdots & \ddots & \vdots & \vdots \\ 0 & 0 & 0 & \dots & P_{N-1,N-1}^{-1} & 0 \\ 0 & 0 & 0 & \dots & 0 & P_{N,N}^{-1} \end{bmatrix} \tag{4.38}$$

Consequently, the computational complexity of Step 1 is approximately Nn_z. The resulting Y has a block tri-diagonal structure, similar with (4.34). Step 2 is carried out by a Cholesky factorization of $Y = LL^T$ followed by a backward and forward substitution to obtain $\Delta\nu$. If the factorization step is performed as described in (4.35), the complexity of Step 2 is again approximately Nn_z. The computation of Step 3 is negligible since the factorization of Φ has already been carried out in Step 1. Step 3 therefore involves only backward and forward substitutions. The solution of the KKT system therefore can be computed efficiently and its complexity grows linearly with the prediction horizon N.

4.3 Approximate Primal Barrier Method

This computational time using a basic primal barrier method can be made even faster without significant decrease in the quality of control law by fixing the barrier parameter and the maximum number of Newton iterations [51].

4.3.1 Fixed t

In the basic primal barrier method, the barrier parameter t is increased by a factor of $\mu > 1$ at each iteration. The variation proposed by [51] is to use a

fixed barrier parameter for all iterations. Fixing t essentially converts the MPC online optimization to a sequence of Newton iterations. This provides a reliable advantage when warm starting is used, to reduce the number of Newton iterations at each step by orders of magnitude, depending on the problem. This is in contrast with the basic primal barrier method where warm starting provides an unreliable and limited advantage. The reason this can be done in an receding horizon MPC setting is because the QP optimization problem at each step is just a heuristic for computing good control which is judged by the objective value and thus solving the QP at each step exactly is not necessary.

4.3.2 Fixed Newton Iterations

Since each step in the online optimization comprises essentially Newton iterations, a further reduction in computational speed is achieved by setting a maximum number of iterations. By quitting prematurely before the primal and dual residuals have converged to a small enough value, primal and dual feasibility might not be achieved. This would imply that a poor quality of control will be obtained in this manner by solving the QP each step crudely. However, extensive numerical simulations by [51] shows that the quality of control obtained is still of high quality and the increase in objective value J is negligible (as long as K^{max} is not too small, for example $K^{max} = 1$). A possible explanation given is that because MPC computes a planned trajectory at each step and only the initial value of input is used. The rest of the inputs are not used but are computed nonetheless to ensure that the current input used does not have significantly adverse affects on the future behavior of the system. This however would remove the guarantee of recursive closed-loop feasibility, which is an advantage of using the TSMPC algorithm. Therefore there is a trade-off between speed and guarantees of feasibility, without significant degradation of the quality of control.

In summary the approximate primal barrier method (or Fast TSMPC) algorithm is as follows:

Algorithm 7. (Fast Tube Stochastic MPC)

1. Given a fixed t and K^{max}, a specified tolerance $\epsilon > 0$, solve (4.30a) to obtain an initial primal feasible trajectory z_0.
2. Solve (4.29) using Infeasible start Newton method to obtain z_k^* or until K^{max} is reached.
3. Warm start.
4. Repeat Step 2 for $k = 1, 2, \ldots$.

4.4 Implementation Results

In this section the implementation results are discussed by two examples. The first example shows the degree of sub-optimality of the QP solution obtained by using the Approximate Primal Barrier Method as compared to solving it exactly. The second example shows the timing profiles compared to using a generic optimization solver for a random system with varying model order, prediction horizon, number of inputs and tube layers.

4.4.1 Second Order Example

To compare the performance of the approximate primal barrier method and exact MPC the following control problem with 2 states and 2 inputs with only soft constraints on the system state is considered. The parameter values for this problem are

$$A^{(0)} = \begin{bmatrix} 1.2 & 0.1 \\ 0.1 & 1.26 \end{bmatrix} \quad A^{(1)} = \begin{bmatrix} 0.04 & 0 \\ 0.01 & 0.04 \end{bmatrix} \quad A^{(2)} = \begin{bmatrix} 0.04 & 0.01 \\ 0 & 0.04 \end{bmatrix}$$

$$B^{(0)} = \begin{bmatrix} 0.5 & 0 \\ 0 & 0.3 \end{bmatrix} \quad B^{(1)} = B^{(2)} = \begin{bmatrix} 0 & 0 \\ 0 & 0 \end{bmatrix}$$

$$d^{(1)} = \begin{bmatrix} 0.1 \\ 0.1 \end{bmatrix} \quad d^{(2)} = \begin{bmatrix} 0 \\ 0 \end{bmatrix} \quad Q = R = \begin{bmatrix} 1 & 0 \\ 0 & 1 \end{bmatrix}$$

For all k, the elements of the random vector q_k are independent with triangular probability distributions supported on $[-\sqrt{6}, \sqrt{6}]$ with variance $\mathbb{E}(q_k q_k^T) = I$. The soft constraints on the system states are

$$F_s = \begin{bmatrix} 2 & 1 \\ -2 & -1 \end{bmatrix}, \quad G_s = \begin{bmatrix} 0 & 0 \\ 0 & 0 \end{bmatrix}, H_s = \begin{bmatrix} 10 \\ 10 \end{bmatrix}.$$

The prediction horizon for this example is chosen to be $N = 10$. The unconstrained LQG optimal feedback law is given as

$$u = \hat{K}x, \quad \hat{K} = \begin{bmatrix} -1.21 & -0.37 \\ -0.30 & -1.84 \end{bmatrix}.$$

The transition probability matrix and vector of constraint violation probabilities, for $\frac{N_{max}}{N_c} = 0.4$, are taken to be:

$$\Pi = \begin{bmatrix} p_{11} & p_{12} \\ p_{21} & p_{22} \end{bmatrix} = \begin{bmatrix} 0.8 & 0.8 \\ 1 & 1 \end{bmatrix}, \quad p = \begin{bmatrix} p_1 \\ p_2 \end{bmatrix} = \begin{bmatrix} 0.3 \\ 0.4 \end{bmatrix}.$$

where these values satisfy $\frac{1}{N_c}\sum_{i=0}^{N_c-1} p(T^{-1}\Pi)^i e_1 \leq \frac{N_{max}}{N_c}$. For the particular choice of $\hat{K}$, the eigenvalues of the nominal closed loop state matrix are

$$\Phi^{(0)} = \begin{bmatrix} 0.61 & 0 \\ 0 & 0.70 \end{bmatrix} \quad \Phi^{(1)} = \begin{bmatrix} 0.05 & -0.01 \\ 0.02 & 0.03 \end{bmatrix} \quad \Phi^{(2)} = \begin{bmatrix} 0.04 & 0.01 \\ 0 & 0.04 \end{bmatrix}.$$

and the corresponding state feedback gain K and the eigenvector matrix are given by

$$K = \begin{bmatrix} 1.16 & -0.48 \\ 0.11 & 1.24 \end{bmatrix} \quad V = \begin{bmatrix} -1.10 & -0.89 \\ -0.15 & -1.41 \end{bmatrix}.$$

For ease of illustration, the number of overlapping tubes is taken to be $\mu = 2$. The approximate primal barrier method parameters are $K^{max} = 20$, $t = 100$, $\alpha = 0.01$, and $\beta = 0.9$.

Firstly, the transformed state trajectories z_k using Exact MPC and FTSMPC is compared in Figure 4.1 for one realization of uncertainty parameters for 20 steps. It is evident that the trajectories are almost identical which shows that almost identical results are obtained for a fraction of the computational speed. Also, the corresponding errors in the input and state trajectories solved using FTSMPC and Exact MPC, are shown in Figure 4.2 and 4.3. The QP which is solved exactly, takes approximately 1.4s while it takes approximately 0.2s using the approximate primal barrier method, leading to a 86% reduction in computational time. Furthermore, a low-level language implementation, for example C, enables further reduction in computational times as evident in the work by [51].

To examine the effects of varying the barrier parameter(t) and the maximum number of Newton steps(K^{max}) , the average stage costs over 100 steps are compared. In Table 4.1, the parameter K^{max} is fixed at 20 while the barrier parameter is varied, $t = 1, 10, 100$. As t is increased by a factor 10 the mean stage cost converges

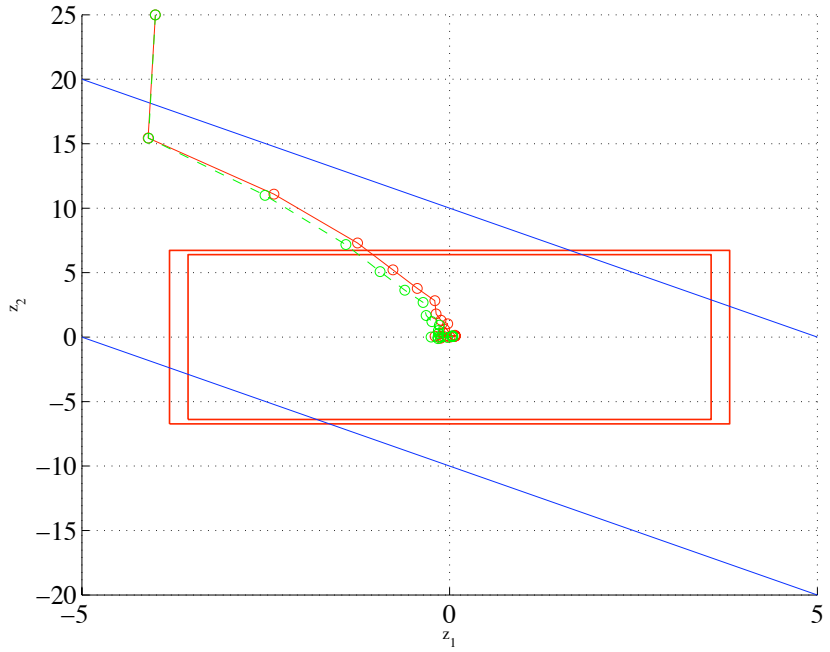

FIGURE 4.1: Trajectories of $z_k, k = 0, \ldots, 20$ for 1 realization of uncertainty. Dashed line:- FSTMPC, Solid line:- Exact MPC. The soft constraints and terminal sets are shown.

to the value computed by using exact MPC. In fact for $t > 10$, the mean stage costs for both methods are essentially the same.

The same analysis is made by fixing $t = 100$ and varying the maximum Newton iterations $K^{max} = 5, 10, 20$. By extensive simulations, primal feasibility is, on average, achieved (as measured by the primal residual) in $K = 4$ steps while dual feasibility is achieved, on average, in $K = 8$ steps. The comparison of mean stage cost for 100 steps is shown in Table 4.2. For $K^{max} > 10$, the mean stage costs is almost identical with the value computed using exact MPC. For $K^{max} = 5$, it is observed that the mean stage costs increases, which implies sub-optimality. This is expected when the iterations are terminated before primal and dual feasibility is achieved.

	Exact MPC	$t = 10$	$t = 100$	$t = 1000$
J_{mean}	37.9	38.6	38.0	37.9

TABLE 4.1: Comparison of mean stage cost J_{mean} as t is increased with $K^{max} = 20$.

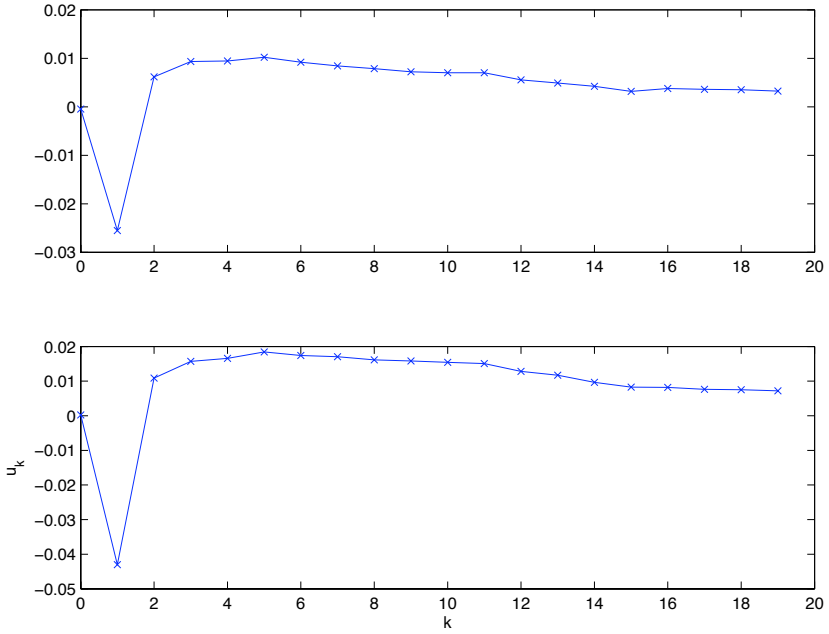

FIGURE 4.2: The difference between input trajectories simulation using FSTMPC and Exact MPC.

	Exact MPC	$K^{max} = 5$	$K^{max} = 10$	$K^{max} = 20$
J_{mean}	37.9	41.3	37.9	37.9

TABLE 4.2: Comparison of mean stage cost J_{mean} as K^{max} is increased with $t = 100$.

Finally, the soft constraint violations are examined by simulating the controlled system for 100 realizations of uncertainties over 20 time steps$(q_k, k = 0, \ldots, 20)$. The trajectory obtained by using an unconstrained optimal controller shows that over a 3 step interval, the worst soft constraint violation rate is 0.8. This clearly violates the soft constraint $\left(\frac{1}{N_c}\sum_{i=1}^{N_c} Pr(F_s z_{k+i} > h_S) \leq 0.45\right)$. On the other hand, the worst soft constraint violation is only 0.3 using the TSMPC algorithm which is solved exactly. The same result is obtained if the TSMPC algorithm is solved using the approximate primal barrier method. Although the soft constraint is satisfied, it is a very conservative result.

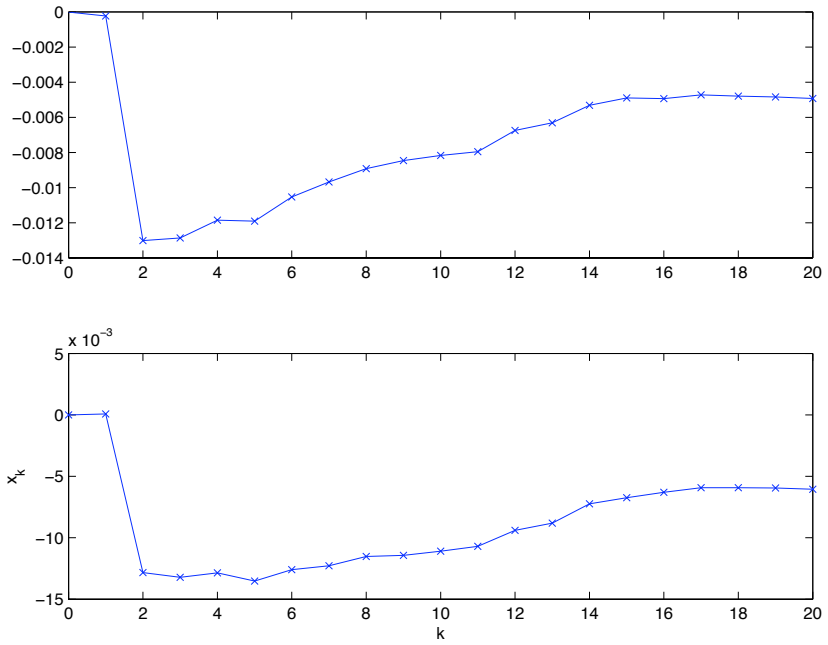

FIGURE 4.3: The difference between state trajectories simulation using FSTMPC and Exact MPC.

4.4.2 Random Systems Example

In this example, the computational times for a randomly generated example with varying system order n, inputs m, horizon N, and number of overlapping tubes μ is shown in Table 4.3. The QP size is shown in the format (n_z/w) where n_z is the number of variables and w is total number of inequalities. The average computational times per step over 10 steps for solving an exact QP and using an approximate primal barrier method are shown and indicates that FTSMPC is at least 10 times faster than MPC solved using the exact QP solver.

4.5 Conclusion

The Tube MPC algorithm is essentially an optimization problem, specifically a QP program. There is considerable structure to the problem. Both the inequality and equality constraints have block tridiagonal and block-diagonal structure

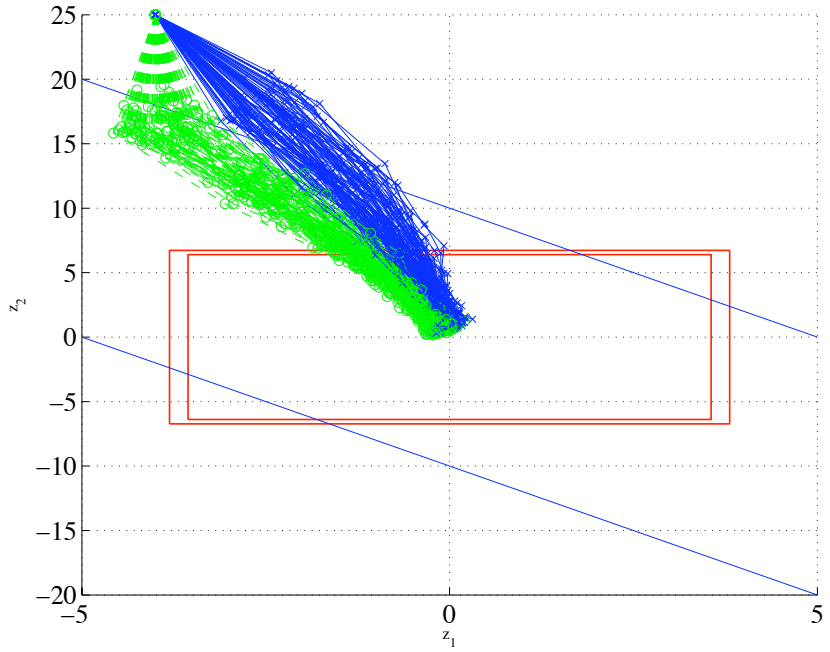

FIGURE 4.4: The trajectories of z_k for 100 realizations of uncertainty. The circles represent the FSTMPC while the crosses is the unconstrained optimal.

n	m	N	μ	QP Size	Exact(s)	FTSMPC(s)
2	2	10	2	80/3272	1.8	0.1
2	2	15	2	120/4892	2.5	0.2
2	2	30	2	240/9752	4.4	0.4
3	3	5	2	60/ 9726	5.7	0.6
3	3	10	2	120/19356	14.4	1.3
3	3	15	2	180/28986	15.0	1.6
4	4	5	2	80/51496	34.2	3.2
4	4	10	2	160/102736	57.0	6.6
4	4	15	2	240/153976	116.6	12.7

TABLE 4.3: Time taken to solve each QP for Randomly Generated Examples

which can be exploited to solve the QP efficiently.This method solves an optimization problem with linear equality and inequality constraints by reducing it to a sequence of linear equality constrained problems, which is solved using Newton's methods.The equality constrained minimization problem is reduced to an unconstrained problem, in particular, reduced to a system of linear equations. The computational time using a basic primal barrier method is made faster without significant decrease in the quality of control law by fixing the barrier parameter and maximum number of Newton iterations. The computational improvement is

shown using two examples. The first example shows the degree of sub-optimality of the QP solution obtained by using the Approximate Primal Barrier Method as compared to solving it exactly is minimal. The second example shows the timing profiles compared to using a generic optimization solver for a random system with varying model order, prediction horizon, number of inputs and tube layers. As a consequence the computational complexity grows linearly with the horizon length as opposed to cubicly if structure is not exploited.

Chapter 5

TSMPC for Systems with Time Correlated Uncertainty

In this chapter the TSMPC algorithm applied to linear systems with hard and probabilistic constraints is adapted to handle the case where the model uncertainty is not time-invariant and temporally independent. Time correlated uncertainty for any probability distribution is relevant in real-world applications modeled using discrete time models because if the sampling time $[t, t + \delta t]$ is small. An example in the field of renewable wind energy is the control of variable pitch wind turbine blades [55]. Pitch control of blades is used to ensure that the energy captured is limited which is important for the safety and overall efficiency of the wind turbine operation.

For a typical wind turbine, the area spanned by the rotor blades covers an area of up to 10^3m^2 and therefore mean and turbulent components of wind speeds at different points of the area varies significantly. This fluctuation of the wind speed produces cyclic perturbations to the aerodynamic thrust force and rotational torque that must be supported by the blades. Furthermore, some frequency components of these perturbations propagate down the drive-train and structure.

These aerodynamic loads have a direct impact on the cost of energy. In fact, they reduce the useful life of the wind turbine and deteriorate the quality of the power supplied to the grid. Increasingly, modern wind turbines include control systems that mitigate these loads. The uncertainty caused by the change of wind speed and direction is modeled more accurately with a temporally dependent distribution. Therefore, control systems which are able to take into account time-correlated uncertainty performs better.

When the uncertainty is not temporally independent, an infinite horizon cost function based on the expected value of a quadratic stage cost cannot be written compactly as a quadratic expression in terms of the degrees of freedom. However, an infinite horizon cost function based on the nominal trajectory generated by an uncertainty-free system can be defined. Constraints are handled using the same strategy of defining a sequence of overlapping tubes, corresponding to a sequence of confidence levels depending on time-step k on the predicted future plant state, and imposing a set of constraints the one-step-ahead predictions. A guarantee of the recursive feasibility of the online optimization ensures the closed loop system trajectories satisfy both hard and soft constraints. The approach is illustrated by a numerical example.

5.1 Problem Description

Consider the discrete-time system model and uncertainty description

$$x_{k+1} = \hat{A}_k x_k + \hat{B}_k u_k + \hat{d}_k \tag{5.1}$$

$$\begin{bmatrix} \hat{A}_k & \hat{B}_k & \hat{d}_k \end{bmatrix} = \begin{bmatrix} \hat{A}^0 & \hat{B}^0 & 0 \end{bmatrix} + \sum_{j=1}^{\rho} \begin{bmatrix} \hat{A}^{(j)} & \hat{B}^{(j)} & \hat{d}^{(j)} \end{bmatrix} q_{jk} \tag{5.2}$$

where $x \in \mathbb{R}^n$, $u \in \mathbb{R}^m$, $\hat{d} \in \mathbb{R}^n$ denote the model state, control input and an additive disturbance, and q_{jk} denotes a random variable with a finitely supported distribution as in previous chapters, $\{q_{i,k}, q_{j,k}\}$ are assumed to be independent for $i \neq j$, but $\{q_{j,k}, q_{j,k+1}, \ldots\}$ are not identically distributed and temporally independent.

5.1.1 Time-correlated uncertainty

Let $q_k = [q_{1k}, \ldots, q_{\rho k}]^T$ then the sequence of random variables $\{q_1, q_2, \ldots\}$ is assumed to be generated by

$$q_{k+1} = \lambda q_k + v_k \tag{5.3}$$

where λ is a scalar and $v_k = [v_{1k}, \ldots, v_{\rho k}]^T$ is a random vector drawn from a symmetric, unimodal, and finitely supported distribution which is identical and independently distributed with mean $\mathbb{E}(v_k) = 0$ and variance $\mathbb{E}(v_k v_k^T) = \sigma_v^2 I$. It can be assumed without loss of generality that the scalar λ satisfies $0 \leq \lambda < 1$ since v_k has a symmetric distribution about 0 and hence (as we show below) q_k is also symmetrically distributed. It can also be assumed without loss of generality that $q_0 = 0$. For example, even if $q_0 \neq 0$, q_k can be treated as consisting of a deterministic and zero-mean random component, $q_k = \hat{q}_k + \tilde{q}_k$ where

$$\hat{q}_{k+1} = \lambda \hat{q}_k + \mathbb{E}(v_k), \quad \hat{q}_0 = q_0, \tag{5.4a}$$

$$\tilde{q}_{k+1} = \lambda \tilde{q}_k + v_k - \mathbb{E}(v_k) \quad \tilde{q}_0 = 0. \tag{5.4b}$$

Note that with $q_0 = 0$, (5.3) is equivalent in distribution with

$$q_{k+1} = q_k + \lambda^k v_k. \tag{5.5}$$

Using the z-transform on (5.3) the system Z transfer function $F(z)$ can be treated as a low pass filter. $F(z)$ can be used to shape the power spectral density function of the disturbance. White noise have a flat power spectral density. The output from the low pass filter simulates the 1st and 2nd moments of an arbitrary random process when driven by a white noise input.

It is now shown that the random vector q_k has a finite support for all k and for $0 \leq \lambda < 1$ with $q_0 = 0$. If (5.3) is generated for $k = 1, 2, \ldots$, then the limit as $k \to \infty$

$$\lim_{k\to\infty} q_k = \lambda^{k-1} v_0 + \lambda^{k-2} v_1 + \ldots + v_k$$

If $|v_k| \leq \bar{v}$ then

$$\begin{aligned}\lim_{k\to\infty} |q_k| &\leq \bar{v}(1 + \lambda + \lambda^2 + \ldots + \lambda^{k-1}) \\ &= \bar{v}\frac{1-\lambda^k}{1-\lambda}.\end{aligned}$$

Therefore the elements of the random vector q_k are bounded by $|q_k| \leq \bar{v}\frac{1-\lambda^k}{1-\lambda}$ for all k.

The variance of q_{k+1} is denoted $\mathbb{E}(q_{k+1}q_{k+1}^T) = \Sigma_{k+1}$ and from (5.3), and assuming that $\mathbb{E}(q_k^T v_k) = 0$, it satisfies the following equation

$$\begin{aligned}\Sigma_{k+1} &= \mathbb{E}\left((\lambda q_k + v_k)(\lambda q_k + v_k)^T\right) \\ &= \lambda^2 \mathbb{E}(q_k q_k^T) + \mathbb{E}(v_k v_k^T) \\ &= \lambda^2 \Sigma_k + \sigma_v^2 I. \end{aligned} \tag{5.6}$$

If $0 \leq \lambda < 1$, (5.6) is stable and converges to a steady state value. By defining the steady state variance to be $\lim_{k\to\infty} \Sigma_k = \Sigma_{ss}$, then the steady state variance

is given by

$$\Sigma_{ss} = \frac{1}{1-\lambda^2}\sigma_v^2 I. \tag{5.7}$$

The support of the random variable is defined as $|q_k| \leq \bar{q}_k$ where $\bar{q}_k$ is generated by $\bar{q}_{k+1} = \lambda\bar{q}_k + \bar{v}$. Hence, for $0 \leq \lambda < 1$, $\bar{q}_k$ increases monotonically to the steady state value $q_{ss} = \frac{\bar{v}}{1-\lambda}$.

5.1.2 Confidence regions

Let $Q_k(p)$ denote the polytopic confidence region containing q_k with probability p (i.e. $Pr(q_k \in Q_k(p)) = p$), where $Q_k(p) = \{q : |q| \leq \theta_k(p)\}$. We next show that $Q_k(p)$ increases monotonically with k, since $\theta_{k+1}(p) \geq \theta_k(p)$, under a mild condition on v. Define f_v to be the probability density function where the random vector v_k is drawn from at time k and for convenience (without loss of generality), consider the case of scalar v. The cumulative density function is then defined by $F(x) = \int_{-\infty}^{x} f_v(v)dv$. The cumulative distribution function for (5.3) is given by

$$\begin{aligned} F_{q_{k+1}}(\theta) &= Pr(q_{k+1} \leq \theta) \\ &= \int_{-\infty}^{\infty}\int_{-\infty}^{(\theta-q)/\lambda} f_{q_k}(q).f_v(v)dqdv. \end{aligned}$$

Since (5.3) is equivalent in distribution with (5.5), then

$$F_{q_{k+1}}(\theta) = \int_{-\infty}^{\infty}\int_{-\infty}^{\theta-\lambda^k v} f_{q_k}(q)dq f_v(v)dv$$

and noting that $\int_{-\infty}^{\theta-\lambda^k v} f_{q_k}(\theta)dq = F_{q_k}(\theta - \lambda^k v)$ which therefore yields

$$F_{q_{k+1}}(\theta) = \int_{-\infty}^{\infty} F_{q_k}(\theta - \lambda^k v) f_v(v)dv. \tag{5.8}$$

Lemma 4. If f_v and f_{q_k} are be unimodal and symmetric then

$$f_{q_{k+1}}(\theta) = \int_{-\infty}^{\infty} f_{q_k}(\theta - \lambda^k v) f_v(v) dv \tag{5.9}$$

is also symmetric and unimodal .

Proof. The proof is given in [56]. □

Throughout this chapter, we assume that f_v is symmetric and unimodal, so f_{q_k} is symmetric and unimodal for all k by Lemma 4.

Lemma 5. If q_k is generated by (5.3) with $q_0 = 0$ and $|q_k| \leq \theta_k(p)$ with probability p, then $\theta_{k+1}(p) \geq \theta_k(p)$ for all k, for any given $p \in [0, 1]$.

Proof. The proof is to show that $F_{q_{k+1}}(\theta) \leq F_{q_k}(\theta)$ for any $\theta > 0$ where $F(x)$ is the cumulative distribution function (CDF) for a given probability density function (PDF) $f(x)$ and we consider (without loss of generality) the case of scalar q_k and v_k. An example of a CDF is shown in Figure 5.1. Since f_{q_k} is by assumption, symmetric and unimodal, the following inequality holds for all $v' \geq 0$ and $\theta \geq 0$

$$0 \leq F_{q_k}(\theta + v') - F_{q_k}(\theta) \leq F_{q_k}(\theta) - F_{q_k}(\theta - v') \tag{5.10}$$

From (5.10) we have, for $\theta \geq 0$ and all $v \geq 0$:

$$F_{q_k}(\theta + \lambda^k v) f_v(v) - F_{q_k}(\theta) f_v(v) \leq F_{q_k}(\theta) f_v(v) - F_{q_k}(\theta - \lambda^k v) f_v(v)$$

Therefore, for all $\theta \geq 0$ we have

$$2 \int_{-\infty}^{0} F_{q_k}(\theta) f_v(v) dv \geq \int_{0}^{\infty} F_{q_k}(\theta - \lambda^k v) f_v(v) dv + \int_{0}^{\infty} F_{q_k}(\theta + \lambda^k v) f_v(v) dv$$

and since $f_v(v)$ is symmetric, it follows that

$$F_{q_k}(\theta) \geq \int_0^\infty F_{q_k}(\theta - \lambda^k v) f_v(v) dv + \int_{-\infty}^0 F_{q_k}(\theta - \lambda^k v) f_v(v) dv.$$

From (5.8), the RHS of this inequality is $F_{q_{k+1}}(\theta)$, so this completes the proof that $F_{q_{k+1}}(\theta) \leq F_{q_k}(\theta)$. Consequently, if $F_{q_k}(\theta_k) = p$, then $F_{q_{k+1}}(\theta_{k+1}) = p$ only if $\theta_{k+1} \geq \theta_k$. □

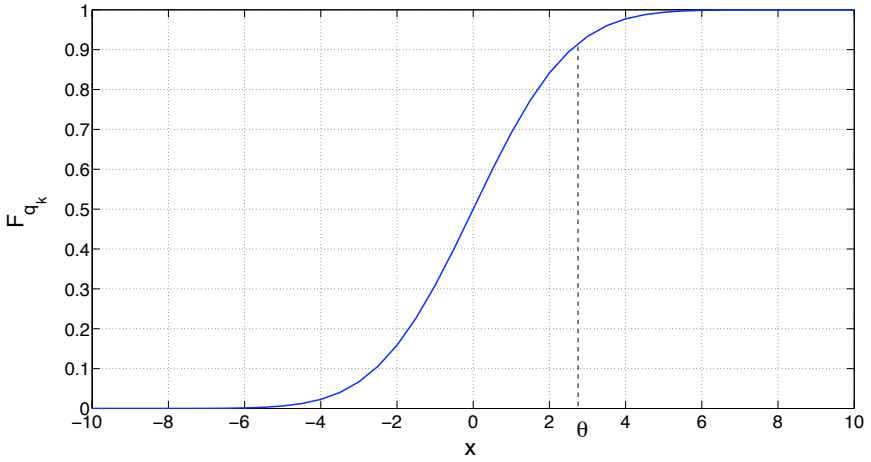

FIGURE 5.1: Plot of a CDF $F_{q_k}(x)$.

5.1.3 Input and state constraints

Using the closed-loop paradigm, the predicted control sequence at time k is given by

$$\begin{aligned} u_{k+i|k} &= \hat{K} x_{k+i|k} + c_{i|k} \quad i = 0, 1, \ldots, N-1 \quad \textit{Mode 1} \\ c_{i|k} &= 0, \quad i = N, N+1, \ldots \quad \textit{Mode 2} \end{aligned} \tag{5.11}$$

where $c_{i|k}$, $i = 0, \ldots, N-1$ are free optimization variables.

Combining (5.11) with the transformation $z = Vx$ allows (5.1) to be reformulated as

$$z_{k+i|k} = \Phi_{k+i|k} z_{k+i|k} + B_{k+i|k} c_{i|k} + d_{k+i|k} \tag{5.12}$$

where from (5.2), we have

$$[\Phi_{k+i|k}\ B_{k+i|k}\ d_{k+i|k}] = [\Phi^0\ B^0\ 0] + \sum_{j=1}^{\rho} [\Phi^{(j)}\ B^{(j)}\ d^{(j)}] q_{jk}$$

with Φ^0,B^0,d^0 and $\Phi^{(j)}$,$B^{(j)}$,$d^{(j)}$ defined by

$$\Phi^0 = V(\hat{A}^0 + \hat{B}^0 \hat{K})W, \quad B^0 = V\hat{B}^0, \quad d^0 = V\hat{d}^0$$
$$\Phi^{(j)} = V(\hat{A}^{(j)} + \hat{B}^{(j)} \hat{K})W, \quad B^{(j)} = V\hat{B}^{(j)}, \quad d = V\hat{d}^{(j)}$$

In this setting the control law of (5.11) can be rewritten as

$$u_{k+i|k} = K z_{k+i|k} + c_{i|k}, \quad K = \hat{K} V^{-1}. \tag{5.13}$$

The constraints imposed on the system are hard constraints and probabilistic (soft) constraints. The hard and soft constraints on the transformed system take the form

$$\psi_k^H = F_H z_k + G_H c_k \leq h_H \tag{5.14}$$
$$\psi_k^S = F_s z_k + G_s c_k \leq h_S. \tag{5.15}$$

Hard constraints (5.14) are constraints which can not be violated at any time. The probabilistic constraints (5.15) instead are constraints which can be violated at any given time k, but with the average rate of violation over a fixed horizon N_c

must not exceed a specified bound $\frac{N_{max}}{N_c}$

$$\frac{1}{N_c}\left\{\sum_{i=1}^{N_c} Pr\{F_s z_{k+i} + G_s c_{k+i} > h_S\}\right\} \leq \frac{N_{max}}{N_c}. \tag{5.16}$$

We define nominal trajectory of the system by

$$\overline{x}_{k+i+1|k} = \hat{A}^0 \overline{x}_{k+i|k} + \hat{B}^0 \overline{u}_{k+i|k}, \quad \overline{x}_{k|k} = x_k. \tag{5.17}$$

Here $\overline{x}_{k+i|k}$ denotes the nominal state prediction i at time k and does not denote the expectation, i.e. $\overline{x}_{k+i|k} \neq \mathbb{E}(\overline{x}_{k+i|k})$. The corresponding nominal input prediction $\overline{u}_{k+i|k} = \hat{K}\overline{x}_{k+i|k} + c_{i|k}$ from (5.11) is substituted into (5.17) to give

$$\overline{x}_{k+i+1|k} = (\hat{A}^0 + \hat{B}^0\hat{K})\overline{x}_{k+i|k} + \hat{B}^0 c_{i|k}. \tag{5.18}$$

5.2 Constraint Handling

To handle constraints on the distribution of predicted states and inputs in a computationally efficient manner, the same method of using a sequence of μ nested tubes comprising of polytopes $Z_{i|k}^{(l)}$ centred on the nominal trajectory given by (5.18) in Mode 1 and polytopes $Z_t^{(l)}$ centred around the origin in Mode 2 is used.

The same strategy of constraining the probabilities that, for each i, the i-step-ahead predicted state lies in any particular set $Z_{i|k}^{(l)}$(or $Z_t^{(l)}$ for $i > N$) is utilized here again. This is ensured by constraining the probabilities of transition from $Z_{h|k}^{(m)}$ to $Z_{h+1|k}^{(l)}$, for $h = 0, 1, \ldots, N-1$ and from $Z_t^{(m)}$ to $Z_t^{(l)}$, to be no less than p_{lm} for $l, m = 1, \ldots, \mu$. Further constraints are imposed in order to ensure that the probability of violating system constraints at prediction time $i+1$ does not exceed p_l for $l = 1, \ldots, \mu$ whenever the i-step-ahead predicted state lies within $Z_{i|k}^{(l)}$(or $Z_t^{(l)}$ for $i > N$). One of the main advantages of this strategy as demonstrated here, is

the ability to handle more general cases, where the uncertainty distributions are not independent and identically distributed. Furthermore, this method provides a more computational tractable algorithm over explicit computation of distributions using multivariate integrations or Monte Carlo methods which are computationally intensive and hence limit application to systems of small order.

The distributions for q_k are finitely supported, time-varying and converge to a steady state distribution as $k \to \infty$. Polytopic confidence regions, as explained in Chapter 3, are utilized to express sufficient conditions for satisfaction of probabilistic and hard constraints in the form of deterministic linear constraints. The difference here is that the polytopic confidence regions ($Q_k(p)$ in q-space) are time varying and hence at time k, $Q_k(p)$ is defined in terms of its vertices $q_k^{(s)}(p), s = 1, \ldots, v$ with the property $Pr\{q_k \in Q_k(p)\} \geq p$. After a finite number of time-steps k, we set $Q_k(p)$ equal to a steady state and hence a constant confidence region which is denoted $Q_t(p)$.

The probabilities p_{lm}, p_l for $l, m = 1, \ldots, \mu$ are design parameters chosen such (3.31a)-(3.31c) and (3.36) in Chapter 3 are satisfied. In summary, the hard constraint (5.14) and the probabilistic bounds (5.16) on the predicted number of violations of the soft constraint (5.15), are satisfied via the following constraints:

1. terminal constraint
2. one-step-ahead transitional probability constraints
3. universality constraint on outer polytope
4. one-step-ahead constraint violation probability
5. feasibility of outer polytope w.r.t hard constraint
6. nestedness constraint

The above constraints can be ensured respectively by invoking a set of inequalities involving the vertices of the polytopes defining the tubes and the vertices of the polytopic confidence regions, $Q_k(p)$ at time k (as the derivations of these linear inequalities are similar, it is not repeated here and the reader is referred back to Chapter 3):

$$\left| z^c_{k+N|k} + D_r \overline{z}^{(l)}_{k+N|k} \right| \leq \overline{z}^{(l)}_T \tag{5.19}$$

$$\begin{aligned} \Big| \Phi(q^{(s)}_{k+i|k}(p_{ml}))[z^c_{k+i|k} + D_r \overline{z}^{(l)}_{k+i|k}] + B(q^{(s)}_{k+i|k}(p_{ml}))c_{i|k} + d(q^{(s)}_{k+i|k}(p_{ml})) \\ - z^c_{k+i+1|k} \Big| \leq \overline{z}^{(m)}_{k+i+1|k} \end{aligned} \tag{5.20a}$$

$$\left| \Phi(q^{(s)}_t(p_{ml}))D_r \overline{z}^{(l)}_T + d(q^{(s)}_t(p_{ml})) \right| \leq \overline{z}^{(m)}_T \tag{5.20b}$$

$$\begin{aligned} \Big| \Phi(q^{(s)}_{k+i|k}(1))[z^c_{k+i|k} + D_r \overline{z}^{(\mu)}_{k+i|k}] + B(q^{(s)}_{k+i|k}(1))c_{i|k} + d(q^{(s)}_{k+i|k}(1)) \\ - z^c_{k+i+1|k} \Big| \leq \overline{z}^{(\mu)}_{k+i+1|k} \end{aligned} \tag{5.21a}$$

$$\left| \Phi(q^{(s)}_t(1))D_r \overline{z}^{(\mu)}_T + d(q^{(s)}_t(1)) \right| \leq \overline{z}^{(\mu)}_T \tag{5.21b}$$

$$\begin{aligned} F_S \Big\{ \Phi(q^{(s)}_{k+i|k}(1-p_l))[z^c_{k+i|k} + D_r \overline{z}^{(l)}_{k+i|k}] + B(q^{(s)}_{k+i|k}(1-p_l))c_{i|k} \\ + d(q^{(s)}_{k+i|k}(1-p_l)) \Big\} + G_S c_{i+1|k} \leq h_S \end{aligned} \tag{5.22a}$$

$$F_S \left\{ \Phi(q^{(s)}_t(1-p_l))D_r \overline{z}^{(l)}_T + d(q^{(s)}_t(1-p_l) \right\} \leq h_S \tag{5.22b}$$

$$F_H[z^c_{k+i|k} + D_r\overline{z}^{(\mu)}_{k+i|k}] + G_H c_{i|k} \leq h_H \tag{5.23a}$$

$$F_H D_r \overline{z}^{(\mu)}_T \leq h_H \tag{5.23b}$$

$$\overline{z}^{\mu}_{i|k} \geq \overline{z}^{\mu-1}_{i|k} \geq \ldots \geq \overline{z}^{1}_{i|k} > 0 \tag{5.24a}$$

$$\overline{z}^{\mu}_{T} \geq \overline{z}^{\mu-1}_{T} \geq \ldots \geq \overline{z}^{1}_{T} > 0 \tag{5.24b}$$

The terminal set parameters $\{\overline{z}^{(l)}_t \, l = 1, \ldots, \mu\}$ are determined off-line by:

$$\max_{\overline{z}^{(l)}_T \, l=1,\ldots,\mu} \prod_{l=1}^{\mu} \text{prod}(\overline{z}^{(l)}_T) \quad \text{s.t. (5.20b), (5.21b), (5.22b), (5.23b)and(5.24b)} \tag{5.25}$$

which maximizes the products of the volumes of $Z^{(l)}_T$, $l = 1, \ldots, \mu$ thereby making the terminal constraints (5.19) less stringent hence enlarging the region of attraction of the proposed method.

5.3 The Receding Horizon Algorithm

For a stochastic system, the predicted states will be random over a prediction horizon and the corresponding cost will also be random. Therefore, a suitable cost is defined by using the expectation operator, as previously defined in Chapter 3 given by

$$J_k = \sum_{i=0}^{\infty} \mathbb{E}_k(x^T_{k+i} Q x_{k+i} + u^T_{k+i} R u_{k+i}).$$

However, for the case of temporally dependent random variables such as the one generated by (5.3) the expected cost function given above is unsuitable. One of the

main advantages of using an expected value of the infinite cost function is that it is finitely parameterized in terms of a quadratic function of c_k as shown in (3.57a). This can be done with an assumption that the random variables are independent. With the assumption of independence, it is shown that $\lim_{i\to\infty} E_k(z_{k+i}) = 0$ if there exist a positive definite matrix P such that $P - \hat{\Psi}^{(0)T} P \hat{\Psi}^{(0)} - \sum_{s=1}^{\rho} \hat{\Psi}^{(s)T} P \hat{\Psi}^{(s)} > 0$ as shown in Lemma 3. On the other hand, the recursion of (5.1) (rewritten in terms of an augmented autonomous state space form, as given in (3.43) in Section 3.4.1) gives:

$$\begin{aligned}
\chi_1 &= \hat{\Psi}_0 \chi_0 + \tilde{d}_0, \\
\chi_2 &= \hat{\Psi}_1 \hat{\Psi}_0 \chi_0 + \hat{\Psi}_1 \tilde{d}_0 + \tilde{d}_1, \\
\chi_3 &= \hat{\Psi}_2 \hat{\Psi}_1 \hat{\Psi}_0 \chi_0 + \hat{\Psi}_2 \hat{\Psi}_1 \tilde{d}_0 + \hat{\Psi}_2 \tilde{d}_1 + \tilde{d}_2, \\
&\vdots
\end{aligned}$$

Taking the expectations yields

$$\begin{aligned}
\mathbb{E}(\chi_1) &= \hat{\Psi}_0 \chi_0 + \tilde{d}_0, \\
\mathbb{E}(\chi_2) &= \mathbb{E}(\hat{\Psi}_1 \hat{\Psi}_0) \chi_0 + \mathbb{E}(\hat{\Psi}_1 \tilde{d}_0) + \mathbb{E}(\tilde{d}_1), \\
\mathbb{E}(\chi_3) &= \mathbb{E}(\hat{\Psi}_2 \hat{\Psi}_1 \hat{\Psi}_0) \chi_0 + \mathbb{E}(\hat{\Psi}_2 \hat{\Psi}_1 \tilde{d}_0) + \mathbb{E}(\hat{\Psi}_2 \tilde{d}_1) + \mathbb{E}(\tilde{d}_2) \\
&\vdots
\end{aligned}$$

Since $\hat{\Psi}_0, \hat{\Psi}_1, \hat{\Psi}_2, \ldots$ and $\tilde{d}_0, \tilde{d}_1, \ldots$ are not independent, the expectations of the product of these terms needs to be evaluated, and over an infinite horizon, this is intractable.

Alternatively, to develop the receding horizon algorithm, a predicted cost to be optimized online can be defined as

$$J_k = \sum_{i=0}^{\infty} \overline{x}_{k+i|k}^T Q \overline{x}_{k+i|k} + \overline{u}_{k+i|k}^T R \overline{u}_{k+i|k}. \tag{5.26}$$

The predicted cost used here is a nominal performance index based on the nominal predicted trajectory of (5.18).

Theorem 5. The predicted cost above can be rewritten in terms of the degrees of freedom $c_k = \left[c_0^T, \ldots, c_{N-1}^T\right]^T$ and its minimization leads to the same optimal solution as the minimization of

$$J_k^c = c_k^T P_c c_k \tag{5.27}$$

where

$$P_c = \begin{bmatrix} B^{0T}P_xB^0 + R & 0 & \ldots & 0 \\ 0 & B^{0T}P_xB^0 + R & & 0 \\ \vdots & \vdots & \ddots & \\ 0 & 0 & \ldots & B^{0T}P_xB^0 + R \end{bmatrix}$$

and P_x is the solution of the $P_x - \Phi^{0T}P_x\Phi^0 = Q + \hat{K}^T R\hat{K}$.

Proof. By substituting (5.18) into (5.26) the following is obtained

$$\begin{aligned} J_k &= \sum_{i=0}^{\infty} \begin{bmatrix} \overline{x}_{k+i|k} \\ c_k \end{bmatrix}^T \begin{bmatrix} Q + \hat{K}^T R\hat{K} & e^T R\hat{K} \\ \hat{K}^T Re & e^T Re \end{bmatrix} \begin{bmatrix} \overline{x}_{k+i|k} \\ c_k \end{bmatrix} \\ &= \sum_{i=0}^{\infty} \begin{bmatrix} \overline{x}_{k+i|k} \\ c_k \end{bmatrix}^T \widetilde{Q} \begin{bmatrix} \overline{x}_{k+i|k} \\ c_k \end{bmatrix}. \end{aligned}$$

This is equivalent to

$$J_k = \begin{bmatrix} \overline{x}_{0|k} \\ c_k \end{bmatrix}^T P_z \begin{bmatrix} \overline{x}_{0|k} \\ c_k \end{bmatrix} \tag{5.28}$$

where P_z is the solution of the Lyapunov equation

$$P_z - \Psi^T P_z \Psi = \widetilde{Q} \tag{5.29}$$

and

$$\Psi = \begin{bmatrix} A^0 + B^0\hat{K} & B^0 E \\ 0 & M \end{bmatrix}, M = \begin{bmatrix} 0 & I & 0 & \dots & 0 \\ 0 & 0 & I & \dots & 0 \\ \vdots & \vdots & & & \vdots \\ 0 & 0 & 0 & \dots & 0 \end{bmatrix}, E = [I\ 0\ \dots\ 0].$$

where I is the $m \times m$ identity matrix. Partitioning $P_z = \begin{bmatrix} P_x & P_{xc} \\ P_{cx} & P_c \end{bmatrix}$ and expanding the cost function yields

$$J_k = \overline{x}_{0|k}^T P_x \overline{x}_{0|k} + 2\overline{x}_{0|k}^T P_{xc} c_k + c_k^T P_c c_k.$$

Define the optimal value for c_k to be c_k^*, that is

$$\begin{aligned} c_k^* &= \arg\min_{c_k} J_k \\ &\Rightarrow 2\overline{x}_{0|k}^T P_{xc} + 2P_c c_k^* = 0 \\ &\Rightarrow c_k^* = -P_c^{-1} P_{xc}^T \overline{x}_{0|k} \neq 0 \quad \forall \overline{x}_{0|k} \neq 0. \end{aligned}$$

If $\hat{K}$ is LQ optimal for (A^0, B^0), then $c_k^* = 0$, since c_k are perturbations away from the unconstrained optimal given by the linear feedback law $u_{k+i|k} = \hat{K} x_{k+i|k}$. thus implying that $P_{xc} = P_{cx} = 0$. Therefore (5.28) is written as

$$J_k = \overline{x}_{0|k}^T P_x \overline{x}_{0|k} + c_k^T P_c c$$

and (5.29) is written as two separate equations

$$P_x - (A^0 + B^0\hat{K})^T P_x (A^0 + B^0\hat{K}) = Q + \hat{K}^T R\hat{K}$$
$$P_c - M^T P_c M = E^T RE.$$

Since the first term of J_k is a constant, it can be ignored and P_c has the analytical solution as given. □

The algorithm is outlined as follows:

Algorithm 8. (TSMPC for Correlated Systems)

1. (OFF-LINE): Perform the optimization of (5.25) in order to maximize the invariant terminal sets.
2. (ONLINE): At each time instant $k = 0, 1, \ldots$ perform the optimization

$$\min_{\overline{z}^{(l)}_{k+i|k}, c_k} J_k \quad \text{s.t } (5.19), (5.20a), (5.21a), (5.22a), (5.23a), (5.24a) \tag{5.30}$$

3. Implement $u_k = Kz_k + c^*_{0|k}$ where c^* is optimal for (5.30).

Lemma 6. Using Lemma 5, if the constraint $\Phi(q_{ss})z + d(q_{ss}) \in \Omega_T \ \forall z \in \Omega_T$ is satisfied, it implies that $\Phi(q_k)z + d(q_k) \in \Omega_T \ \forall z \in \Omega_T, k = N, N+1, \ldots$.

Proof. The constraint above is ensured by the inequality constraints given by terminal constraint, (5.19) and universality constraints (5.21b). The polytopic confidence region $Q_t(p)$ in Mode 2 is chosen to be $Q_t = Q_{ss}$. Invoking (5.21b) for all the vertices of $Q_t(p)$ gives

$$-\overline{z}^{(\mu)}_T \leq \Phi(q) D_r \overline{z}^{(\mu)}_T + d(q) \leq \overline{z}^{(\mu)}_T$$

for all $q \in Q_t(1)$. Since $q_{k+1} > q_k$ is monotically increasing for $k = N, N+1, \ldots$ and converges to q_{ss} and since (5.21b) is affine in q_k, it follows that the constraint is also feasible for all q_k, $k = N, N+1, \ldots$, if feasible for q_{ss}. □

Theorem 6. If the online optimization is feasible at initial time $k = 0$ then it is guaranteed to remain feasible and the closed-loop system state converges to the minimal robust invariant set for (5.1) under $u_k = Kx_k$ with no constraints.

Proof. Feasibility at time k implies feasibility at $k+1$ because shifting by one time instant all the previously computed trajectories, both in terms of the perturbations c and the polytopic upper bounds $\overline{z}^{(l)}$, will define at least one feasible set of trajectories. This follows from the fact that c is chosen to be zero in Mode 2, and from the terminal condition $Z^{(l)}_{k+N|k} \subseteq Z^{(l)}_T$ according to which the last element in Mode 1 of the feasible $\overline{z}^{(l)}$ trajectory can be chosen to be $\overline{z}^{(l)}_T$. Let c^*_k be a feasible trajectory computed from the online optimization and the corresponding optimal cost to be J^{c*}_k at time k. Then $Mc^*_k = c_{k+1}$ provides a feasible trajectory for the next time step $k+1$. Then the following is true

$$
\begin{aligned}
&J^{c*}_{k+1} \leq J^c_{k+1} \leq c_k^T M^T P_c M c_k = c_k^T P_c c_k - c_k^T E^T (B^{0T} P_x B^0 + R) E c_k \\
&\Leftrightarrow J^c_k - J^c_{k+1} \geq c_k^T E^T (B^{0T} P_x B^0 + R) E c_k
\end{aligned}
$$

Since $(B^{0T} P_x B^0 + R)$ is a positive definite matrix, the following inequality holds

$$J^c_k - J^c_{k+1} > 0.$$

and that $Ec_k \to 0$ as $k \to \infty$ which implies $u_k \to Kx_k$ which implies $x_k \to \mathcal{S}$ where $\mathcal{S}$ is the minimal robust invariant set under $u_k = Kx_k$ with no constraints. □

Theorem 7. If the online optimization is feasible at $k = 0$, then it remains feasible at all times $k = 1, 2, \ldots$ and consequently the closed loop system under the

algorithm satisfies the hard constraints (5.14) and the probabilistic bound (5.16) on soft constraints.

Proof. The proof is the same as Theorem 4 except with time varying polytopic confidence regions $Q_{k+i|k}(p)$. □

5.4 Numerical Example

As an example, the evolution of the probability density functions (pdfs) of the correlated random variables for $k = 1, \ldots, 10$ is shown in Figure 5.2. The pdfs are generated for the case of $\lambda = 0.5$ by firstly taking a discrete approximation of a uniform distribution and then recursively performing the convolution operation. When the distribution has reached a steady state, the constraints are time invariant across the prediction horizon. The steady state distribution is finitely supported on $[-2, 2]$ with mean $\mathbb{E}(q_k) = 0$ and variance of $\mathbb{E}(q_k q_k^T) = \sigma_{ss}^2 I$ where $\sigma_{ss}^2 = \frac{4}{9}$.

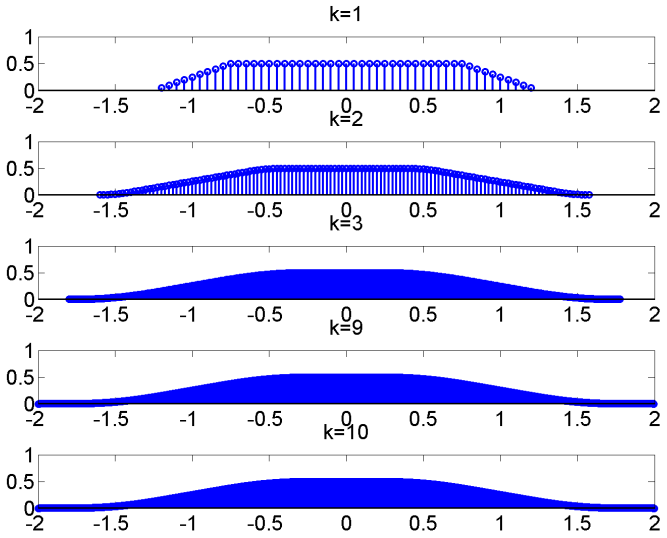

FIGURE 5.2: The evolution of the probability density function for $k = 1, \ldots, 10$ for $\mu = 0.5$. The pdfs approaches a steady state distribution as $k > 9$.

Consider the system for which the parameters of the model (5.1) and (5.2) are given by:

$$\hat{A}^0 = \begin{bmatrix} 1.2 & 0.1 \\ 0.1 & 1.26 \end{bmatrix} \quad \hat{A}^{(1)} = \begin{bmatrix} 0.1 & 0 \\ 0 & 0.1 \end{bmatrix} \quad \hat{A}^{(2)} = \begin{bmatrix} 0.1 & 0 \\ 0 & 0.1 \end{bmatrix}$$

$$\hat{B}^0 = \begin{bmatrix} 0.5 \\ 0.4 \end{bmatrix} \quad \hat{B}^{(1)} = \begin{bmatrix} 0 \\ 0 \end{bmatrix} \quad \hat{B}^{(2)} = \begin{bmatrix} 0 \\ 0 \end{bmatrix}$$

$$\hat{d}^0 = \begin{bmatrix} 0 \\ 0 \end{bmatrix} \quad \hat{d}^{(1)} = \begin{bmatrix} 0.02 \\ 0 \end{bmatrix} \quad \hat{d}^{(2)} = \begin{bmatrix} 0 \\ 0.2 \end{bmatrix}$$

For simplicity, consider only soft constraints on the system states defined by

$$F_s = \begin{bmatrix} 2 & 1 \\ -2 & -1 \end{bmatrix}, \quad G_s = \begin{bmatrix} 0 & 0 \\ 0 & 0 \end{bmatrix}, H_s = \begin{bmatrix} 1.8 \\ 1.8 \end{bmatrix}.$$

The prediction horizon for this example is chosen to be $N = 4$, and the cost of (5.26), for $Q = I$,$R = 1$, leads to the unconstrained optimal feedback law:

$$u = \hat{K}x, \quad \hat{K} = [1.8 \ -4.9].$$

The transition probability matrix and vector of constraint violation probabilities, for $\frac{N_{max}}{N_c} = 0.80$, are taken to be:

$$\Pi = \begin{bmatrix} p_{11} & p_{12} \\ p_{21} & p_{22} \end{bmatrix} = \begin{bmatrix} 0.9 & 0.3 \\ 1 & 1 \end{bmatrix}, \quad p = \begin{bmatrix} p_1 \\ p_2 \end{bmatrix} = \begin{bmatrix} 0.4 \\ 0.95 \end{bmatrix}.$$

where these values satisfy $\frac{1}{N_c}\sum_{i=0}^{N_c-1} p(T^{-1}\Pi)^i e_j \leq \frac{N_{max}}{N_c}$ $j = 1, 2$. The number of

overlapping tubes is taken to be $\mu = 2$. For the particular choice of $\hat{K}$, the eigenvalues of the nominal closed loop state matrix and eigenvector matrix respectively are given by

$$\Phi^{(0)} = \begin{bmatrix} 0.87 & 0 \\ 0 & 0.54 \end{bmatrix} \quad V = \begin{bmatrix} 5.3 & -7.9 \\ -4.4 & 8.4 \end{bmatrix}.$$

The results shown compares three algorithms, namely, the LQ Optimal feedback under $u_k = \hat{K}x_k$, the TSMPC with time invariant polytopic confidence regions, which is defined using the steady state distribution q_{ss}, (denoted TSMPC2a) and the algorithm presented in this Chapter, where time varying polytopic confidence regions are used, (denoted TSMPC2b).

The choice of initial condition has significant effect on the performance of the TSMPC2b algorithm when comparing with the LQ Optimal feedback case and TSMPC2a. A set of initial points are chosen from a grid of $z_1 \in [-5, 5]$ and $z_2 \in [-20, 20]$. For initial points which start inside the feasible set (does not violated any constraints at time $k = 0$) the performance of TSMPC2b over the other algorithm as measured by the sum of stage costs is the same. Furthermore, all algorithm are feasible with respect to the constraints. Therefore, there is no clear advantage of using the TSMPC2b algorithm for points inside the feasible set. For points outside the feasible set, as an example if f $z_0 = [-5\ 20]^T$ is chosen, the advantage of using TSMPC2b can be better highlighted.

Figure 5.3 show the closed loop response for the states over 100 realizations of the uncertain sequence $(q_k, k = 1, \ldots, 20)$ for an initial condition of $z_0 = [-5,\ 20]^T$. The terminal sets computed off-line are $\overline{Z}_t^{(1)} = [0.45,\ 1.43]^T$ and $\overline{Z}_t^{(2)} = [0.50,\ 1.61]^T$. The corresponding closed loop response for the input and states are shown in Figure 5.4 and 5.5.

Firstly the nominal closed loop cost for the 3 cases are compared. The nominal closed loop cost are: 837.1 (for LQ Optimal), 954.2 (for TSMPC2a), and 910.2 (for TSMPC2b). As expected, LQ optimal control achieves a lower value of nominal closed loop cost but achieves this at the expense of violating the probabilistic constraint of the problem. TSMPC2b achieves are much higher cost but is feasible with respect to the probabilistic constraints. TSMPC2b achieves a lower closed loop cost compared to TSMPC2a.

The frequency of soft constraint violations over a horizon of N_c is shown in Table 5.1. Indeed, for LQ Optimal control the worst constraint violation rate is exhibited in the first 3 steps of the closed loop response, during which the expected number of constraint violations equal to 0.96, clearly exceeding the allowable limit of $\frac{N_{max}}{N_c} = 0.8$. By contrast the worst expected constraint violation rate for the TSMPC2a algorithm over any 3-step interval is 0.35 which is within the allowable limit. TSMPC2b achieves a less conservative result of 0.43. The reason here is that since the polytopic confidence regions are time-varying and this information is included in the receding horizon optimization, a less conservative result is obtained in terms of soft constraint violations and a lower closed loop cost.

k	0	1	2	3	4	5
LQ Optimal	100	87	90	100	100	100
TSMPC2a	100	6	0	0	0	0
TSMPC2b	100	30	0	0	0	0

TABLE 5.1: Soft constraint violations for under LQ optimal control, TSMPC2a, and TSMPC2b at time step k over a horizon N_c over 100 realizations of uncertainty.

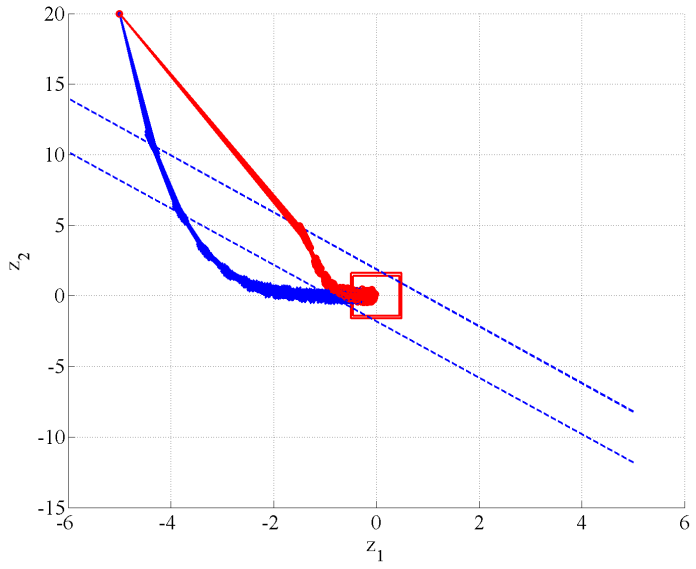

FIGURE 5.3: Plot of the trajectories of z_k for k=1, . . . , 6 and 100 realizations. The blue line shows the trajectory under the unconstrained LQ Optimal control while the red is under the TSMPC algorithm. The dotted line shows the soft constraints imposed on the states. The red polytopes are the terminal sets.

5.5 Conclusion

The TSMPC algorithm applied to linear systems with hard and probabilistic constraints is adapted to handle the case where the model uncertainty is not temporally independent. When the uncertainty is not temporally independent, an infinite horizon cost function based on expected value of a quadratic stage cost cannot be written compactly as a quadratic expression in terms of the degrees of freedom. However, an infinite horizon cost function based on the nominal trajectory generated by uncertainty free system can be defined. Constraints are handled using the same strategy of defining a sequence of overlapping tubes, corresponding to a sequence of confidence levels depending on time-step k on the predicted future plant state, and imposing a set of constraints the one-step-ahead predictions. A guarantee of the recursive feasibility of the online optimization ensures the closed loop system trajectories satisfy both hard and soft constraints. It was shown that the TSMPC algorithm adapted to handle temporally dependent uncertainty is less

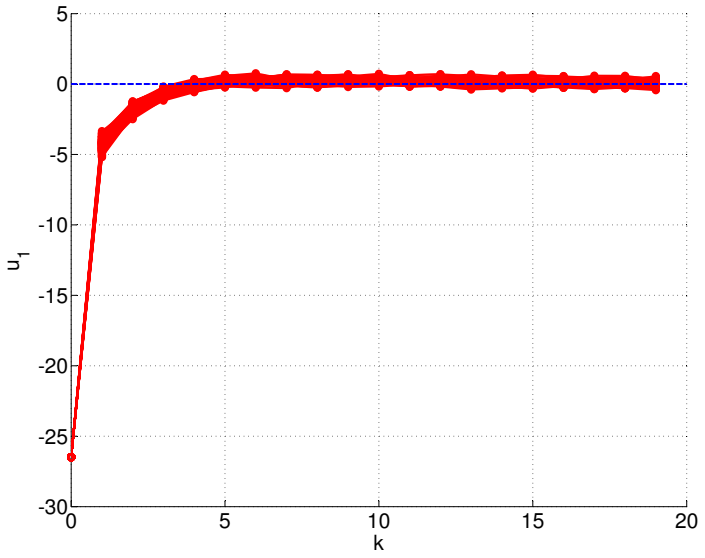

FIGURE 5.4: Plot of the input trajectories $u_k = \hat{K}x_k + c_k$ for the 100 realizations of uncertainty for algorithm TSMPC2b.

conservative compared to the case where the original TSMPC algorithm for the case of temporally independent uncertainties.

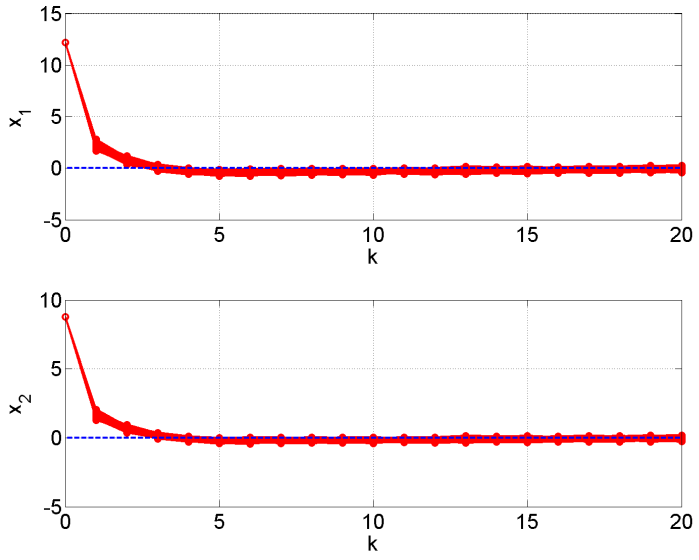

FIGURE 5.5: Plot of the state trajectories in the x domain for the 100 realizations of uncertainty for algorithm TSMPC2b.

Chapter 6

Application of TSMPC to Sustainable Development

6.1 Problem Description

6.1.1 The Sustainable Development Problem

Model Predictive Control (MPC) solves, in a receding horizon manner, a series of open-loop optimization problems, thus providing tractable solutions to an infinite horizon constrained optimal control problem. It can be applied to wider class of problems, where the aim is to maximize a suitably defined benefit while keeping risk or cost within constraints. One such problem is prevalent in the field of Sustainable Development (SD). Sustainable Development is defined by the United Nations as 'development that meets the needs of the present without compromising the ability of future generations to meet their own needs' [57]. In this context, the sustainable development paradigm needs to be incorporated in the decision making process. An example of a decision making process is the resource allocation problem where a finite amount of resource needs to be allocated to maximize

benefit or minimize cost. Therefore the quantitative assessment of policies needs to reflect the tradeoff between the pattern of present resource consumption and in the future. A purely quantitative assessment (as opposed to quasi-quantitative or qualitative) is needed to allow a direct objective comparison of one policy against another. This is equivalent to a constrained optimization of future benefits over a given time horizon. At all future times, the sustainable development context will still be relevant and therefore the optimization is effectively performed in a receding horizon manner, making it similar with MPC.

Predicting how current development will affect the potential for development in the future is inherently random. Assuming there is some statistical regularity, a stochastic model can be used to generate predictions. The resource allocation problem (SD problem) here concerns the allocation of research and development investments between different power generating technologies. Several measures of performance can be used which include price of energy and CO_2 emissions. Constraints can be placed on these measures such as a limit on CO_2 emission in 3 years time. The goal here is therefore to allocate investments to give the 'best' measure of predicted performance subject to constraints. The stochastic model used to make predictions is an economic model called 'Prometheus' [58]. In MPC terms, this is equivalent to controlling a system subject to model parameter uncertainty and additive disturbance. Hence, the Tube Stochastic MPC can be applied directly to solve the resource allocation problem.

This chapter is arranged as follows. In Section 1, the economic model Prometheus is further defined. Section 2 discusses the previous work on the SD problem. Section 3 describes the ARX model, which is used to give a closed-form approximate model of Prometheus. The application of the Tube Stochastic MPC to the SD problem is discussed in the Section 4. Finally, the numerical results and simulations are presented in Section 5.

6.1.2 Prometheus

Prometheus is an economic model which relates research and development (R&D) investments on 15 alternative power generating technologies to 8 measurable indicators [58]. These measurable indicators include energy cost or CO_2 emission and are classified by world region. It provides yearly outputs (indicators) with varying inputs (investments) for a prediction horizon of 30 years. Two types of predictions can be made using Prometheus namely 'deterministic outputs', where the uncertain model parameters are set to their mean values, and 'stochastic outputs', where a random sample of the uncertain parameters are taken from a known probability distribution. The aim of this chapter is only to highlight the applicability of the TSMPC algorithm to the SD problem and therefore for simplicity, the focus is only on two outputs and two inputs.The two outputs and inputs are

y_1**:** The energy cost for non-European signees of the Convention on the Organization for Economic Co-operation and Development (OECD).

y_2**:** The CO_2 emissions over the whole world.

u_1**:** R&D Investment on Gas Turbine in Combined Cycle (GCC) technology.

u_2**:** R&D Investment on Wind Turbine technology.

Inputs here are the spending levels (measured in arbitrary units) above an underlying baseline investment. The effect of this baseline investment is removed from the Prometheus outputs, so that all outputs reflect the consequence of additional investments. Consequently, all units on the inputs and outputs are ignored as these are now relative units. The assumption is made that over 30 years, the total amount of extra investments should lie within 0 to 10% of the baseline investment. This would form a budgetary constraint. For example, if 10% of the baseline investment into GCC technology is 6408, the sum of the yearly investments should not exceed this amount.

A distinction needs to be formed between yearly inputs (shocks) u_i and cumulative inputs v_i (stocks) which is the cumulative investment to current time, i.

The step responses obtained from the stochastic version of Prometheus, averaged over a large number of samples is shown in Figure 6.1. It shows that investments into either technology results in a decrease in CO_2 emissions over a 30 year period, which would be expected. However, investment in wind turbine technology (u_2) has a effect of increasing energy costs in the first 10 years. This is also expected due to higher initial costs associated with wind powered energy generation. An optimization based on minimizing expected energy cost alone would result in a bulk of investments going into GCC technology (u_1). With a TSMPC formulation of the optimization problem however, the variances (because we use the expected value of a quadratic cost) of the output responses are taken into account and therefore lead to a more balanced decision especially when probabilistic constraints on CO_2 emissions are imposed.

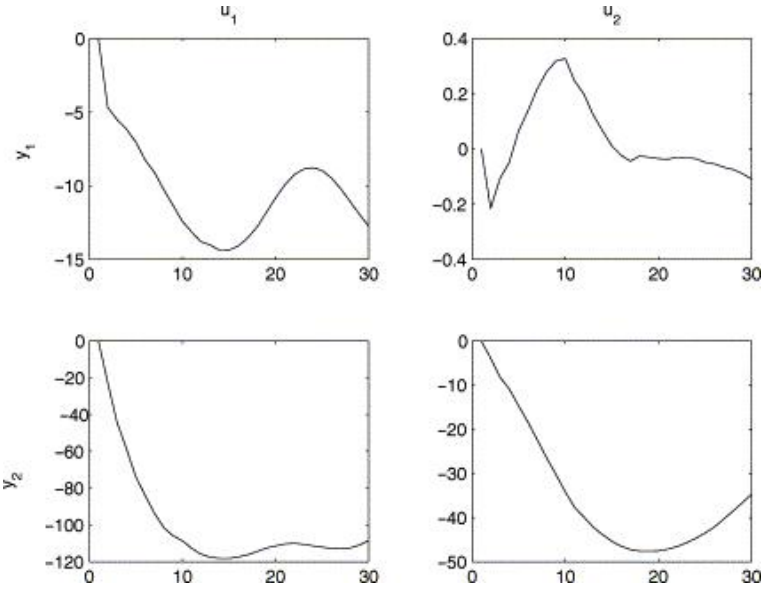

FIGURE 6.1: Prometheus responses to step changes in u_1 and u_2. Image source: [16]

6.2 Previous Work and Motivation

In this section previous solutions to the SD problem are described. An initial solution was a static formulation [59] where the static models are used through equations such as

$$y_i = r_i^T v \tag{6.1}$$

where y_i, i=1, . . . , 8 is an cumulative indicators associated with the various targets (CO_2, Energy Cost) over a 30 year period, r_i is a vector of impact coefficients associated with y_i and v is the vector of inputs (investment allocations, $v_j, j = 1, \ldots, 8$), associated with the different technologies. Due to the stochastic nature of Prometheus, the elements of r_i are random and assumed to be normal, $r_i \sim N(\rho_i, V_i)$. The mean and covariance matrix of the normal distribution are computed from Monte Carlo simulations.

The optimization problem can be posed in terms of expected values, however this would remove the significant stochastic components of the problem. Instead the optimization is cast in a stochastic (chance constrained) framework as

$$\max_u \Pr(y_1 > A_1) \tag{6.2a}$$

$$\text{s.t } \Pr(y_i > A_i) \geq p_i \tag{6.2b}$$

$$\sum_{i=1}^{15} v_j \leq B \tag{6.2c}$$

for a set of thresholds A_i, probabilities p_i, and budget B which provides a flexible tool for a multi-objective policy assessment. The multi-objective is such that the primary output y_1 is optimized while respecting constraints (probabilistic) on the other outputs (y_i). It is shown that for $p_i > 0.5$ the optimization is convex and

therefore has a unique optimum which can be computed reliably and efficiently using Second-Order Conic Programming (SOCP) [60].

Normalize the probabilistic constraints and rewrite them in the form of a second order conic constraint in the vector of decision variables, u:

$$\Pr(y_i > A_i) \geq p_i \tag{6.3a}$$

$$\Leftrightarrow \Pr(X > z_i) \geq p_i \text{ where } X \sim \mathcal{N}(0, I) \text{ and } z_i = \frac{\rho_i^T v - A_i}{\sqrt{v^T V_i v}} \tag{6.3b}$$

$$\Leftrightarrow \rho_i^T v - A_i \geq \kappa_i \sqrt{v^T V_i v} \text{ where } \Pr(X \leq \kappa_i) = p_i \tag{6.3c}$$

$$\Leftrightarrow \|V_i^{0.5} v\|_2 \leq \frac{1}{\kappa_i}(\rho_i^T v - A_i). \tag{6.3d}$$

Likewise, the objective function can be written in the same form.

$$\max_v \Pr(y_1 > A_1) \tag{6.4a}$$

$$= \max_v \Pr(X \leq z_1) \text{ where } X \sim \mathcal{N}(0, I) \text{ and } z_1 = \frac{\rho_1^T v - A_1}{\sqrt{v^T V_1 v}} \tag{6.4b}$$

$$= \min_v \frac{A_1 - \rho_1^T v}{\sqrt{v^T V_1 v}} \tag{6.4c}$$

$$= \min_{v,s} \ s \tag{6.4d}$$

$$\text{s.t. } \frac{A_1 - \rho_1^T v}{\sqrt{v^T V_1 v}} \leq s. \tag{6.4e}$$

Optimization (6.2) can be rewritten as

$$\min_{v,s} s \tag{6.5a}$$

$$\text{s.t. } \|V_i^{0.5} v\|_2 \leq \frac{1}{s}(\rho_1^T v - A_1) \tag{6.5b}$$

$$\text{s.t. } \|V_i^{0.5} v\|_2 \leq \frac{1}{\kappa_i}(\rho_i^T v - A_i) \tag{6.5c}$$

$$\sum_{i=1}^{15} v_j \leq B$$

The two main problems with the static formulation are that no consideration is given to closed-loop effects and the dynamic response of the economic model. Therefore there are no guarantees of feasibility and stability when applied in a receding horizon manner.

The budget allocation adjustments are applied once only at initial time and the optimization is based on cumulative effects of these changes to the output the end of the 30 year horizon, which is well beyond the transient behavior of outputs and therefore is a severe restriction. If the dynamics of the outputs are taken into account in the optimization problem this would lead to improvements in the optimal solution due to more degrees of freedom. The incorporation of the degrees of freedom requires a dynamic model which considers the dependence of $y_i(k+i|k)$, the i^{th} step ahead prediction of y_i at time k, on the past, current, and future predicted values of u_j. This forms the motivation for the work in [16, 20, 61, 62]

Two types of dynamic model are suitable for this application: an Auto Regressive Model with External inputs (ARX) model or a Moving Average (MA) model. Previous work has focused on MA models because it preserves the assumption that the predicted values are drawn from a normal distribution. The predictions are generated using the MA model recursively

$$y_i(k+1|k) = \sum_{j=1}^{2} \sum_{l=0}^{q-1} g_{ij}(l) v_j(k-l), \quad i = 1, 2 \tag{6.6}$$

where y_i refers to the actual rather than cumulative value of the i^{th} output. $g_{ij}(l)$ are the elements of the impulse respose from the j^{th} shock to the i^{th} output.

Using this dynamic model, a SMPC formulation is used. The SMPC formulation is divided to two phases. Phase 1 computes a set-point in some optimal manner while Phase 2 provide the receding horizon optimization which guides the primary output to the region above the set-point.

Phase 1:

$$\max_{v^{ss},A_1} A_1 \tag{6.7a}$$

$$\text{s.t.} \Pr(y_1^{ss} \geq A_1) \geq p_1 \tag{6.7b}$$

$$\Pr(y_i^{ss} \geq A_i) \geq p_i \quad i = 2, \ldots, n_y \tag{6.7c}$$

$$v^{ss} \leq B, \quad v^{ss} \geq 0 \tag{6.7d}$$

Phase 2:

$$\min_{v(k+l|l),s(l|k),t(l|k)} J(k) = \sum_{i=l}^{N} s^2(l|k) \tag{6.8a}$$

$$\text{s.t.} \quad s(l|k) \geq t(l|k) - t^{ss}, \; s(l|k) \geq 0 \tag{6.8b}$$

$$\Pr(y_1(k+l|k) \geq r - t(l|k)) \geq p_1 \quad l = 1, \ldots, N \tag{6.8c}$$

$$\Pr(y_1(k+l|k) \leq r + t(l|k)) \geq p_1 \quad l = 1, \ldots, N \tag{6.8d}$$

$$\Pr(y_i(k+l|k) \geq A_i) \geq p_i \quad l = 1, \ldots, N \tag{6.8e}$$

$$v_j(k+m+1|k) \geq v_j(k+m|k) \quad m = 0, \ldots, N-q \tag{6.8f}$$

$$v_j(k|k) \geq v_j(k-1) \tag{6.8g}$$

Linear combinations of normal distributions are themselves normal and this justifies the choice of MA models. The linear combinations involve products of random coefficients with past inputs which are deterministic. However MA models are non-parsimonious. By using an ARX model, the past inputs and outputs are used thus enabling a more suitable model. However, ARX predictions involve products terms of random coefficients with predicted output values, both which are random, and therefore do not have a normal distribution.

6.3 Using an ARX Model

The TSMPC in the previous section algorithm requires a (closed form) linear state-space model. Since Prometheus is a very detailed, nonlinear, and stochastic model, it is not feasible to write it in an analytic form for use with MPC. However, an approximation can be made by fitting a closed-form dynamic model to Prometheus. Here, an ARX model is used to approximate the predictions from Prometheus.

Prometheus is a multi-input multi-output (MIMO) model and hence each output can be modeled with an ARX model. Each of these outputs (y_1 and y_2) are represented separately by an ARX model which relates the current output to past outputs and inputs. The ARX model for the case of 1 of these outputs, y_1 with 2 inputs takes the form

$$A(z,\theta)y_1(k+1) = z^{-n_D}B_1(z,\theta)v_1(k) + z^{-n_D}B_2(z,\theta)v_2(k) + \varepsilon_1(k) \tag{6.9}$$

where n_D is the number of samples of delay and

$$\begin{aligned} A(z,\theta) &= 1 + a_1 z^{-1} + \ldots + a_{n_a} z^{-n_a} = 1 + \sum_{i=1}^{n_a} a_i z^{-i} \\ B_1(z,\theta) &= b_0^1 + b_1^1 z^{-1} + \ldots + b_{n_b}^1 z^{-n_b} = \sum_{i=0}^{n_b} b_i^1 z^{-i} \\ B_2(z,\theta) &= b_0^2 + b_1^2 z^{-1} + \ldots + b_{n_b}^2 z^{-n_b} = \sum_{i=0}^{n_b} b_i^2 z^{-i}. \end{aligned}$$

Note that $A(z,\theta)$ is monic (leading coefficient is 1). The number of parameters define the leading order of the poles (n_a), the leading order of the zeroes (n_{b1},n_{b2}), and z^{-1} is the backward shift operator. The parameter vector θ is then

$$\theta = [a_1 \ \ldots \ a_{n_a} \ b_0^1 \ \ldots \ b_{n_b}^1 \ b_0^2 \ \ldots \ b_{n_b}^2]^T. \tag{6.10}$$

and it is assumed that θ and $\varepsilon_1(k)$ are independent and identically distributed with a normal distribution:

$$\theta \sim \mathcal{N}(\overline{\theta}, \Theta) \tag{6.11}$$

$$\varepsilon_1(k) \sim \mathcal{N}(0, \sigma_1^2) \tag{6.12}$$

The mean $\overline{\theta}$, covariance matrix Θ, and noise variance σ_1^2 can be estimated by fitting the model to multiple realizations of Prometheus as will be explained in detail in the next section. Note that the normal distribution is only used as an approximation to model the parameter distributions and the noise, and this assumption needs to be validated. Model (6.9) can be used as a prediction model to predict future values based on past outputs and inputs.

6.3.1 Fitting the Model

In this section, the identification process to obtain estimates (denoted $\hat{\theta}$) of the approximation of the true system (denoted θ_0) is explained. The assumption is made that a good linear approximation of the true system, which is nonlinear and of unknown order, exists. The process consists of several steps and the main steps are detailed, all which follows standard procedure, (see e.g [63]).

Data Collection

The first step is to collect data from Prometheus. Since each input constitutes a shock at a given year, the total shocks in a 30 year time length is ensured to a predefined budget. Note that these shocks are relative to a baseline so any shocks are deemed as additional spending. Budgets are therefore given as a percentage of the baseline spend. Monetary investments are by definition positive, meaning that no divestments can be made. The budgetary constraint for investments to Wind

Energy Technology and Combined Gas Cycle Turbine are chosen to be 1510.1 and 6404.8 respectively.

One of the inputs is excited by a random input signal drawn from a uniform distribution with a range of $[0, 1]$ while the other inputs are set to zero. The input realization is then scaled so that the budgetary constraint is satisfied over the 30 years. Since Prometheus is a stochastic model, the outputs measurements are repeated to obtain several realizations of outputs based on the same input. This measurement process is repeated for different realizations of the random inputs. Therefore we have a collection of 40 data sets (each data set contains 30 realizations of outputs from the same input realization):

$$Z_1^{(r)} = \{v_1^{(r)}(t), [y_1^{(1)}(t), \ldots, y_1^{(30)}(t)],\ [y_2^{(1)}(t), \ldots, y_2^{(30)}(t)]\},$$
$$Z_2^{(r)} = \{v_2^{(r)}(t), [y_1^{(1)}(t), \ldots, y_1^{(30)}(t)], [y_2^{(1)}(t), \ldots, y_2^{(30)}(t)]\},$$

for $t = 1, \ldots, 30$, $r = 1, \ldots, 20$.

Parameter Estimation via Least Squares

The recurrence equation is obtained by expanding (6.9), the sequence of predictions for output $\hat{y}^i$, which is based on past and future inputs and outputs is written

as (for $n_{b1} = 1$, $n_{b2} = 2$, $n_D = 1$)

$$\begin{bmatrix} \hat{y}_1^i(k) \\ \hat{y}_1^i(k+1) \\ \vdots \\ \hat{y}_1^i(k+N) \\ \hat{y}_2^i(k) \\ \hat{y}_2^i(k+1) \\ \vdots \\ \hat{y}_2^i(k+N) \end{bmatrix} = \begin{bmatrix} -y_1^i(k-1) & \dots & -y_1^i(k-n_{ai}) & v_l^1(k-1) & 0 \\ -y_1^i(k) & \dots & -y_1^i(k-n_{ai}+1) & v_l^1(k) & 0 \\ & \vdots & & \vdots & \vdots \\ -y_1^i(k+N) & \dots & -y_1^i(k-n_{ai}+N) & v_l^1(k+N) & 0 \\ -y_2^i(k-1) & \dots & -y_2^i(k-n_{ai}) & 0 & v_l^2(k-1) \\ -y_2^i(k) & \dots & -y_2^i(k-n_{ai}+1) & 0 & v_l^2(k) \\ & \vdots & & \vdots & \vdots \\ -y_2^i(k+N) & \dots & -y_2^i(k-n_{ai}+N) & 0 & v_l^2(k+N) \end{bmatrix} \theta_i \tag{6.13}$$

Note zero initial conditions is assumed and therefore $y^i(k) = 0$ and $v^j(k) = 0$ for $k < 0$. The equation above is rewritten in more compact form

$$\hat{y}^i(k) = M(k)\theta_i. \tag{6.14}$$

Due to uncertainty or disturbances, the predicted and measured outputs are never equal, and the residuals $e(k) = \hat{y}(k) - y(k)$ should be minimized by the choice of parameters. That is the identification problem is cast as an optimization problem

$$\min_{\theta} \sum_{j=1}^{N} \varepsilon_j^2. \tag{6.15}$$

Because the predictors are linear, the minimization to the least-squares problem above has a closed form solution given by

$$\hat{\theta}_i = (M^T M)^{-1} M^T y^i(k). \tag{6.16}$$

Since the estimated parameter vector $\hat{\theta}_i$ is a random sample from an underlying

distribution, we can estimate the mean and covariance of the underlying distribution by solving the least-squares problem for multiple realizations of output generated from Prometheus. Hence, for each $i = 1, \ldots, \kappa$ realizations, we repeatedly solve the least squares problem, (6.16). Consequently the mean, $\overline{\theta}$, in (6.11) can be estimated from:

$$\begin{aligned} \overline{\theta} &= \mathbb{E}\theta_i \\ &= \frac{1}{\kappa}\sum_{i=1}^{\kappa}\theta_i \end{aligned} \tag{6.17}$$

and the covariance ,Θ, in (6.11) can be estimated

$$\begin{aligned} \Theta &= \mathbb{E}(\theta_i - \overline{\theta_i})^T(\theta_i - \overline{\theta_i}) \\ &= \frac{1}{\kappa - 1}\sum_{i=1}^{\kappa}(\theta_i - \overline{\theta_i})^T(\theta_i - \overline{\theta_i}) \end{aligned} \tag{6.18}$$

To determine the best model order, the Aikake Information Criterion (AIC) [64] is used:

$$AIC = ln(RSS) + \frac{2l}{N} \tag{6.19}$$

where l is the number of parameters, $RSS = \frac{1}{N}\sum_{j=1}^{N}\varepsilon_j^2$ is the residual sum squared and N is the number of observations. The AIC can be used as a measure the goodness of fit which then used to compare the different models. A lower AIC represent a good tradeoff between bias and variance. Given a data set, several candidate models may be ranked according to their AIC, with the model having the minimum AIC being the best. Since we are estimating the mean and covariance of the random parameters by repeating the identification process for each $i = 1, \ldots, \kappa$ realizations, the mean value of the AIC is used.

6.3.2 State-space Form

With the assumption of linearity, the dynamics of Prometheus are described by a m-input n-output discrete time matrix transfer function. Here, only the cases of $m = 2$ inputs and $n = 2$ output is considered:

$$\begin{bmatrix} Y^1(z) \\ Y^2(z) \end{bmatrix} = \begin{bmatrix} G_{11}(z) & G_{12}(z) \\ G_{21}(z) & G_{22}(z) \end{bmatrix}_k \begin{bmatrix} V^1(z) \\ V^2(z) \end{bmatrix} \tag{6.20}$$

where $G_{ij} = \frac{B^{ij}(z)}{A^i(z)}$ relates input j to output i. Note that the parameters of the matrix of transfer function is a realization at time k drawn from its probability distribution function. For ease of notation, note that the time dependence is not explicitly shown (i.e $\theta_k = \theta$).

The recurrence equations between the inputs $j = 1, 2$ and output $i = 1$ are written by expanding (6.9) with $n_k = 1$ thus obtaining

$$\begin{aligned} y^1(k+1) = -a_1 y^1(k) + \ldots - a_{n_{a1}} y^1(k - n_a) + \\ b_1^{11} v_1(k) + \ldots b_{n_{b2}}^{11} v_1(k - n_{b2}) + b_1^{21} v_2(k) + \ldots + b_{n_{b2}}^{21} v_2(k - n_{b2}) \end{aligned} \tag{6.21}$$

There are many state-space realizations of a transfer functions and a detailed explanation is given in [65]. In order to allow the coefficients of the ARX model

(6.21) to be random and time varying, we use a non-minimal state space realization. Thus the dynamics of (6.20) are written as

$$x(k+1) = \begin{bmatrix} y^1(k+1) \\ \vdots \\ y^1(k-n_{a1}) \\ y^2(k+1) \\ \vdots \\ y^2(k-n_{a2}) \\ v^1(k) \\ \vdots \\ v^1(k-n_{b1}) \\ v^2(k) \\ \vdots \\ v^2(k-n_{b2}) \end{bmatrix} \qquad x(k) = \begin{bmatrix} y^1(k) \\ \vdots \\ y^1(k-n_{a1}-1) \\ y^2(k) \\ \vdots \\ y^2(k-n_{a2}-1) \\ v^1(k-1) \\ \vdots \\ v^1(k-n_{b1}-1) \\ v^2(k-1) \\ \vdots \\ v^2(k-n_{b2}-1) \end{bmatrix} \tag{6.22}$$

and the vector of input stocks as

$$v(k) = \begin{bmatrix} v^1(k) \\ v^2(k) \end{bmatrix}. \tag{6.23}$$

The realization of the matrix transfer function in state-space form is given by

$$x(k+1) = A_k x(k) + B_k v(k) + d_k \tag{6.24}$$

$$y(k) = Cx(k) \tag{6.25}$$

where $x(k) \in \mathbb{R}^{n_{a1}+n_{a2}+n_{b1}+n_{b2}-2}$, $v(k) \in \mathbb{R}^m$, $y(k) \in \mathbb{R}^n$, and

$$A_k = \begin{bmatrix}
-a_1^1 & & \dots & -a_{n_{a1}}^1 & & & & & b_2^{11} & \dots & b_{n_{b1}}^{11} & b_2^{12} & \dots & b_{n_{b2}}^{12} \\
1 & 0 & \dots & 0 & & & & & 0 & \dots & 0 & 0 & \dots & 0 \\
0 & 1 & \dots & 0 & & & & & & \vdots & & & \vdots & \\
0 & \dots & 1 & 0 & & & & & 0 & \dots & 0 & 0 & \dots & 0 \\
 & & & & -a_1^2 & & \dots & -a_{n_{a2}}^2 & b_2^{21} & \dots & b_{n_{b1}}^{21} & b_2^{22} & \dots & b_{n_{b2}}^{22} \\
 & & & & 1 & 0 & \dots & 0 & 0 & \dots & 0 & 0 & \dots & 0 \\
 & & & & 0 & 1 & \dots & 0 & & \vdots & & & \vdots & \\
 & & & & 0 & \dots & 1 & 0 & 0 & \dots & 0 & 0 & \dots & 0 \\
 & & & & & & & & 0 & \dots & 0 & & & \\
 & & & & & & & & 1 & \dots & 0 & & & \\
 & & & & & & & & \vdots & \ddots & 0 & & & \\
 & & & & & & & & \dots & 1 & 0 & & & \\
 & & & & & & & & & & & 0 & \dots & 0 \\
 & & & & & & & & & & & 1 & \dots & 0 \\
 & & & & & & & & & & & \vdots & \ddots & 0 \\
 & & & & & & & & & & & \dots & 1 & 0
\end{bmatrix} \tag{6.26}$$

$$B_k = \begin{bmatrix} b_1^{11} & b_1^{12} \\ 0 & 0 \\ \vdots & \vdots \\ 0 & 0 \\ b_1^{21} & b_1^{22} \\ 0 & 0 \\ \vdots & \vdots \\ 0 & 0 \\ 1 & \\ 0 & \\ \vdots & \\ 0 & \\ & 1 \\ & 0 \\ & \vdots \\ & 0 \end{bmatrix} \qquad d_k = \begin{bmatrix} \varepsilon_1(k) \\ 0 \\ \vdots \\ 0 \\ \varepsilon_2(k) \\ 0 \\ \vdots \\ 0 \\ 0 \\ 0 \\ \vdots \\ 0 \\ 0 \\ 0 \\ \vdots \\ 0 \end{bmatrix}. \tag{6.27}$$

$$C = \begin{bmatrix} 1 & 0 & \dots & 0 & & & & 0 & 0 & \dots & 0 & & & \\ & & & & 1 & 0 & \dots & 0 & & & & 0 & 0 & \dots & 0 \end{bmatrix}. \tag{6.28}$$

Note that the missing elements of the time varying system matrices A_k, B_k, and output matrix C are all zeros.

Since the model coefficients and disturbances are random variables, the state space model can be written as a linear expansion over a set of scalar random variables

$\{q^{(1)}, \ldots, q^{(\rho)}\}$

$$[A_k \ B_k \ d_k] = [\bar{A} \ \bar{B} \ 0] + \sum_{i=1}^{\rho} [A^{(i)} \ B^{(i)} \ d^{(i)}] q_k^{(i)} \tag{6.29}$$

where $q_k = [q_k^{(1)}, \ldots, q_k^{(\rho)}]^T$ is a random vector with zero mean and known (estimated) covariance matrix S_q. The basis $\{A^{(i)} \ B^{(i)} \ d^{(i)}\}$ can be chosen so that the elements of q_k are uncorrelated ($S_q = I$). This can be shown as follows by firstly substituting (6.29) into (6.24)

$$\begin{aligned} x(k+1) = \bar{A}x(k) + \bar{B}v(k) + \\ [A^{(1)}x(k) + B^{(1)}v(k) + d^{(1)} \ldots A^{(\rho)}x(k) + B^{(\rho)}v(k) + d^{(\rho)}]q_k. \end{aligned} \tag{6.30}$$

The covariance matrix S_q is necessarily symmetric positive definite and can be decomposed into $S_q = RR^T$ (using Cholesky decomposition). By defining $\hat{q}_k = R^{-1}q_k$, then $\hat{q}_k$ has mean

$$\mathbb{E}(\hat{q}_k) = R^{-1}\mathbb{E}(q_k) = 0$$

and covariance matrix

$$\begin{aligned} \mathbb{E}(\hat{q}_k \hat{q}_k^T) &= \mathbb{E}(R^{-1} q_k q_k^T R) \\ &= R^{-1}\mathbb{E}(q_k q_k^T)R \\ &= R^{-1} S_q R = I. \end{aligned}$$

Substituting $q_k = R\hat{q}_k$ into (6.30),

$$\begin{aligned} x(k+1) = \bar{A}x(k) + \bar{B}v(k) + \\ [A^{(1)}x(k) + B^{(1)}v(k) + d^{(1)} \ldots A^{(\rho)}x(k) + B^{(\rho)}v(k) + d^{(\rho)}]R\hat{q}_k. \end{aligned} \tag{6.31}$$

By denoting r_{ij} as the ij^{th} element of R the following is obtained

$$x(k+1) = \bar{A}x(k) + \bar{B}v(k) + \sum_{i=1}^{\rho}\sum_{j=1}^{\rho}[A^{(i)}\ B^{(i)}\ d^{(i)}] \begin{bmatrix} x(k) \\ v(k) \\ 1 \end{bmatrix} r_{ij}\hat{q}_k^{(j)}$$

$$= \bar{A}x(k) + \bar{B}v(k) + \sum_{j=1}^{\rho}\left(\sum_{i=1}^{\rho}[A^{(i)}\ B^{(i)}\ d^{(i)}]r_{ij}\right) \begin{bmatrix} x(k) \\ v(k) \\ 1 \end{bmatrix} \hat{q}_k^{(j)}. \quad (6.32)$$

Comparing the equation (6.32) with (6.29), it is shown that the basis $\{A^{(i)}\ B^{(i)}\ d^{(i)}\}$ over which the expansion of (6.29) is performed can be replaced by $\{\hat{A}^{(i)}\ \hat{B}^{(i)}\ \hat{d}^{(i)}\}$ where $[\hat{A}^{(i)}\ \hat{B}^{(i)}\ \hat{d}^{(i)}] = \sum_{i=1}^{\rho}[A^{(i)}\ B^{(i)}\ d^{(i)}]r_{ij}$ so that the elements of q_k are uncorrelated.

6.3.3 State-space model with input shocks

The model that is used currently relates stocks to outputs given by (6.24). As an example, consider only the state vectors for the case of $\{n_a = 1, n_{b1} = 2, n_{b2} = 2\}$ for brevity sake, the state and input matrices are given by

$$A_k = \begin{bmatrix} -a_1^1 & 0 & b_2^{11} & b_2^{12} \\ 0 & -a_1^2 & b_2^{21} & b_2^{22} \\ 0 & 0 & 0 & 0 \\ 0 & 0 & 0 & 0 \end{bmatrix} \quad B_k = \begin{bmatrix} b_1^{11} & b_1^{12} \\ b_1^{21} & b_1^{22} \\ 1 & 0 \\ 0 & 1 \end{bmatrix}$$

The relation between input stocks v_k and input shocks u_k is given by

$$v(k) = v(k-1) + u(k). \quad (6.33)$$

This is equivalent to passing input shocks through an integrator to obtain stocks at time k. Constraints in the sustainable development context are imposed on shocks and stocks. It is helpful to parameterize the optimization so that constraints are easily encoded into the problem. This is done by forming a models which relates shocks and also stocks to output. By substituting (6.33) into (6.24) we get

$$x(k+1) = A_k x(k) + B_k v(k-1) + B_k u(k) + d_k \tag{6.34}$$

where the state vector is $x(k) = [y^1(k), y^2(k), v^1(k-1), v^2(k-1)]^T$ and input shocks vector $u(k) = [u^1(k), u^2(k)]^T$. This is equivalent to

$$x(k+1) = A_k^u x(k) + B_k u(k) + d_k \tag{6.35}$$

where

$$A_k^u = \begin{bmatrix} -a_1^1 & 0 & b_1^{11} + b_2^{11} & b_1^{12} + b_2^{12} \\ 0 & -a_1^2 & b_1^{21} + b_2^{21} & b_1^{22} + b_2^{22} \\ 0 & 0 & 1 & 0 \\ 0 & 0 & 0 & 1 \end{bmatrix}$$

The block diagram relating the model with stocks as inputs, and the augmented model with shocks as inputs is shown in Figure 6.2. Stocks are integrated values of shocks reflected by the integrator in the block diagram.

6.4 Application of the TSMPC Algorithm

The Tube Stochastic Model Predictive Control (TSMPC) algorithm, given in Section 3.4 is directly applied to the budget allocation problem in a sustainable development context. The goal of the controller is to compute a sequence of inputs

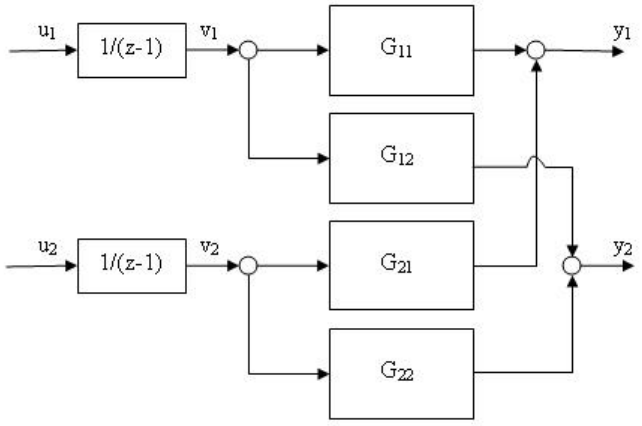

FIGURE 6.2: Block diagram of the identified Prometheus model to be controlled.

so that it optimizes some measure defined by the primary output while the secondary and remaining outputs are feasible with respect to the soft and also hard constraints on the inputs are themselves satisfied.

From the SD problem perspective, the goal is to achieve the lowest possible energy cost subject to budgetary constraints and probabilistic constraints on CO_2 emission. The budgetary constraint form a hard constraint on the shocks so that the vector of stocks, $v_k = [v_k^1, v_k^2]^T$ satisfies:

$$\sum_{j=1}^{2} v_k^j \leq B \quad k = 0, 1 \ldots, \tag{6.36}$$

where B is budget allocation and stocks are always positive (no investment can be taken out):

$$v_k^j \geq 0 \quad j = 1, 2 \text{ and } k = 0, 1, \ldots. \tag{6.37}$$

Probabilistic constraints can be interpreted as over a horizon of N_c years, the expected rate of violation of soft constraints does not exceed a given bound $\frac{N_{max}}{N_c}$. The soft constraint considered here is such that CO_2 emission, y_2 is lower than a

threshold h_S

$$\frac{1}{N_c}\left\{\sum_{k=1}^{N_c} Pr\{y_k^2 > h_S\}\right\} \leq \frac{N_{max}}{N_c}. \tag{6.38}$$

The problem here is a set-point tracking, where a set-point is computed initially and the role of the controller is to minimize the output deviation from this set-point. However, the TSMPC algorithm is tailored for a regulation problem. Therefore, the variables are changed to convert a set-point tracking problem into the one of regulation (that is to drive the state to the origin). But firstly, a optimum set point x_{ss} and the steady-state stock v_{ss} needs to be determined. Since the set point satisfies the $x_{ss} = \overline{A}x_{ss} + \overline{B}v_{ss}$ from the dynamics of (6.35), it implies that the x_{ss} is linearly dependant on v_{ss}. The optimum setpoint can then be determined by varying the elements of the steady-state stocks vector $v_{ss} = [v_{ss}^1, v_{ss}^2]^T$, such that it satisfies $\sum_{j=1}^{2} v_{ss}^j \leq B$. The TSMPC algorithm is then applied. The vector v_{ss} which corresponds to the lowest mean cost is used to determine the optimal setpoint , x_{ss}.

6.5 Numerical Results

The identification results of fitting an ARX model to Prometheus is presented. The data collected from the actual system consists of 30 realizations of 20 random inputs over a 30 year horizon. For each of the 20 input realizations, a set of 30 output responses is obtained correspondingly. The data points are obtained for two sets of inputs and two sets of outputs. The results of model fitting are shown in Figure 6.5.

Firstly, the model order which best fits the dataset is determined using the AIC measure, and the results for both models, for output y_1 and y_2, are shown in

Figure 6.3 and 6.4 respectively. From these values, the lowest AIC measure determines the best model order. It can be seen from both the figures that the AIC does not decrease significantly as the number of parameters are increased. Since the TSMPC algorithm suffers from the severe computation complexity for state-space models with system order greater than 4 ($n > 4$), an ARX model with 4 total number of parameters is chosen to ensure a balance of computation time and accuracy of model when implementing the TSMPC algorithm. Consequently, the model order chosen for y_1 is $\{n_a = 1, n_{b1} = n_{b2} = 2\}$ with a mean AIC of 0.74 and the model order chosen for y_2 is also $\{n_a = 1, n_{b1} = n_{b2} = 2\}$ with a mean AIC of 0.78.

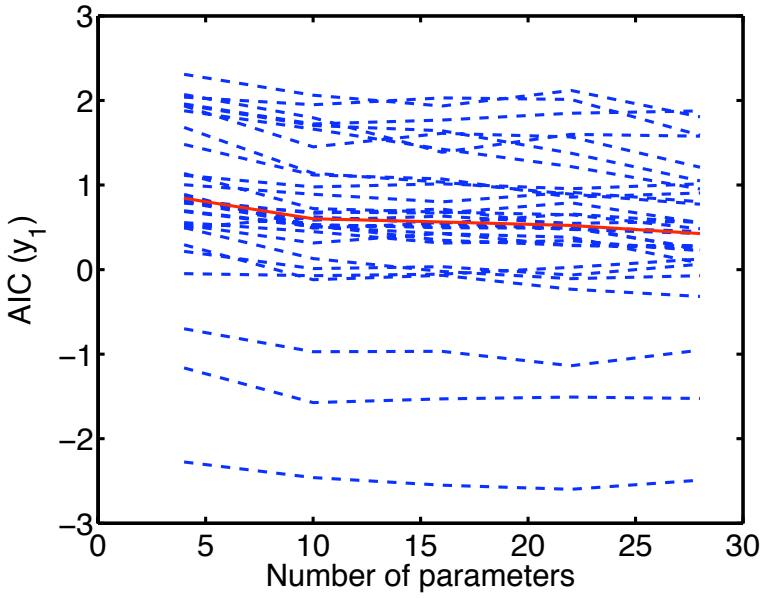

FIGURE 6.3: The AIC for varying number of parameters for output y_1. The order of poles and zeros of the ARX model are varied, and the identification process repeated (shown using blue dashed lines). The ensemble mean AIC is computed over 30 realizations of uncertainty is shown using a red solid line.

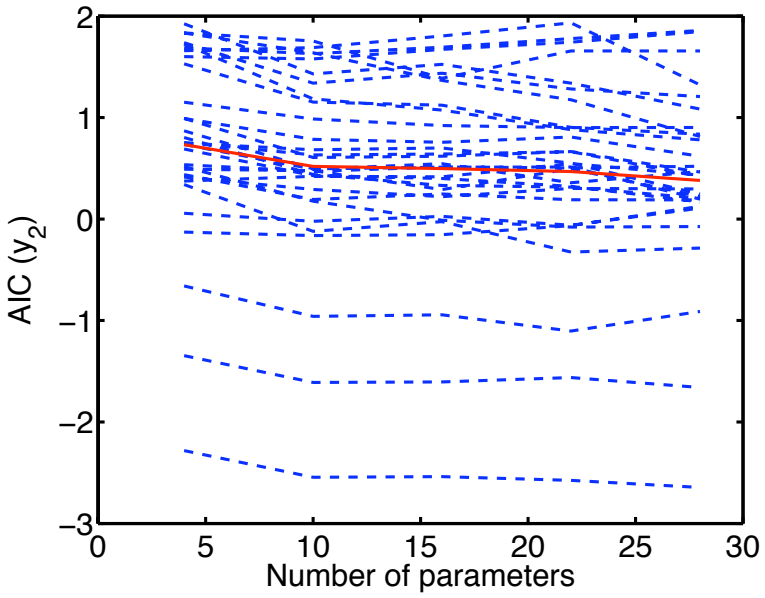

FIGURE 6.4: The AIC for varying number of parameters for output y_2. The order of poles and zeros of the ARX model are varied, and the identification process repeated (shown using blue dashed lines). The ensemble mean AIC is computed over 30 realizations of uncertainty is shown using a red solid line.

The identified system parameters using model order $\{n_a = 1, n_{b1} = n_{b2} = 2\}$ are therefore given by

$$\overline{A} = \begin{bmatrix} 0.7725 & 0 & -0.0001 & -0.0002 \\ 0 & 0.8603 & -0.0016 & -0.0016 \\ 0 & 0 & 1 & 0 \\ 0 & 0 & 0 & 1 \end{bmatrix}$$

$$A^{(1)} = \begin{bmatrix} 0.0332 & 0 & 0 & 0 \\ 0 & 0.0192 & 0 & 0 \\ 0 & 0 & 0 & 0 \\ 0 & 0 & 0 & 0 \end{bmatrix} \quad \overline{B} = \begin{bmatrix} -0.0006 & -0.0010 \\ -0.0073 & -0.0057 \\ 1 & 0 \\ 0 & 1 \end{bmatrix}.$$

From the identified parameters, the variance of the parameters which constitute the matrix B is negligible and therefore deterministic given only by its mean value

$\overline{B}$. The choice of basis of $\rho = 1$ is chosen for simplicity and the matrix $A^{(1)}$ is determined as explained in Section 6.3.2.

The feedback gain matrix and dual eigenvector matrix of $\overline{A} + \overline{B}K_x$ are

$$K_x = \begin{bmatrix} 0.0001 & 0.0020 & -0.3297 & 0 \\ 0.0001 & 0.0019 & 0 & -0.3297 \end{bmatrix}$$

$$V = \begin{bmatrix} -1 & 0 & -0.0006 & -0.0010 \\ 0 & -1 & -0.0070 & -0.0053 \\ 0.0010 & 0.0133 & -0.7981 & -0.6068 \\ 0.0004 & 0.0004 & 0.6631 & -0.7520 \end{bmatrix}.$$

The transformed system parameters are

$$\overline{\Phi} = \begin{bmatrix} 0.4610 & 0 & 0 & 0 \\ 0 & 0.6367 & 0 & 0 \\ 0 & 0 & 0.0109 & 0 \\ 0 & 0 & 0 & 0.0109 \end{bmatrix}$$

$$\Phi^{(1)} = \begin{bmatrix} 0.0332 & 0 & 0 & 0 \\ 0 & 0.0192 & -0.0002 & 0 \\ 0 & -0.0003 & 0 & 0 \\ 0 & 0 & 0 & 0 \end{bmatrix}.$$

The following transition probabilities and probability of soft constraint violations are used

$$\Pi = \begin{bmatrix} 0.9 & 0.6 \\ 1 & 1 \end{bmatrix} \quad p = \begin{bmatrix} 0.4 \\ 0.9 \end{bmatrix}.$$

In the off-line stage, the terminal sets (for $\mu = 2$) are computed to be:

$$Z_t^{(1)} = \begin{bmatrix} 78.1832 \\ 106.9736 \\ 1.4724 \\ 1.2233 \end{bmatrix} \quad Z_t^{(2)} = \begin{bmatrix} 84.2634 \\ 106.9736 \\ 1.4724 \\ 1.2233 \end{bmatrix}.$$

From the discussion in Section 6.4, the optimal set point is determined as $x_{ss} = [-2.4018, -32.0198, 100, 400]^T$. The closed-loop simulations of the system were performed over 20 realizations of uncertainty. The input responses obtained are shown in Figure 6.6. Based on the simulation results, the optimal allocation is to invest in the first 5 years with more emphasis on investments into wind technology. The corresponding output responses are shown in Figure 6.7. The investments on both the technologies has the net effect of reducing both the energy costs and CO_2 levels over a period of 15 years; after 15 years both outputs fluctuate around a steady state value. The soft constraint $\Pr(y_2 > -15) < 0.4$ which represents that the CO_2 levels at year 3 should only exceed -15 with a probability less that 0.4. As the CO_2 levels in year 3 never exceeds -15, the soft constraint is satisfied with probability of 1. This result implies that the TSMPC controller is a conservative one.

6.6 Conclusion

Predicting how current technological development will affect potential for development in the future is inherently random. Assuming there is some statistical regularity, a stochastic model, namely the ARX model can be used to generate predictions. The resource allocation problem (SD problem) here concerns the

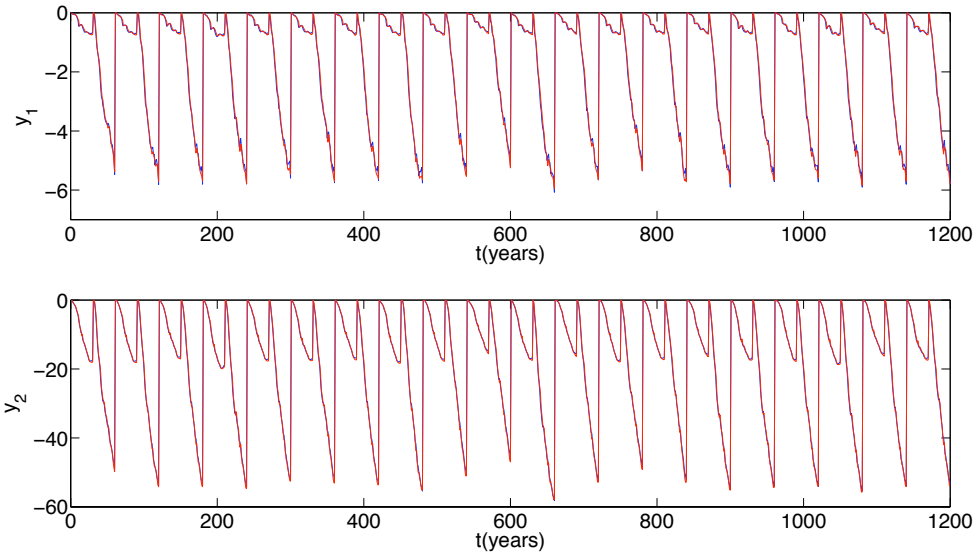

FIGURE 6.5: Plot of mean output over 30 realizations. (Blue:- responses from Prometheus. Red:- responses from the identified model.)

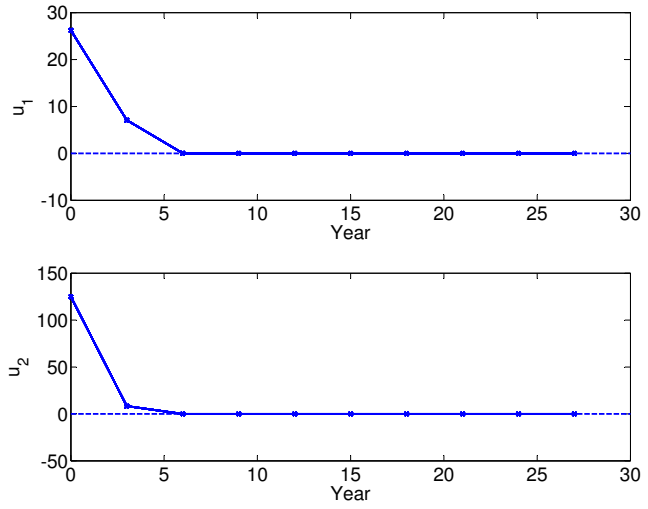

FIGURE 6.6: Input trajectory. R&D Investment on Wind Turbine technology (top) and GGC (bottom).

allocation of research and development investments between different power generating technologies. Several measures of performance can be used which include price of energy and CO_2 emissions. Constraints can be placed on these measures such as a limit on CO_2 emission in 3 years time. The goal here is therefore to allocate investments to give the 'best' measure of predicted performance subject to

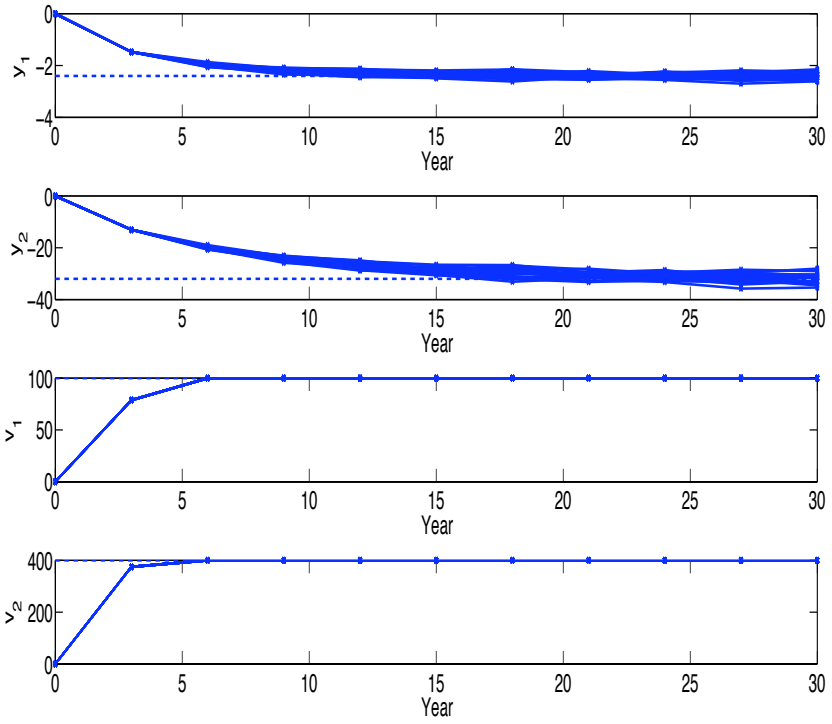

FIGURE 6.7: The output responses where y_1:- Energy Costs and y_2:-CO_2 Emissions. The bottom two plots the stocks which is the cumulative sum of the inputs shocks. The dashed lines represents the steady-state levels.

constraints. The stochastic model used to make predictions is an economic model called 'Prometheus'. In MPC terms, this is equivalent to controlling a system subject to model parameter uncertainty and additive disturbance. Hence, the Tube Stochastic MPC can be directly applied to solve the resource allocation problem.

Chapter 7

Non-linear Stochastic MPC

[1]A Receding Horizon Control methodology is proposed for systems with nonlinear dynamics, additive stochastic uncertainty, and both hard and soft (probabilistic) input/state constraints. Jacobian linearization about predicted trajectories is used to derive a sequence of convex optimization problems. Constraints are handled through the construction of a sequence of tubes and an associated Markov chain model. The parameters defining the tubes are optimized simultaneously with the predicted future control trajectory via online Linear Programming. The tractability of the Non-linear Stochastic Model Predictive Control (NLSMPC) algorithm is demonstrated by a numerical example of a coupled-tank system.

7.1 Problem Formulation

Consider the discrete time nonlinear model with state $x_k \in \mathbb{R}^{n_x}$ and input $u_k \in \mathbb{R}^{n_u}$

$$x_{k+1} = f(x_k, u_k) + d_k, \quad k = 0, 1, \ldots \tag{7.1}$$

[1]The work in this Chapter has been published in [44].

where n_x defines the order of the system while n_u defines the number of inputs. We assume that the control problem is to drive the plant state to a target equilibrium point which, for convenience we take to be the origin of the model (7.1), so that $f(0,0) = 0$. The additive random disturbance d_k is assumed to be finitely supported with zero mean, $(\mathbb{E}(d_k) = 0)$, and d_j and d_l are independent from each other $(j \neq l)$. The distribution of d_k is assumed to be known.

The dynamics of (7.1) are assumed to be continuous throughout the operating region for the state (denoted $\mathcal{X}$) and input (denoted $\mathcal{U}$). More specifically, $f(x_k, u_k)$ in (7.1) should be continuously differentiable over the operating regions. This assumption is important because the entire algorithm here is based upon successive Jacobian linearization about a predicted trajectory.

The hard constraints on states or inputs are written in the form

$$H_l \leq F_h x_k + G_h u_k \leq H_h \tag{7.2}$$

where $F_h \in \Re^{(n_h \times n_x)}$, $G_h \in \Re^{(n_h \times n_u)}$. n_h denotes the number of constraints (upper,$H_h \in \Re^{n_h}$ and lower, $H_l \in \Re^{n_h}$ limits) imposed on the states and/or inputs. The majority of work on SMPC algorithms to date focused on feasibility with respect to hard constraints and the work explored here extends this to include soft constraints. This type of constraint is useful in applications involving constraints on the rate of accumulation of fatigue damage. Soft constraints of this kind can be written as

$$\frac{1}{N_c} \sum_{i=0}^{N_c} Pr\left(F_s x_k + G_s u_k \geq H_s\right) \leq \frac{N_{max}}{N_c} \tag{7.3}$$

where $F_s \in \Re^{(n_s \times n_x)}$, $G_s \in \Re^{(n_s \times n_u)}$. n_s denotes the number of soft constraints imposed on the states and/or inputs. N_{max} is the maximum number of expected constraint violations over a specified horizon of N_c.

The control aim is to regulate the non-linear system to the set-point equilibrium from a given initial condition. This is easily reformulated to a regulation problem. The essence of the SMPC algorithm here is to minimize a measure of performance, or cost, while respecting constraints on the non-linear system in the presence of the additive random disturbance. A suitable cost explored here is the mean 1-norm cost over an infinite horizon, written as

$$J_k(x_k, u_k) = \sum_{k=0}^{\infty} \mathbb{E}_0 \left(\mathbf{1}^T |x_k| + \mathbf{1}^T |u_k| \right). \tag{7.4}$$

The justification (explained in Section 7.5) for using a 1-norm cost is that it casts the optimization problem as a Linear Programming which can be solved efficiently. In addition, a simple upper bound on the infinite horizon cost can be computed off-line which enables the infinite horizon MPC optimization to be parameterized over a set of finite variables.

7.2 Successive linearization MPC

This section describes in outline a method of solving the receding horizon formulation of the control problem defined in Section 7.1. Let $\{u_{k|k}, u_{k+1|k}, \ldots\}$ denote a predicted input sequence at time k and denote $\{x_{k|k}, x_{k+1|k}, \ldots\}$ as the corresponding state trajectory, with $x_{k|k} = x_k$. Following the dual mode prediction paradigm [28], we define the infinite horizon predicted input sequence in terms of a finite number of free variables, $\mathbf{c}_k = \{c_{0|k}, \ldots, c_{N-1|k}\}$ as:

$$u_{k+i|k} = Kx_{i|k} + c_{i|k} \quad i = 0, \ldots, N-1 \quad \text{[MODE 1]} \tag{7.5a}$$

$$u_{k+i|k} = Kx_{i|k} \quad i = N, N+1, \ldots \quad \text{[MODE 2]}. \tag{7.5b}$$

The linear feedback law $u = Kx$ is assumed to stabilize the model (7.1) in a neighborhood of $x = 0$ (the approach allows this to be replaced by a stabilizing nonlinear feedback law if available). The feedback gain K, is specified as the optimal feedback law for the linearized model $\left(\frac{\partial f}{\partial x}\big|_{(0,0)} , \frac{\partial f}{\partial u}\big|_{(0,0)} \right)$ with a suitable quadratic cost. Note that this formulation contains a degree of conservativeness since it leads to an optimization over the variables $\mathbf{c}_k$ rather than closed-loop policies, however it provides a convenient balance of computation and conservativeness.

Under the control law of (7.5), state predictions are governed by the model

$$x_{k+i+1|k} = \phi(x_{k+i|k}, c_{i|k}) + d_{k+i}, \quad x_{k|k} = x_k \tag{7.6}$$

where $\phi : \mathbb{R}^{n_x \times n_u} \to \mathbb{R}^{n_x}$ is defined by the identity

$$\phi(x_k, c_k) = f(x_k, Kx_k + c_k). \tag{7.7}$$

In order to account efficiently for the nonlinearity and uncertainty in the prediction system (7.6), the proposed receding horizon optimization is based on linear models obtained from the Jacobian linearization of (7.6) around nominal trajectories for the predicted state. Let $\{x^0_{k|k}, \ldots, x^0_{k+N|k}\}$ denote a trajectory for the nominal system associated with the expected value of uncertainty in (7.6) and $\mathbf{c}^0_k = \{c^0_{0|k}, \ldots, c^0_{N-1|k}\}$, so that $x^0_{k+i|k}$ evolves according to

$$x^0_{k+i+1|k} = \phi(x^0_{k+i|k}, \mathbf{c}^0_{i|k}), \quad x^0_{k|k} = x_k. \tag{7.8}$$

The combined effects of approximation errors and unknown disturbances can be taken into account through the definition of a sequence of sets centred on a nominal trajectory at prediction times $i = 1, \ldots, N$ and a terminal set centred at the origin for $i > N$. For computational convenience we define these sets as low complexity polytopes of the form $\{x : |V(x - \hat{x}_{i|k})| \leq \overline{z}_{i|k}\}$ for $i = 1, \ldots, N$, and $\{x : |Vx| \leq \overline{z}_t\}$

for the terminal set. Note that the norm operator($|.|$) applies element-wise. Here V is a square full-rank matrix and the parameters $\overline{z}_{i|k} \in \Re^{n_x}$, $\overline{z}_t \in \Re^{n_x}$ determine the relative scaling of the sets. Define V as the transformation matrix such that $\Phi = V \left.\frac{\partial \phi}{\partial x}\right|_{(0,0)} V^{-1}$ is in modal form. Hence under the assumption that $\left.\frac{\partial \phi}{\partial x}\right|_{(0,0)}$ has a simple Jordan form, Φ is diagonal with the diagonal elements all lying inside the unit circle centered at the origin of the complex plane, thereby making nominal invariance easier to meet. Nominal invariance (which is ensured by (7.29)) will be further discussed in Section 7.4. Further details of this approach for the deterministic case can be found in [36].

To simplify presentation, we define a transformed variable $z = Vx$ and denote z^δ and c^δ as the deviations from the nominal trajectories for z and c:

$$z^\delta_{k+i|k} = z_{k+i|k} - z^0_{k+i|k}, \quad z^0_{k+i|k} = Vx^0_{k+i|k} \tag{7.9}$$

$$c^\delta_{i|k} = c_{i|k} - c^0_{i|k}. \tag{7.10}$$

The transformed state evolves according to

$$z^0_{k+i+1|k} + z^\delta_{k+i+1|k} = V\phi(V^{-1}(z^0_{k+i|k} + z^\delta_{k+i|k}), c^0_{i|k} + c^\delta_{i|k}) + \varepsilon_{k+i} \quad \text{[MODE 1]} \tag{7.11a}$$

$$z^\delta_{k+i+1|k} = V\phi(V^{-1}z^\delta_{k+i|k}, 0) + \varepsilon_{k+i} \quad \text{[MODE 2]}. \tag{7.11b}$$

where $\varepsilon_{k+i} = Vd_{k+i}$. The Jacobian linearization of (7.6) about $\{x^0_{k|k}, \ldots, x^0_{k+N|k}\}$ and $\mathbf{c}^0_k$ in Mode 1 and linearization about the origin in Mode 2 can therefore be expressed as

$$z^\delta_{k+i+1|k} = \Phi_{k+i|k} z^\delta_{k+i|k} + B_{k+i|k} c^\delta_{i|k} + \varepsilon_{k+i} + e_{k+i|k} \quad \text{[MODE 1]} \tag{7.12a}$$

$$z^\delta_{k+i+1|k} = \Phi z^\delta_{k+i|k} + \varepsilon_{k+i} + e_{k+i|k} \quad \text{[MODE 2]} \tag{7.12b}$$

where $e_{k+i|k}$ defines the linearization error and the closed loop state matrices Φ and input matrices B are

$$\Phi_{k+i|k} = V \left.\frac{\partial \phi}{\partial x}\right|_{(x^0_{k+i|k}, c^0_{i|k})} V^{-1}, \qquad B_{k+i|k} = V \left.\frac{\partial \phi}{\partial c}\right|_{(x^0_{k+i|k}, c^0_{i|k})} \quad \text{[MODE 1]} \tag{7.13a}$$

$$\Phi = V \left.\frac{\partial \phi}{\partial x}\right|_{(0,0)} V^{-1} \quad \text{[MODE 2]}. \tag{7.13b}$$

The linearization errors in (7.12a) and (7.12b) respectively are given by

$$\begin{aligned} e_{k+i|k} = {} & V\phi(V^{-1}(z^0_{k+i|k} + z^\delta_{k+i|k}), c^0_{i|k} + c^\delta_{i|k}) \\ & - V\phi(V^{-1} z^0_{k+i|k}, c^0_{i|k}) - \Phi_{k+i|k} z^\delta_{k+i|k} - B_{k+i|k} c^\delta_{i|k} \quad \text{[MODE 1]} \end{aligned} \tag{7.14a}$$

$$e_{k+i|k} = V\phi(V^{-1}(z^\delta_{k+i|k}), 0) - \Phi z^\delta_{k+i|k} \quad \text{[MODE 2]}. \tag{7.14b}$$

Next, we show how these linearization errors are bounded linearly in terms of z^δ and c^δ for Mode 1 and Mode 2. The zero-th order Taylor expansion of (7.11a) around $\{x^0_{k|k}, \ldots, x^0_{k+N|k}\}$ and $\mathbf{c}^0_k$ for Mode 1 is given by

$$z^0_{k+i+1|k} + z^\delta_{k+i+1|k} = V\phi(V^{-1} z^0_{k+i|k}, c^0_{i|k}) + \varepsilon_{k+i} + R_{k+i|k} \tag{7.15}$$

where $R_{k+i|k}$ is the remainder term. Since ϕ is continuously differentiable by assumption in the region given by

$$\left(V^{-1} z^\delta_{k+i|k}, K V^{-1} z^\delta_{k+i|k} + c^\delta_{i|k}\right) \in \mathcal{X} \times \mathcal{U},$$

using Taylor's Remainder Theorem, the remainder term is given by

$$R_{k+i|k} = V \left.\frac{\partial \phi}{\partial x}\right|_{(\xi_{k+i|k},\nu_{i|k})} V^{-1} z^{\delta}_{k+i|k} + V \left.\frac{\partial \phi}{\partial c}\right|_{(\xi_{k+i|k},\nu_{i|k})} c^{\delta}_{i|k} \tag{7.16}$$

where $(\xi_{k+i|k}, \nu_{k+i|k}) \in \mathcal{X} \times \mathcal{U}$. Substituting (7.12a) and (7.16) into (7.15) and rearranging yields

$$e_{k+i|k} = \left(V \left.\frac{\partial \phi}{\partial x}\right|_{(\xi_{k+i|k},\nu_{i|k})} V^{-1} - \Phi_{k+i|k} \right) z^{\delta}_{k+i|k} + \left(V \left.\frac{\partial \phi}{\partial c}\right|_{(\xi_{k+i|k},\nu_{i|k})} - B_{k+i|k} \right) c^{\delta}_{i|k}. \tag{7.17}$$

Since $\xi_{k+i|k}$ and $\nu_{k+i|k}$ are defined in the region $(\xi_{k+i|k}, \nu_{k+i|k}) \in \mathcal{X} \times \mathcal{U}$ and ϕ is continuously differentiable everywhere in the region, it follows that

$$\left(V \left.\frac{\partial \phi}{\partial x}\right|_{(\xi_{k+i|k},\nu_{i|k})} V^{-1}, V \left.\frac{\partial \phi}{\partial c}\right|_{(\xi_{k+i|k},\nu_{i|k})} \right) \in T \tag{7.18}$$

where $T \subset \text{Co}\left\{\overline{\Gamma_z}^{(m)}, \overline{\Gamma_c}^{(m)}, m = 1, \ldots, M\right\}$ for some set of matrices $\left\{\overline{\Gamma_z}^{(m)}, \overline{\Gamma_c}^{(m)}, m = 1, \ldots, M\right\}$, with Co$\{.\}$ defined as the convex hull. Hence the linearization error in Mode 1 given by (7.17) belongs to a set defined by the convex hull of

$$e_{k+i|k} \in \text{Co}\left\{ (\overline{\Gamma_z}^{(m)} - \Phi_{k+i|k}) z^{\delta}_{k+i|k} + (\overline{\Gamma_c}^{(m)} - B_{k+i|k}) c^{\delta}_{i|k},\ m = 1, \ldots, M \right\}. \tag{7.19}$$

Therefore if the assumption of continuous differentiability holds in the region $\mathcal{X}$ and $\mathcal{U}$, the linearization error in (7.12a) (for Mode 1) necessarily satisfies the following Lipschitz condition

$$|e_{k+i|k}| \leq \Gamma^{z}_{k+i|k} |z^{\delta}_{k+i|k}| + \Gamma^{c}_{k+i|k} |c^{\delta}_{i|k}| \tag{7.20}$$

for some positive matrices $\Gamma^z_{k+i|k}$, $\Gamma^c_{k+i|k}$. Similarly in Mode 2, the linearization error in (7.12b) is bounded linearly in terms of z^δ given by

$$|e_{k+i|k}| \leq \Gamma_t |z^\delta_{k+i|k}| \tag{7.21}$$

for some positive matrix Γ_t, for all $z_{k+i|k}$ such that

$$\left(V^{-1} z_{k+i|k}, KV^{-1} z_{k+i|k}\right) \in \mathcal{X} \times \mathcal{U}.$$

The matrices $\Gamma^z_{k+i|k}$, $\Gamma^c_{k+i|k}$ are computed online (as discussed in Section 7.6), and Γ_t can be computed off-line with a method of computation as outlined in Algorithm (9).

The bounds (7.20) and (7.21) are combined with bounds on the uncertainty ε_k to construct sets $\mathcal{Z}^{(l)}_{i|k}, i = 0, \ldots, N$ that depend on $\mathbf{c}^\delta_k = \{c^\delta_{0|k}, \ldots, c^\delta_{N-1|k}\}$, thus defining tubes centred on a nominal trajectory containing the predictions of (7.8). These tubes provide a means of bounding the receding horizon performance cost and of ensuring satisfaction of constraints. As a result the process of successively linearizing about $(x^0_{k+i|k}, \mathbf{c}^0_k)$, optimizing $\mathbf{c}^\delta_k$, and then redefining $(x^0_{k+i|k}, \mathbf{c}^0_k)$ by setting $\mathbf{c}^0_k \leftarrow \mathbf{c}^0_k + \mathbf{c}^\delta_k$ necessarily converges to a local optimum for the original nonlinear dynamics.

7.3 Probabilistic Tubes

This section describes a method of constructing a series of tubes around a nominal predicted trajectory so that each tube contains the future predicted state with a prescribed probability. This process provides a means of bounding the predicted value of the cost (7.4) and of ensuring satisfaction of hard constraints (7.2) and

probabilistic constraints (7.3) along future predicted trajectories. The probabilities of transition between tubes from one sampling instant to the next and the probability of constraint violation within each tube are governed by the fixed probabilities that are determined offline. However the parameters determining the size of each tube are retained as optimization variables, and this allows the effects of stochastic model uncertainty and linearization errors (which depend on the predicted input trajectory) to be estimated non-conservatively over the prediction horizon.

Instead of fixing the nominal trajectory (7.8), it is allowed to be shifted. At each $i = 0, \ldots, N-1$, the nominal trajectory $z^0_{k+i|k}$ is shifted by an amount $\hat{z}_{k+i|k}$ and it evolves according to

$$\hat{z}_{i+1|k} = \Phi_{k+i|k}\hat{z}_{i|k} + B_{k+i|k}c^{\delta}_{i|k} \quad \hat{z}_{0|k} = 0. \tag{7.22}$$

By defining the nominal trajectory with the optimization parameters $c^{\delta}_{i|k}$, a better performance with respect to the cost is obtained.

The tubes are defined to be low-complexity nested polytopic sets (more specifically, orthotopes) centred on the nominal trajectories in Mode 1 and the origin in Mode 2,

$$z^{\delta} \in \mathcal{Z}^{(l)}_{i|k} = \left\{ \hat{z}_{i|k} + v_{i|k} : |v_{i|k}| \leq \overline{z}^{(l)}_{i|k} \right\} \quad l = 1, \ldots, \mu \quad \text{[MODE 1]} \tag{7.23a}$$

$$z^{\delta} \in \mathcal{Z}^{(l)}_{t} = \left\{ |z^{\delta}| \leq \overline{z}^{(l)}_{t} \right\} \quad l = 1, \ldots, \mu \quad \text{[MODE 2]} \tag{7.23b}$$

where $\overline{z}_{i|k}$ and $\overline{z}_t$ define the respective sizes. Note that the polytopic sets are nested, that is

$$\mathcal{Z}^{\mu}_{i|k} \supseteq \mathcal{Z}^{\mu-1}_{i|k} \supseteq \ldots \supseteq \mathcal{Z}^{1}_{i|k} \quad \text{[MODE 1]} \tag{7.24}$$

$$\mathcal{Z}^{\mu}_{t} \supseteq \mathcal{Z}^{\mu-1}_{t} \supseteq \ldots \supseteq \mathcal{Z}^{1}_{t} \quad \text{[MODE 2]}. \tag{7.25}$$

An illustration of our notation above is shown in Figure 7.1.

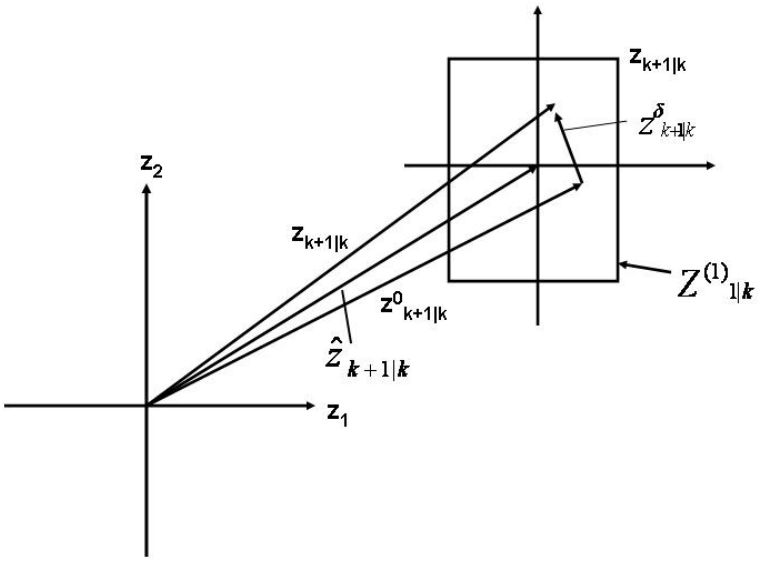

FIGURE 7.1: An illustration of a low complexity polytope ($l = 1$)defined by $\mathcal{Z}^l_{i|k} = \{z^\delta = \hat{z}_{i|k} + v_{i|k} : |v_{i|k}| \leq \overline{z}^{(l)}_{i|k}\}$ for a 2 dimensional system $n_x = 2$.

Having defined the bounded polytopes above along the prediction horizon, the transitional probabilities between these sets can be defined. Since the sets are bounded and finite, the one-step-ahead probabilities can be expressed in a matrix form as

$$\Pi = \begin{bmatrix} p_{11} & \cdots & p_{1\mu} \\ \vdots & \ddots & \vdots \\ p_{\mu 1} & \cdots & p_{\mu\mu} \end{bmatrix}. \tag{7.26}$$

By induction, the probability of a state belonging to a particular tube l at i steps ahead is given below. Note that at $i = 0$, the initial condition is known and

therefore specified to be in the innermost (l=1) tube with certainty($p_0^{(1)} = 1$).

$$\begin{bmatrix} p_i^{(1)} \\ \vdots \\ p_i^{(\mu)} \end{bmatrix} = (T^{-1}\Pi)^i e_1 \tag{7.27}$$

$$e_1 = [1\ 0\ \ldots\ 0], \quad T = \begin{bmatrix} 1 & 0 & \ldots & 0 \\ 1 & 1 & \ldots & 0 \\ \vdots & \vdots & \ddots & \vdots \\ 1 & 1 & \ldots & 1 \end{bmatrix}.$$

To ensure that the predicted state trajectories lie within these layered tubes, constraints are imposed for each step along the prediction horizon by specifying one-step-ahead transitional probabilities. In addition, constraints are further imposed so that the trajectories always satisfy hard constraints. For soft constraint handling, one-step-ahead soft constraint violation probabilities are specified. These constraints are outlined below (note that the notation $\Pr(X|Y)$ denotes the *maximum* probability of X given Y)

1. One-step-ahead Transitional Probability Constraint

$$\Pr\left(z_{k+i+1|k} \in \mathcal{Z}_{i|k}^{(l)} | z_{k+i|k} \in \mathcal{Z}_{i|k}^{(m)}\right) \geq p_{lm} \quad \text{[MODE 1]} \tag{7.28a}$$

$$\Pr\left(z_{k+i+1|k} \in \mathcal{Z}_{t}^{(l)} | z_{k+i|k} \in \mathcal{Z}_{t}^{(m)}\right) \geq p_{lm} \quad \text{[MODE 2]} \tag{7.28b}$$

2. Universality Constraint

$$\Pr\left(z_{k+i+1|k} \in \mathcal{Z}_{i|k}^{(\mu)} | z_{k+i|k} \in \mathcal{Z}_{i|k}^{(l)}\right) = 1 \quad \text{[MODE 1]} \tag{7.29a}$$

$$\Pr\left(z_{k+i+1|k} \in \mathcal{Z}_{t}^{(\mu)} | z_{k+i|k} \in \mathcal{Z}_{t}^{(l)}\right) = 1 \quad \text{[MODE 2]} \tag{7.29b}$$

3. One-step-ahead Soft Constraint Violation Probability Constraint

$$\Pr\left(F_s z_k + G_s u_k \geq H_s | z_{k+i|k} \in \mathcal{Z}_{i|k}^{(l)}\right) \leq p_l \quad \text{[MODE 1]} \tag{7.30a}$$

$$\Pr\left(F_s z_k + G_s u_k \geq H_s | z_{k+i|k} \in \mathcal{Z}_{t}^{(l)}\right) \leq p_l \quad \text{[MODE 2]} \tag{7.30b}$$

4. Feasibility Of Hard Constraint

$$H_l \leq F_h x_k + G_h u_k \leq H_h \quad \forall \mathcal{Z}_{i|k}^{(\mu)} \quad \text{[MODE 1]} \tag{7.31a}$$

$$H_l \leq F_h x_k + G_h u_k \leq H_h \quad \forall \mathcal{Z}_{t}^{(\mu)} \quad \text{[MODE 2]} \tag{7.31b}$$

Using the definition of tubes, together with the probabilistic constraints imposed above (7.28)-(7.31), and the transitional probabilities (7.26), it can be shown that the tube satisfies hard constraints (7.2) and the probability of soft constraint violations (7.3) at i steps along the prediction horizon is bounded by

$$\Pr\left(F_s z_{k+i} + G_s u_{k+i} \geq H_s\right) \leq [p_1 \ \ldots \ p_\mu]^T (T^{-1}\Pi)^i e_1 \tag{7.32}$$

The proof is given in Lemma 2 of Chapter 3.

Since the cost is given over an infinite horizon, the tubes must be feasible at all prediction times. Since constraints imposed in Mode 2 ensures feasibility from N to infinity, the controller should drive the state into the terminal set within N steps over Mode 1 and this can be enforced by

$$z_{k+N|k} + z_{k+N|k}^{\delta} \in \mathcal{Z}_t \quad \forall \quad z_{k+N|k}^{\delta} \in \mathcal{Z}_{N|k}^{(l)} \tag{7.33}$$

7.4 Probabilistic Tube Constraints

In the previous section, probabilistic constraints are imposed on the transition of states between the tubes along the prediction horizon. These tubes are guaranteed to be feasible with respect to hard constraints. From the transitional probabilities and the probability of one-step-ahead soft constraint violations in the tubes it is possible to determine an upper bound on the probability of violating a soft constraint at i steps ahead. This section translates the imposed constraints onto a set of linear constraints on parameters to be optimized on-line, namely, c^{δ},$\overline{z}_{k+i|k}$, and $\overline{z}_t$.

The probability of one-step-ahead soft constraint violation will be smaller for points located nearer to the origin on the current tube as compared to points nearer to the boundary of the tubes. Therefore the probability p_l of violating the soft constraint one-step-ahead given that the current state lies in $\mathcal{Z}^{(l)}$ should be chosen so that

$$0 < p_1 < p_2 < \ldots < p_\mu < 1 \tag{7.34}$$

The choice of one-step-ahead transitional probabilities between the tubes should be chosen so that the probability of transition into the inner sets is greater than the transition to the outer sets. Also, the universality constraint implies that all state transitions must lie within the outermost tube

$$p_{lm} > p_{lm+1}, \quad p_{\mu m} = 1, \quad l = 1, \ldots, \mu - 1; m = 1, \ldots, \mu. \tag{7.35}$$

Finally, the choice of Π and p_l should be such that the average probability of soft constraint violations over i steps (7.32) does not exceed a given specified bound

$$\frac{1}{N_c}\sum_{i=0}^{N_c-1}[p_1 \ \ldots \ p_\mu]^T(T^{-1}\Pi)^i e_1 \leq \frac{N_{max}}{N_c}. \tag{7.36}$$

Due to the nested properties of the tubes, the constraint (7.24) is equivalent to

$$0 \leq \overline{z}^{(1)}_{k+i|k} \leq \ldots \leq \overline{z}^{(\mu)}_{k+i|k} \quad \text{[MODE 1]} \tag{7.37}$$

$$0 \leq \overline{z}^{(1)}_{t} \leq \ldots \leq \overline{z}^{(\mu)}_{t} \quad \text{[MODE 2]}. \tag{7.38}$$

To invoke probabilistic constraints we use confidence intervals based on the probability distribution of $\varepsilon_k = Vd_k$ in (7.12). For the case of a two-dimensional random variable, we can take the confidence region to be a rectangular with with vertices (a,b). These vertices are non-unique and $\int_{-a}^{a}\int_{-b}^{b} T(a,b)dadb = p$ where $T(a,b)$ is a given probability distribution function. For convenience, the confidence region can be chosen to be a square and therefore the confidence interval of each random variables (in the two dimensional case) will then be over $\sqrt{p}$. The confidence regions of ε_k given by the Π and p_l are denoted

$$\Pr(|\varepsilon_k| \leq \xi_{lm}) = p_{lm} \quad \Pr(|\varepsilon_k| \leq \xi_l) = 1 - p_l \tag{7.39}$$

$$\Pr(|\varepsilon_k| \leq \overline{\xi}) = 1. \tag{7.40}$$

The probabilistic constraints on the tubes can be invoked via linear inequalities. Constraints (7.28)-(7.31) and (7.33) are imposed by the following inequalities.

$$\overline{z}^{(m)}_{i+1|k} \geq |\Phi_{k+i|k} D_p \overline{z}^{(l)}_{i|k}| + \Gamma_z|\hat{z}_{i|k} + D_p\overline{z}^{(m)}_{i|k}| + \Gamma_c|c^{\delta}_{i|k}| + \xi_{lm}\text{[MODE 1]} \tag{7.41}$$

$$\overline{z}^{(m)}_{t} \geq (|\Phi| + \Gamma_t)\overline{z}^{(l)}_{t} + \xi_{lm}\text{[MODE 2]} \tag{7.42}$$

$$\overline{z}^{(\mu)}_{i+1|k} \geq |\Phi_{k+i|k} D_p \overline{z}^{(l)}_{i|k}| + \Gamma_z |\hat{z}_{i|k} + D_p \overline{z}^{(l)}_{i|k}| + \Gamma_c |c^{\delta}_{i|k}| + \overline{\xi} \quad \text{[MODE 1]} \tag{7.43}$$

$$\overline{z}^{(\mu)}_{t} \geq (|\Phi| + \Gamma_t)\overline{z}^{(l)}_{t} + \overline{\xi} \quad \text{[MODE 2]} \tag{7.44}$$

$$\begin{aligned}(F_S + G_S K)W(z^0_{k+i+1|k} + \hat{z}_{i+1|k} + \Phi_{k+i|k} D_p \overline{z}^{(l)}_{i|k} + G_S(c^0_{i+1|k} + c^{\delta}_{i+1|k}) \\ + |(F_S + G_S K)W|(\Gamma_z |\hat{z}_{i|k} + D_p \overline{z}^{(l)}_{i|k}| + \Gamma_c |c^{\delta}_{i|k}| + \xi_l) \leq H_s \quad \text{[MODE 1]}\end{aligned} \tag{7.45}$$

$$|(F_S + G_S K)W|\{(|\Phi| + \Gamma_t)\overline{z}^{(l)}_{t} + \xi_l\} \leq H_s \quad \text{[MODE 2]} \tag{7.46}$$

$$H_l \leq (F_H + G_H K)W(z^0_{k+i|k} + \hat{z}_{i|k} + D_p \overline{z}^{(\mu)}_{i|k}) + G_H(c^0_{i|k} + c^{\delta}_{i|k}) \leq H_h \quad \text{[MODE 1]} \tag{7.47}$$

$$H_l \leq |(F_H + G_H K)W|\overline{z}^{(\mu)}_{t} \leq H_h \quad \text{[MODE 2]} \tag{7.48}$$

$$z^0_{k+N|k} + \hat{z}_{k+N|k} + D_p \overline{z}^{(l)}_{k+N|k} \leq \overline{z}^{(l)}_{t} \tag{7.49}$$

The derivations for the linear inequality constraints above are shown here:

1. **One-step-ahead Transitional Probability Constraint**

   The one-step-ahead transitional probability constraint (7.28) under control law (7.5) in Mode 1 is ensured by imposing (7.41) and (7.42).

From (7.12),(7.20), and (7.22) the following bound is obtained for $v_{k+i|k} = z^{\delta}_{k+i+1|k} - \hat{z}_{i+1|k}$

$$\begin{aligned} z^{\delta}_{k+i+1|k} - \hat{z}_{k+i+1|k} &= \Phi_{k+i|k} z^{\delta}_{k+i|k} - \Phi_{k+i|k}\hat{z}_{k+i|k} + e_{k+i|k} + \varepsilon_{i|k} \\ |z^{\delta}_{k+i+1|k} - \hat{z}_{i+1|k}| &\leq |\Phi_{k+i|k}(z^{\delta}_{k+i|k} - \hat{z}_{i|k})| + \Gamma_z |z^{\delta}_{k+i|k}| + \Gamma_c |c^{\delta}_{i|k}| + |\varepsilon_{k+i}| \\ |v_{i+1|k}| &\leq |\Phi_{k+i|k} v_{i|k}| + \Gamma_z |\hat{z}_{i|k} + v_{i|k}| + \Gamma_c |c^{\delta}_{i|k}| + |\varepsilon_{k+i}| \end{aligned}$$

The one-step-ahead transition from $v_{i|k} \in \mathcal{Z}^{(m)}_{i|k}$ to $v_{i+1|k} \in \mathcal{Z}^{(l)}_{i+1|k}$ is at least p_{lm} is sufficiently ensured by

$$\overline{z}^{(m)}_{i+1|k} \geq |\Phi_{k+i|k} D_p \overline{z}^{(l)}_{i|k}| + \Gamma_z |\hat{z}_{i|k} + D_p \overline{z}^{(m)}_{i|k}| + \Gamma_c |c^{\delta}_{i|k}| + \xi_{lm} \quad \text{[MODE 1]}.$$

In Mode 2, the tubes are centered on the origin, $v_{i|k} = z^{\delta}_{k+i|k}$

$$\begin{aligned} z^{\delta}_{k+i+1|k} &= \Phi z^{\delta}_{k+i|k} + e_{k+i|k} + \varepsilon_{i|k} \\ |z^{\delta}_{k+i+1|k}| &\leq |\Phi z^{\delta}_{k+i|k}| + \Gamma_t |z^{\delta}_{k+i|k}| + |\varepsilon_{k+i}| \\ |v_{i+1|k}| &\leq (|\Phi| + \Gamma_t)|v_{i|k}| + |\varepsilon_{k+i}| \end{aligned}$$

To ensure that the one-step-ahead transition from $v_{i|k} \in \mathcal{Z}^{(m)}_{t}$ to $v_{i+1|k} \in \mathcal{Z}^{(l)}_{t}$ is at least p_{lm}, the vertices $v_{i+1|k} = D_p \overline{z}_t$ should be lower bounded by the vertices at the current step $v_{i|k} = D_p \overline{z}_t$ and the confidence interval ξ_{lm}. This is sufficiently ensured by

$$\overline{z}^{(m)}_{t} \geq (|\Phi| + \Gamma_t)\overline{z}^{(l)}_{t} + \xi_{lm} \quad \text{[MODE 2]}.$$

2. **Universality Constraint**

The universality constraint (7.29) under control law (7.5) in Mode 1 and 2 is sufficiently ensure by imposing (7.43) and (7.44).

The proof is similar as above except that the one-step-ahead transition probability from $v_{i|k} \in \mathcal{Z}_{i|k}^{(l)}$ to $v_{i+1|k} \in \mathcal{Z}_{i+1|k}^{(\mu)}$ is 1. Hence, the vertices $v_{i+1|k} = D_p \overline{z}_{i+1|k}$ is lower bounded by the vertices at the current step $v_{i|k} = D_p \overline{z}_{i|k}$ and the confidence interval $\overline{\xi}$ for $i = 0, 1, \ldots$.

3. **One-step-ahead Soft Constraint Violation Probability Constraint**
The probabilistic one-step-ahead soft constraint violations (7.30) under control law (7.5) in Mode 1 is such that

$$\begin{aligned} F_S W z_{k+i+1|k} + G_S(KW z_{k+i+1|k} + c_{i+1|k}) &\leq H_s \\ (F_S + G_S K) W z_{k+i+1|k} + (G_S) c_{i+1|k} &\leq H_s \\ (F_S + G_S K) W (z^0_{k+i+1|k} + \hat{z}_{k+i+1|k} + v_{k+i+1|k}) + (G_S) c_{i+1|k} &\leq H_s. \end{aligned}$$

From (7.12),(7.20), and (7.22)

$$v_{k+i+1|k} = z^{\delta}_{k+i+1|k} - \hat{z}_{k+i+1|k} = \Phi_{k+i|k} z^{\delta}_{k+i|k} - \Phi_{k+i|k} \hat{z}_{k+i|k} + e_{k+i|k} + \varepsilon_{i|k}.$$

Therefore

$$\begin{aligned} (F_S + G_S K) W (z^0_{k+i+1|k} + \hat{z}_{k+i+1|k} + \Phi_{k+i|k} z^{\delta}_{k+i|k} - \Phi_{k+i|k} \hat{z}_{k+i|k} + e_{k+i|k} + \varepsilon_{i|k}) & \\ + (Gs)(c^0_{i+1|k} + c^{\delta}_{i+1|k}) &\leq H_s \\ (F_S + G_S K) W (z^0_{k+i+1|k} + \hat{z}_{k+i+1|k} + \Phi_{k+i|k} v_{k+i|k}) + & \\ |(F_s + G_s K) W| (|e_{k+i|k}| + |\varepsilon_{i|k}|) + (Gs)(c^0_{i+1|k} + c^{\delta}_{i+1|k}) &\leq H_s \end{aligned}$$

The maximum soft constraint violation occurs at the vertices $v_{k+i|k} = D_p \overline{z}_{i|k}$. Using the confidence intervals (7.39), the maximum soft constraint violation if $z^{\delta} \in \mathcal{Z}_{i|k}^{(l)}$ is ensured to be less than p_l. Hence, (7.30) is ensured by imposing

constraint (7.45) given by

$$(F_S + G_S K)W(z^0_{k+i+1|k} + \hat{z}_{i+1|k} + \Phi_{k+i|k} D_p \overline{z}^{(l)}_{i|k} + G_S(c^0_{i+1|k} + c^\delta_{i+1|k}) \\ +|(F_S + G_S K)W|(\Gamma_z|\hat{z}_{i|k} + D_p \overline{z}^{(l)}_{i|k}| + \Gamma_c|c^\delta_{i|k}| + \xi_l) \leq H_s \quad \text{[MODE 1]}.$$

For Mode 2, the derivation is similar to Mode 1 as follows

$$\begin{aligned} F_s W z^\delta_{k+i+1|k} + Gs W z^\delta_{k+i+1|k} &\leq H_s \\ (F_s + G_s K)W z^\delta_{k+i+1|k} &\leq H_s \\ |(F_s + G_s K)W|\{|\Phi z^\delta_{k+i|k} + e_{k+i|k} + \varepsilon_{k+i|k}|\} &\leq H_s \\ |(F_s + G_s K)W|\{(|\Phi| + \Gamma_t)|D_p \overline{z}^{(l)}_t| + \xi_l\} &\leq H_s. \end{aligned}$$

Therefore (7.30) is sufficiently ensured in Mode 2 by imposing constraint (7.46)

$$|(F_S + G_S K)W|\{(|\Phi| + \Gamma_t)\overline{z}^{(l)}_t + \xi_l\} \leq H_s \quad \text{[MODE 2]}.$$

4. **Feasibility Of Hard Constraint**

The hard constraint (7.31) in Mode 1 is such that

$$\begin{aligned} H_l \leq F_H W z_{k+i+1|k} + G_H(KW z_{k+i+1|k} + c_{i+1|k}) &\leq H_h \\ H_l \leq (F_H + G_H K)W z_{k+i+1|k} + G_H(c_{i+1|k}) &\leq H_h \\ H_l \leq (F_H + G_H K)W(z^0_{k+i+1|k} + \hat{z}_{k+i+1|k} + v_{k+i+1|k}) + G_H(c_{i+1|k}) &\leq H_h \end{aligned}$$

Due to the nested properties of the tube, hard constraints are satisfied as long as the outer most tube is feasible,

$$H_l \leq (F_H + G_H K)W(z^0_{k+i|k} + \hat{z}_{i|k} + D_p \overline{z}^{(\mu)}_{i|k}) + G_H(c^0_{i|k} + c^\delta_{i|k}) \leq H_h \quad \text{[MODE 1]}.$$

Similarly in Mode 2, we require that

$$\begin{aligned} H_l \leq F_H W z_{k+i+1|k} + G_H(KW z_{k+i+1|k}) &\leq H_h \\ H_l \leq (F_H + G_H K) W z_{k+i+1|k} &\leq H_h \\ H_l \leq (F_H + G_H K) W(v_{k+i+1|k}) &\leq H_h \\ H_l \leq (F_H + G_H K) W(D_p \overline{z}_t^{(\mu)}) &\leq H_h \\ H_l \leq |(F_H + G_H K) W| \overline{z}_t^{(\mu)} &\leq H_h \quad \text{[MODE 2]}. \end{aligned}$$

7.5 Cost Function

The 1-norm cost function over an infinite horizon is defined in (7.4). Due to the random uncertainty in the system model, the expectation of the cost function is taken over the assumed distribution of uncertainties. However, since the uncertainty appears additively in the model, the expectation of the steady state stage cost will not tend to zero, and therefore its summation would diverge to infinity. Hence, a bound on the expectation of the steady state stage cost is subtracted from the stage cost to ensure a finite value cost function is achieved.

The expected stage cost is defined in terms of perturbations as

$$l_k = \mathbb{E}(1^T |W z_{k+i|k}| + 1^T |K z_{k+i|k} + c_{i|k}|).$$

Hence an upper bound on the steady state stage cost is defined as

$$\mathbb{E}(1^T |W z_{ss}| + 1^T |KW z_{ss}|) \leq l_{ss}.$$

From (7.12) and (7.20), the one-step-ahead linearized state trajectory in Mode 2 is bounded by

$$|z_{k+1}| \leq (|\Phi| + \Gamma_t)|z_k| + |\varepsilon_k|.$$

Define $r_{k+1} = (|\Phi| + \Gamma_t)|z_k| + |\varepsilon_k|$ where z. The steady-state r_{ss} is given by

$$r_{ss} = (|\Phi| + \Gamma_t)r_{ss} + |\varepsilon_k|$$
$$r_{ss} = [I - (|\Phi| + \Gamma_t)]^{-1}|\varepsilon_k|.$$

As $k \to \infty$ the state trajectory

$$\lim_{k\to\infty} |z_k| \leq \lim_{k\to\infty} (|\Phi| + \Gamma_t)^k |z_0| + \sum_{i=1}^{k} (|\Phi| + \Gamma_t)^{i-1} |\varepsilon_{k-i}|.$$

If the eigenvalues of $(|\Phi| + \Gamma_t)$ are less than 1, then $|z_k| \to |z_{ss}|$ where

$$|z_{ss}| \leq r_{ss} = [I - (|\Phi| + \Gamma_t)]^{-1}|\varepsilon|.$$

$$\begin{aligned}
\mathbb{E}(1^T|Wz_{ss}| + 1^T|KWz_{ss}|) &\leq \mathbb{E}(1^T|W||z_{ss}| + 1^T|KW||z_{ss}|) \\
&\leq \mathbb{E}(1^T|W|[I - (|\Phi| + \Gamma_t)]^{-1}|\varepsilon| + 1^T|KW|[I - (|\Phi| + \Gamma_t)]^{-1}|\varepsilon|) \\
&= 1^T|W|[I - (|\Phi| + \Gamma_t)]^{-1}\mathbb{E}(|\varepsilon|) + 1^T|KW|[I - (|\Phi| + \Gamma_t)]^{-1}\mathbb{E}(|\varepsilon|)
\end{aligned}$$

Hence, the upper-bound to be subtracted from the infinite horizon costs is

$$l_{ss} = 1^T|W|[I - (|\Phi| + \Gamma_t)]^{-1}\mathbb{E}(|\varepsilon|) + 1^T|KW|[I - (|\Phi| + \Gamma_t)]^{-1}\mathbb{E}(|\varepsilon|) \tag{7.50}$$

where $\mathbb{E}(|\varepsilon|) = \int_0^a xp(x)dx$, and $p(x)$ is the symmetric compact probability distribution defined at $[-a, a]$.

In Mode 2, the cost function from $N, N+1, \ldots$ can be defined in term of upper

bounds based on the nested tubes. Since the linearization error bounds Γ_t and tube sizes $\overline{z}_t$ are constant throughout Mode 2, the Mode 2 cost function can be upper- bounded in terms of the size of $z_{k+N|k}$.

The stage cost at step i in Mode 2 is bounded by

$$\mathbf{1}^T|Wz_{k+i|k}| + \lambda\mathbf{1}^T|KWz_{k+i|k}| - l_{ss} \leq q^T|Wz_{k+i|k}| - \mathbb{E}_{k+i}(q^T|Wz_{k+i|k}|)$$

Using (7.12),(7.20), and (7.40), the inequality is expanded to

$$\mathbf{1}^T|Wz_{k+i|k}| + \lambda\mathbf{1}^T|KWz_{k+i|k}| - l_{ss} \leq q^T|W|(|z_{k+i|k}| + |\Phi z_{k+i|k}| - \Gamma_t|z_{k+i|k}| - \zeta).$$

By summing over $i = N, N+1, \ldots$ and taking the expectations the following bound is obtained

$$\sum_{i=N}^{\infty} \mathbb{E}_k(\mathbf{1}^T|Wz_{k+i|k}| + \lambda\mathbf{1}^T|KWz_{k+i|k}| - l_{ss}) \leq q^T|Wz_{k+N|k}|. \tag{7.51}$$

Therefore, the summation of the stage cost in Mode 2 is finitely bounded in terms of $z_{k+N|k}$. In Mode 2, all state trajectories lie within the terminal set if $z_{k+N|k} \in \mathcal{Z}_t^{(l)}$. Using the results above, the optimal bound on the Mode 2 cost can be determined by solving for $q^{(l)}$ for $l = 1, \ldots, \mu$:

$$\begin{aligned} q^{(l)} = &\arg\min_q q^{(l)T}|W|\overline{z}_t^{(l)} \\ &\text{s.t } q^{(l)T}|W|(\overline{z}_t^{(\mu)} - |\Phi D_p \bar{z}_t^{(\mu)}| - \Gamma_t \overline{z}_t^{(\mu)} - \zeta) \geq \\ &\mathbf{1}^T|WD_p\overline{z}_t^{(\mu)}| + \lambda\mathbf{1}^T|KWD_p\overline{z}_t^{(\mu)}| - l_{ss}, \quad p = 1, \ldots, 2^{n_x} \end{aligned} \tag{7.52}$$

The infinite horizon cost can now be upper-bounded and finitely parameterized. Define V as the bound given by

$$V(\mathbf{c}_k^{\delta}, \overline{z}_{i|k}^{(l)}, x_{k+i|k}^0, \mathbf{c}_k^0) = \sum_{j=1}^{\mu} \left\{ \sum_{i=0}^{N-1} \max_{z_{i|k}^{\delta} \in \mathcal{Z}_{i|k}^{(j)}} \left(\mathbf{1}^T |W z_{k+i|k}| + \lambda |KW z_{k+i|k} + c_{i|k}^0 + c_{i|k}^{\delta}| - l_{ss} \right) p_i^{(j)} + q^{(j)T} |W z_{k+N|k}| p_N^{(j)} \right\} \tag{7.53}$$

7.6 Receding Horizon NLSMPC

The implementation of the NLSMPC algorithm requires the computation of Γ_t in (7.21) and $\Gamma_{k+i|k}^z, k = 1, 2, \ldots, i = 1, \ldots, N$ in in (7.20). The computation of Γ_t is performed offline by firstly gridding the operating regions $\mathcal{X}$ with equally spaced points. Then for each point on the grid, compute the linearization errors (7.14b). The matrix Γ_t is computed by solving the following optimization problem

$$\min_{\Gamma_t} \max_{(V^{-1} z^{\delta}) \in \mathcal{X}} \|\Gamma_t\|_1 \tag{7.54}$$
$$\text{subject to (7.21).}$$

The computation of $\Gamma_{k+i|k}^z, k = 1, 2, \ldots, i = 1, \ldots, N$, however, is performed online. Using the same points from the grid in the set $\mathcal{X}$, compute the linearization errors in (7.14a). The matrices $\Gamma_{k+i|k}^z$ are computed by solving the following optimization problem for $k = 0, 1, \ldots$ and $i = 1, \ldots, N$

$$\min_{\Gamma_{k+i|k}^z} \max_{(V^{-1} z_{k+i|k}^{\delta}) \in \mathcal{X}} \|\Gamma_{k+i|k}^z\|_1 \tag{7.55}$$
$$\text{subject to (7.20).}$$

In the online receding horizon optimization, the last tube in the prediction horizon is forced to lie within the terminal set, and it is therefore desirable to maximize this terminal set. The offline computation of a maximum volume, feasible and invariant terminal set is performed by solving:

$$\arg \max_{(\overline{z}_t^{(1)},\ldots,\overline{z}_t^{(\mu)})} \prod_{j=1}^{\mu} vol(\mathcal{Z}_t^{(j)}) \tag{7.56}$$

$$\text{subject to} (7.38), (7.42), (7.44), (7.46), \text{and} (7.48).$$

Finally, the full receding horizon control algorithm is outlined. It is divided into two parts, namely, the off-line and online stage.

Algorithm 9. (Nonlinear Stochastic MPC)

1. (OFF-LINE:) Given p_j, p_{jm} satisfying (7.34)-(7.36), compute parameters K,V, terminal sets $\overline{Z}_t^{(l)}, l = 1, \ldots, \mu$, the terminal weights $q^{(j)}$, and Γ_t as outlined in Algorithm (7.56), Algorithm (7.52), and Algorithm (7.54) respectively.

2. (ONLINE:) At times $k = 0, 1, \ldots$: Given $\mathbf{c}_k^0$, calculate $x_{k+i|k}^0$, and $\Phi_{k+i|k}$, $B_{k+i|k}$, $\Gamma_{k+i|k}^z$, for $i = 0, \ldots, N$ and solve

$$\mathbf{c}_k^{\delta *} = \arg \min_{\mathbf{c}_k^\delta, \{\overline{z}_{i|k}^{(l)}\}} V(\mathbf{c}_k^\delta, \{\overline{z}_{i|k}^{(l)}\}, \{x_{k+i|k}^0\}, \mathbf{c}_k^0) \tag{7.57}$$

$$\text{subject to } (7.42) - (7.49).$$

3. Set $u_k = Kx_k + c_{0|k}^0 + c_{0|k}^{\delta *}$ and $\mathbf{c}_{k+1}^0 = \left\{c_{1|k}^0 + c_{1|k}^{\delta *}, \ldots, c_{N-1|k}^0 + c_{N-1|k}^{\delta *}, 0\right\}$.

Theorem 8. In closed-loop operation, the NLSMPC algorithm has the properties:

1. the optimization (7.57) is feasible for all $k > 0$ if feasible at $k = 0$

2. the optimal value $V^*(x^0_{k+i|k}, \mathbf{c}^0_k)$ of the objective (7.53) satisfies

$$\mathbb{E}_k[V^*(x^0_{k+i+1|k+1}, \mathbf{c}^0_{k+1})] - V^*(x^0_{k+i|k}, \mathbf{c}^0_k) \leq l_{ss} - \mathbf{1}^T|x_k| - \lambda \mathbf{1}^T|u_k| \quad (7.58)$$

3. constraints (7.2) and (7.3) are satisfied at all times k and

$$\lim_{n\to\infty} \frac{1}{n} \sum_{k=0}^{n} \mathbb{E}_0(\mathbf{1}^T|x_k| + \lambda \mathbf{1}^T|u_k|) \leq l_{ss}. \quad (7.59)$$

Proof. 1 and 2 follow from feasibility of $\mathbf{c}^\delta_k = 0$ in (7.57). Constraint satisfaction in 3 follows from 1, and (7.59) results from summing (7.58) over $0 \leq k \leq n$ and noting that $V^*(x^0_{k+i|k}, \mathbf{c}^0_k)$ is finite. □

The optimization (7.57) to be solved online is formulated as a linear program. Note that the number of constraints in (7.57) depends linearly on the horizon N and the number of tubes r, but grows exponentially with the dimension of the model state due the exponential growth in the number of vertices of $Z^{(j)}_{i|k}$. The required online computation therefore grows rapidly with model size.

If the constraints on online computation allow for more than one optimization at each sample, then setting $\mathbf{c}^0_k \leftarrow \mathbf{c}^0_k + \mathbf{c}^{\delta *}_k$ and repeating Step 1 results in non-increasing optimal cost values $V^*(x^0_{k+i|k}, \mathbf{c}^0_k)$. This process generates a sequence of iterates $\mathbf{c}^{\delta *}_k$ that converges to an optimum point for the problem of minimizing (7.53) for the nonlinear dynamics (7.9) at time k.

7.7 Numerical Example

In this section, the NLSMPC algorithm is applied to the model of a coupled tank system shown in Figure 7.2. The system is governed by the principal that the input flow is equal to the output flow plus accumulation in each tank. Water flow

is explained by Bernoulli's equation which states that the flow is proportional to the square root of the water level. The process parameters are taken from [66] and outlined in Table 7.1. The objective of the control problem is to adjust the

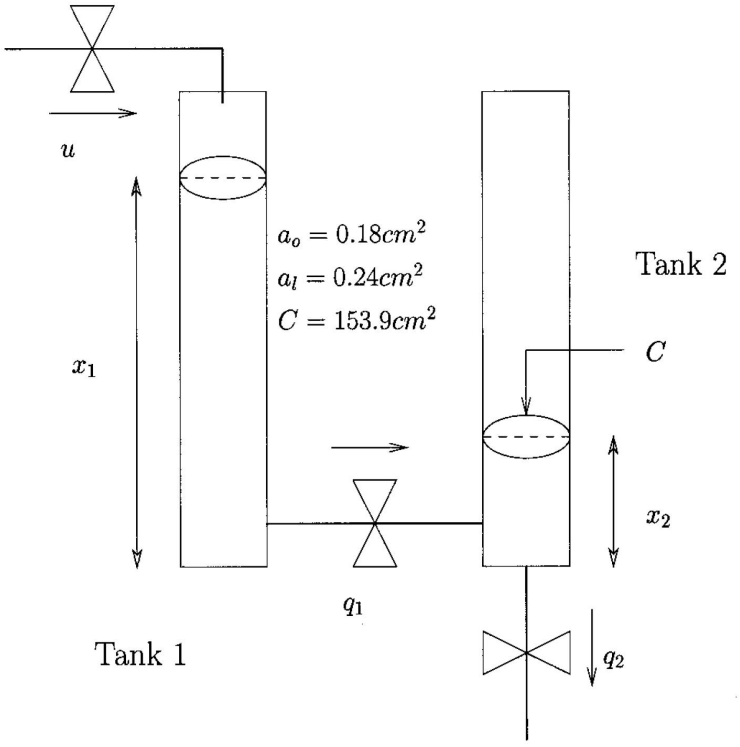

FIGURE 7.2: Coupled Tank System: a_o and a_l are the cross-sectional area of the inlet and outlet flow pipe.C is the cross-sectional area of the tanks.

input flow u such that the height of the second tank h_2 is maintained at a desired point. The fluid level heights of the first and second tank is given by $h_1 = x_1 + x_1^r$ and $h_2 = x_2 + x_2^r$ respectively. The set points corresponding to a flow rate of $u_r = 35cm^3/s$ are $x_1^r = 30.14cm$ and $x_2^r = 19.29cm$.

The system is described by the following continuous-time nonlinear state space equations

$$f(x,u) = \begin{bmatrix} -a_1\sqrt{h_1 - h_2} + \frac{1}{C}(u^r + u) \\ a_1\sqrt{h_1 - h_2} - a_2\sqrt{h_2} \end{bmatrix} \tag{7.60}$$

where $a_1 = \frac{\sigma_l\sqrt{2g}}{C}$ and $a_2 = \frac{\sigma_0\sqrt{2g}}{Ca}$.Also, x_1^r, x_2^r, and u_r are the equilibrium states and input and defined by $a_1\sqrt{x_1^r - x_2^r} = a_2\sqrt{x_2^r} = \frac{1}{C}u^r$ respectively.

The continuous-time model is Euler discretized using a sampling interval of $T_s = 10s$ giving the following discrete-time nonlinear model

$$f(x_k, u_k) = \begin{bmatrix} x_{1,k} + T_s\left(-a_1\sqrt{h_{1,k} - h_{2,k}}\right) \\ x_{2,k} + T_s\left(a_1\sqrt{h_{1,k} - h_{2,k}} - a_2\sqrt{h_{2,k}}\right) \end{bmatrix} + \begin{bmatrix} \frac{T_s}{C} \\ 0 \end{bmatrix}(u^r + u_k) \quad (7.61)$$

where $x_{1,k}$ and $x_{2,k}$ denote the first and second element of x_k respectively and the origin is an equilibrium point ($f(0,0) = 0$).

Under the control law of $u_k = Kx_k + c_k$, define

$$\begin{aligned} \phi(x_k, c_k) &= f(x_k, Kx_k + c_k) \\ &= \begin{bmatrix} x_{1,k} + T_s\left(-a_1\sqrt{h_{1,k} - h_{2,k}} + \frac{Kx_k + u^r}{C}\right) \\ x_{2,k} + T_s\left(a_1\sqrt{h_{1,k} - h_{2,k}} - a_2\sqrt{h_{2,k}}\right) \end{bmatrix} + \begin{bmatrix} \frac{T_s}{C} \\ 0 \end{bmatrix} c_k \end{aligned} \quad (7.62)$$

$$\left.\frac{\partial\phi}{\partial x}\right|_{(x_k, c_k)} = \begin{bmatrix} 1 & 0 \\ 0 & 1 \end{bmatrix} + T_s \begin{bmatrix} -h_d + \frac{K_1}{C} & h_d + \frac{K_2}{C} \\ h_d & -h_d - \frac{a_2}{2}(h_2)^{-0.5} \end{bmatrix} \quad (7.63)$$

where $h_d = \frac{a_1}{2}(h_1 - h_2)^{-0.5}$, and K_1 and K_2 denotes the first and second element of K respectively.

$$\left.\frac{\partial\phi}{\partial c}\right|_{(x_k, c_k)} = \begin{bmatrix} \frac{Ts}{C} \\ 0 \end{bmatrix} \quad (7.64)$$

The state predictions are governed by the model

$$x_{k+i+1|k} = \phi(x_{k+i|k}, c_{i|k}) + d_{k+i} \quad (7.65)$$

σ_0	0.18
σ_l	0.24
C	153.9
g	10
Equilibrium (x^r, u^r)	$([30.14, 19.29]^T$,35)
Hard Input constraint	$u_k \in [0, 70]$
Hard State constraint	$x_{1,k}, x_{2,k} \in [0, 40]$
Soft State constraint	$h_k < [1.0, 3.0]^T$
Sampling Period	$T_s = 10$

TABLE 7.1: Parameter settings for the case study.

σ_0	Orifice Areas
σ_l	Orifice Areas
C	Cross Sectional Area of Tanks
g	Gravitational constant

TABLE 7.2: Relevant constants for the Coupled Tanks dynamic model.

where d_{k+i} is the additive disturbance, which for this example, is taken to be a finitely supported triangular distribution over $[-\xi, \xi]$ ($\xi = 0.2$)with zero mean. The triangular distribution is taken to model the perturbations on the water surfaces of both tanks as water is continuously pumped into the first tank. The algorithm here is flexible in the sense that it enables any distribution with finite support to be used. The physical justification of using the NLSMPC controller here is so that the variations in the pump output is reduced. This effectively reduces the fatigue damage on the pump which arises from continuous usage.

For simplicity of illustration, the number of overlapping tubes are chosen to be $\mu = 2$. The transition probabilities between tubes and probability of one-step-ahead soft constraint violations are chosen to be

$$\Pi = \begin{bmatrix} 0.9 & 0.6 \\ 1 & 1 \end{bmatrix} \quad p = [0.4\ 0.7]^T$$

$$F_s = \begin{bmatrix} 1 & 0 \\ 0 & 1 \end{bmatrix} \quad H_s = \begin{bmatrix} 1 \\ 3 \end{bmatrix}$$

For a given horizon of $N_c = 3$, the corresponding maximum number of constraint violations,N_{max} based on the transitional probabilities are computed to be $\frac{1}{N_c}\sum_{i=0}^{N_c-1}[p_1\ p_2](T^{-1}\Pi)^i e_j \leq 0.56, j = 1, 2.$

Using the system parameter settings as outlined in Table 7.1, the following state space matrices and control parameters (in Mode 2) are computed off-line:

$$A = \left.\frac{\partial f}{\partial x}\right|_{(0,0)} = \begin{bmatrix} 0.8988 & 0.1012 \\ 0.1012 & 0.8418 \end{bmatrix} \quad B = \left.\frac{\partial f}{\partial u}\right|_{(0,0)} = \begin{bmatrix} 0.0628 \\ 0 \end{bmatrix}$$

$$K = \begin{bmatrix} -6.5660 & -2.7096 \end{bmatrix}$$

The matrix V is formed by eigenvectors of $A + BK$ as columns and the diagonal matrix Φ contains the eigenvalues of $A + BK$, and $W = V^{-1}$. These matrices are computed respectively to be

$$V = \begin{bmatrix} -1.1143 & -0.2294 \\ -0.3297 & -1.0889 \end{bmatrix} \quad W = \begin{bmatrix} -0.9571 & 0.2017 \\ 0.2898 & -0.9795 \end{bmatrix}$$

$$\Phi = \begin{bmatrix} 0.5074 & 0 \\ 0 & 0.8210 \end{bmatrix}$$

The operating region is defined as a finite region of space centred on the nominal nonlinear trajectory $\{z^0_{k|k}, \ldots, z^0_{k+N|k}\}$ in Mode 1 and centered on the origin in Mode 2. The linearization errors are computed over a set of points forming a regularly spaced grid over this region. These values are then used to compute the

matrices satisfying the Lipschitz condition. In this example, a grid of $|z^\delta| \leq 4$ is used. The bound obtained for Mode 2 is

$$\Gamma_t = \begin{bmatrix} 0.0314 & 0.0806 \\ 0.0806 & 0.0101 \end{bmatrix}.$$

The terminal sets and terminal weights are computed off-line and given by $\bar{z}_t^{(1)} = [2.56, 3.95]^T$, $\bar{z}_t^{(2)} = [2.63, 4.00]^T$ and $q^{(1)} = q^{(2)} = [7.33 - 0.70]^T$ respectively.

In the online stage, an initial condition of $z_0 = [3, 1]^T$ is chosen. The NLSMPC algorithm is simulated for $k = 10$ steps and due to uncertainty, the algorithm has to be simulated for a wide range of possible realizations of uncertainties (100 realizations were deemed to be sufficient).

Figure 7.3 shows the closed-loop responses of the height of Tank 1 and 2 and the input trajectories. Figure 7.4 show the closed loop state trajectories for z_k generated by the NLSMPC algorithm as compared to the trajectory generated by the linearized model ($z_{k+1} = \Phi z_k$ with linear feedback $u_k = KWz_k$) for 100 realizations of uncertainty. It can be seen from Figure 7.4 that over 100 realizations, the first element of z_k violates the soft constraint at time step $k = 0$ and $k = 1$ for all 100 realizations. On the contrary the trajectory generated by the NLSMPC algorithm violates the soft constraint only 2 times out of the 100 realizations at time $k = 1$.

If the time constraints on online computation allow for more than one optimization at each sample, then setting $\mathbf{c}_k^0 \leftarrow \mathbf{c}_k^0 + \mathbf{c}_k^{\delta *}$ and repeating the optimization results in non-increasing optimal cost values $V^*(x_{k+i|k}^0, \mathbf{c}_k^0)$, as shown in Table 7.3.

$V^*(x^0_{k+i\|k}, \mathbf{c}^0_k)$	$k=1$	$k=2$	$k=3$
Iteration 1	26.09	18.28	14.11
Iteration 2	25.54	18.22	14.06
Iteration 3	25.53	18.21	14.05

TABLE 7.3: The optimization is repeated 3 times at each sample for 3 time steps and by setting $\mathbf{c}^0_k \leftarrow \mathbf{c}^0_k + \mathbf{c}^{\delta *}_k$ generates a sequence of iterates $\mathbf{c}^{\delta *}_k$ that converges to an optimum point.

7.8 Conclusion

This chapter extend the TSMPC algorithm to nonlinear systems. Jacobian linearization about predicted trajectories is used to derive a sequence of convex optimization problems. Linearizations about predicted trajectories allow for an efficient online optimization which may be terminated after a single iteration. Constraints are handled through the construction of a sequence of tubes and an associated Markov chain model. The parameters defining the tubes are optimized simultaneously with the predicted future control trajectory via online Linear Programming. The tractability of the Non-linear Stochastic Model Predictive Control (NLSMPC) algorithm is demonstrated by an example of a coupled-tank system. The algorithm has the advantage that it has guarantees of feasibility and stability and the ability to handle probabilistic constraints. However, it suffers from a growth in computational complexity as the system order is increased.

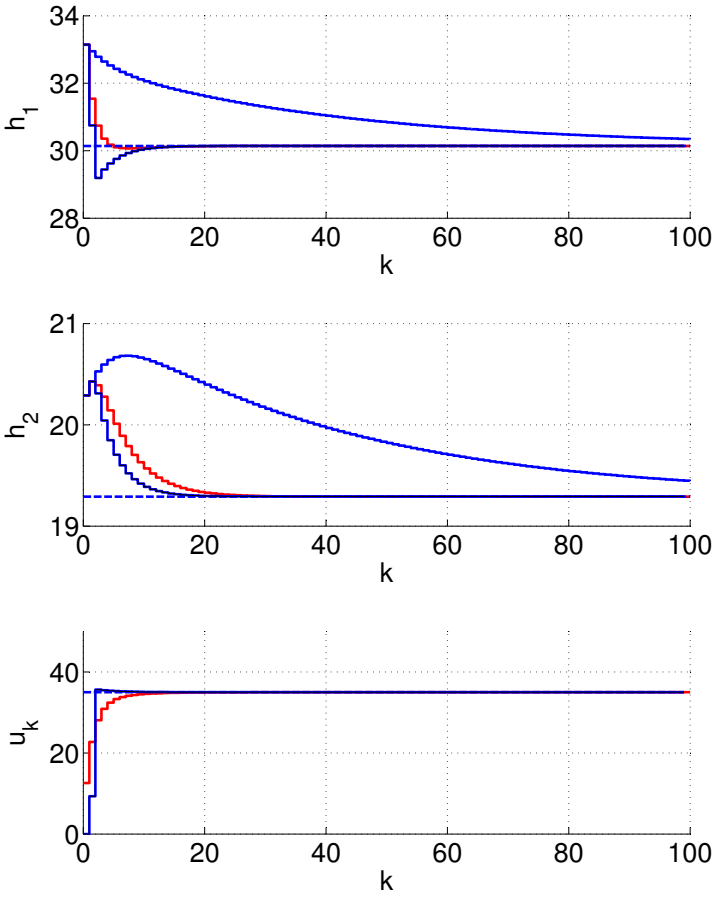

FIGURE 7.3: Plot of the closed loop trajectory for one realization of uncertainty. Top: Height of Tank 1,Middle: Height of Tank 2, Bottom: Input. Blue: $u_k = u_r$, Red: $u_k = Kx_k$, Black:$u_k = Kx_k + c_k$

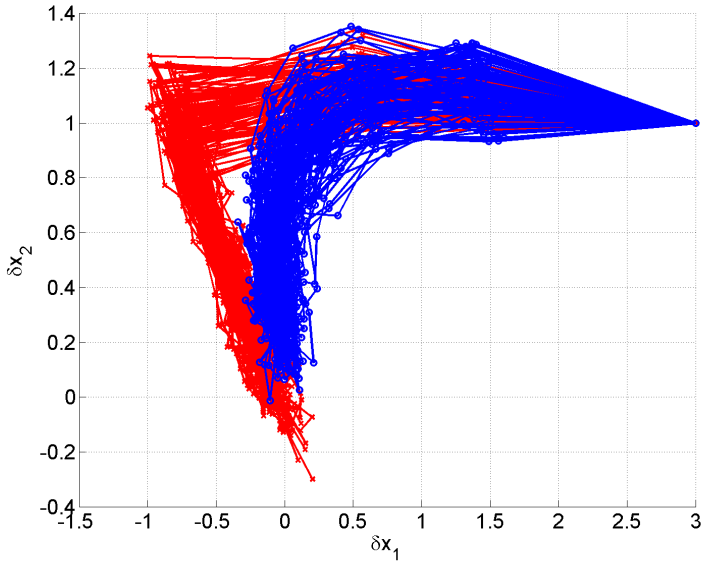

FIGURE 7.4: Plot of the trajectories of z_k for $k = 1, \ldots, 6$ and 100 realizations of uncertainty. The blue line shows the trajectory under the unconstrained LQ Optimal control on the linearized model while the red is under the NLTSMPC algorithm.

Chapter 8

Conclusion

A novel SMPC algorithm (denoted TSMPC) based on the receding horizon control methodology is developed for linear systems with additive and multiplicative bounded disturbances subjected to hard and probabilistic constraints. The algorithm is shown to handle stochastic uncertainty and constraints efficiently.

The strategy of the algorithm is to construct a sequence of nested polytopic sets (or tubes) centred around the nominal predicted trajectory. The probability of constraint violations at the next time step, given that the current state lies in a particular polytopic set is constrained. Furthermore, the transition probability of states between these sets from the current time step to the next is constrained and forms the basis of a Markov Chain Model. The series of nested tubes and Markov Chain Model forms the framework for probabilistic constraint handling. It is shown that a series of constraints on the tubes which are linear in the parameters, can be derived ensuring constraint satisfaction along the prediction horizon.

The control law employs the dual mode paradigm, where an infinite cost is parameterized by a finite number of decision variables. The dual mode paradigm is divided into Mode 1 and Mode 2. Mode 1 spans the length of a prediction horizon over which constraints are handled explicitly and Mode 2 spans from the end of this

initial prediction horizon to infinity. The control law is a linear optimal feedback law throughout the infinite horizon of Mode 2 with perturbations along the finite prediction horizon in Mode 1. These perturbations are the degrees of freedom to be optimized with respect to a performance cost, subject to constraints.

The performance measure is in the form of an infinite horizon quadratic objective function, and is taken to be the expectation across all possible realizations of model uncertainty. Without additive uncertainty, the objective function is well defined because the cost converges to zero in the steady state. However, in the presence of persistent additive uncertainty, the stage cost converges to a non-zero value and when the infinite sum is taken, it will diverge to infinity. Therefore, the objective function is redefined by subtracting from the stage cost the non-zero asymptotic value of the stage cost.

The use of terminal invariant sets into which the state at the end of the Mode 1 prediction horizon are driven ensures unconstrained optimality in Mode 2. In the interest of maximizing the region of attraction, an off-line optimization of the terminal sets is performed. The tube sequences provide a means of bounding the receding horizon performance cost and satisfaction of constraints.

Therefore, the online algorithm essentially minimizes the objective function subject to linear constraints with free parameters defining the sizes and location of probabilistic tubes along the predicted horizon at each step. The first input is implemented and the optimization is repeated for the next step. The optimization performed is a Quadratic Program which can be solved very efficiently.

The QP problem can be solved reliably using a variety of methods and one such method is the Primal Barrier Interior-Point method. The main advantage of this method is that it exploits the structure of the problem. Evidently, the QP problem has considerable structure. Both the inequality and equality constraints have block tridiagonal and block-diagonal structure which can be exploited to solve

the QP efficiently.This method, like any interior point method solves an optimization problem with linear equality and inequality constraints by reducing it to a sequence of linear equality constrained problems, which is solved using Newton's methods.The equality constrained minimization problem is reduced to an unconstrained problem, in particular, reduced to a system of linear equations. The computational time using a basic primal barrier method is made faster without significant decrease in the quality of control law by fixing the barrier parameter and maximum number of Newton iterations. The computational improvement is shown using two examples. The first example shows the degree of sub-optimality of the QP solution obtained by using the Approximate Primal Barrier Method as compared to solving it exactly is minimal. The second example shows the timing profiles compared to using a generic optimization solver for a random system with varying model order, prediction horizon, number of inputs and tube layers.

Predicting how current technological development will affect potential for development in the future is inherently random. Assuming there is some statistical regularity, a stochastic model can be used to generate predictions. The resource allocation problem (SD problem) here concerns the allocation of research and development investments between different power generating technologies. Several measures of performance can be used which include price of energy and CO_2 emissions. Constraints can be placed on these measures such as a limit on CO_2 emission in 3 years time. The goal here is therefore to allocate investments to give the 'best' measure of predicted performance subject to constraints. The stochastic model used to make predictions is an economic model called 'Prometheus'. In MPC terms, this is equivalent to controlling a system subject to model parameter uncertainty and additive disturbance. Hence, the Tube Stochastic MPC can be directly applied to solve the resource allocation problem.

The TSMPC algorithm applied to linear systems with hard and probabilistic constraints is adapted to handle the case where the model uncertainty is not temporally independent. When the uncertainty is not temporally independent, an infinite horizon cost function based on expected value of a quadratic stage cost cannot be written compactly as a quadratic expression in terms of the degrees of freedom. However, an infinite horizon cost function based on the nominal trajectory generated by uncertainty free system can be defined. Constraints are handled using the same strategy of defining a sequence of overlapping tubes, corresponding to a sequence of confidence levels depending on time-step k on the predicted future plant state, and imposing a set of constraints the one-step-ahead predictions. A guarantee of the recursive feasibility of the online optimization ensures the closed loop system trajectories satisfy both hard and soft constraints. It was shown that the TSMPC algorithm adapted to handle temporally dependent uncertainty is less conservative compared to the case where the original TSMPC algorithm for the case of temporally independent uncertainties.

A Receding Horizon Control methodology was proposed for systems with nonlinear dynamics, additive stochastic uncertainty, and both hard and soft (probabilistic) input/state constraints. Jacobian linearization about predicted trajectories is used to derive a sequence of convex optimization problems. Linearizations about predicted trajectories allow for an efficient online optimization which may be terminated after a single iteration. Constraints are handled through the construction of a sequence of tubes and an associated Markov chain model. The parameters defining the tubes are optimized simultaneously with the predicted future control trajectory via online Linear Programming. The tractability of the Non-linear Stochastic Model Predictive Control (NLSMPC) algorithm is demonstrated by an example of a coupled-tank system.

The main drawback of the algorithms proposed in this thesis is that invoking the transitional and violation probability constraints over a confidence polytopes

results in a large number of variables and linear inequalities in the online optimization. The number of constraints, (and hence the computational complexity) grows exponentially with the system order, number of tube layers, and prediction horizon. However, by exploiting the structure inherent in the MPC optimization problem, the computation complexity grows linearly with the prediction horizon. Nonetheless this still results in limitations of applications to low-dimensional systems even if the number of tube layers is small. For small number of tube layers, the handling of probabilistic constraints becomes conservative. Furthermore, the confidence region corresponding to a given probability p is not unique, yet affects the degree of conservatism in closed loop performance. A possible solution is to use layered ellipsoidal tubes centered on a nominal trajectory. Preliminary work on this approach is presented in [67]. Note however that this approach does not handle multiplicative uncertainiy, which is considered in this thesis. The scalings which define the ellipsoidal sizes and the nominal trajectory can be allowed to vary with time. The evolution of the tubes can be described by a simple dynamical system which implies a significant reduction in the number of optimization variables. The dynamical system governing the tube scalings is stochastic and the computation of the predicted distributions of tube scalings is done using a process of discretization. These distributions enable bounds to be imposed on the probability of violation of state and input constraints. These computations are performed offline and therefore allow many tube layers to be used without a significant increase in the online computation.

Bibliography

[1] J. Richalet, A. Rault, J.L. Testud, and J. Papon. Model predictive heuristic control: Applications to industrial processes. *Automatica*, 14(5):413–428, 1978.

[2] C.R. Cutler and B.L. Ramaker. Dynamic matrix control-a computer control algorithm. In *Proceedings of the Joint Automatic Control Conference*, pages 13–15, 1980.

[3] D.Q. Mayne, J.B. Rawlings, C.V. Rao, and P.O.M. Scokaert. Constrained model predictive control: Stability and optimality. *Automatica*, 36(6):789–814, 2000.

[4] C.E. Garcia and A.M. Morshedi. Quadratic programming solution of dynamic matrix control (QDMC). *Chemical Engineering Communications*, 46(1):73–87, 1986.

[5] S.J. Qin and T.A. Badgwell. A survey of industrial model predictive control technology. *Control Engineering Practice*, 11(7):733–764, 2003.

[6] D.W. Clarke, C. Mohtadi, and P.S. Tuffs. Generalized Predictive Control-Part I The basic algorithm. *Automatica*, 23(2):137–148, 1987.

[7] D.W. Clarke, C. Mohtadi, and P.S. Tuffs. Generalized Predictive Control-Part II Extensions and interpretations. *Automatica*, 23(2):149–160, 1987.

[8] D.W. Clarke and R. Scattolini. Constrained receding-horizon predictive control. In *Proceedings of the IEE, Part D, Control Theory and Applications*, volume 138, pages 347–354, 1991.

[9] E. Mosca and Z.X. Jing. Stable redesign of predictive control. *Automatica*, 28(6):1229–1233, 1992.

[10] D.H. van Hessem and O.H. Bosgra. A conic reformulation of Model Predictive Control including bounded and stochastic disturbances under state and input constraints. In *Proceedings of the 41st IEEE Conference on Decision and Control*, volume 4, pages 4643–4648, 2002.

[11] I. Batina, A.A. Stoorvogel, and S. Weiland. Optimal control of linear, stochastic systems with state and input constraints. In *Proceedings of the 41st IEEE Conference on Decision and Control*, volume 2, pages 1564 – 1569, 2002.

[12] P. Couchman, B. Kouvaritakis, and M. Cannon. MPC on state space models with stochastic input map. In *45th IEEE Conference on Decision and Control*, pages 3216–3221, 2006.

[13] M. Cannon, B. Kouvaritakis, and X. Wu. Probabilistic constrained MPC for systems with multiplicative and additive stochastic uncertainty. *IEEE Transactions on Automatic Control*, 54(7):1626–1632, 2009.

[14] M. Cannon, B. Kouvaritakis, and X. Wu. Model predictive control for systems with stochastic multiplicative uncertainty and probabilistic constraints. *Automatica*, 45(1):167–172, 2009.

[15] C.V. Rao, S.J. Wright, and J.B. Rawlings. Application of interior-point methods to model predictive control. *Journal of Optimization Theory and Applications*, 99(3):723–757, 1998.

[16] B. Kouvaritakis, M. Cannon, and V. Tsachouridis. Recent developments in stochastic MPC and sustainable development. *Annual Reviews in Control*, 28 (1):23–35, 2004.

[17] J.A. Primbs. Portfolio Optimization Applications of Stochastic Receding Horizon Control. In *American Control Conference*, pages 1811–1816, 2007.

[18] P.J. Meindl. Dynamic hedging of single and multi-dimensional options with transaction costs: a generalized utility maximization approach. *Quantitative Finance*, 8(3):299–312, 2008.

[19] J. Yan and R.R. Bitmead. Incorporating state estimation into model predictive control and its application to network traffic control. *Automatica*, 41(4): 595–604, 2005.

[20] P. Couchman, B. Kouvaritakis, and M. Cannon. LTV models in MPC for sustainable development. *International Journal of Control*, 79(1):63–73, 2006.

[21] H. Chen and F. Allgower. Quasi-infinite horizon nonlinear model predictive control scheme with guaranteed stability. *Automatica*, 34(10):1205–1217, 1998.

[22] R. Bellman. Dynamic Programming. *Science*, 153(3731):34–37, 1966.

[23] F. Blanchini. Set invariance in control. *Automatica*, 35(11):1747–1767, 1999.

[24] S.P. Boyd, L.E. Ghaoui, E. Feron, and V. Balakrishnan. *Linear Matrix Inequalities in System and Control Theory*. Society for Industrial & Applied Mathematics, 1994.

[25] Y.I. Lee and B. Kouvaritakis. Robust receding horizon predictive control for systems with uncertain dynamics and input saturation. *Automatica*, 36(10): 1497–1504, 2000.

[26] B. Kouvaritakis, M. Cannon, A. Karas, B. Rohal-Ilkiv, and C. Belavy. Asymmetric constraints with polytopic sets in MPC with application to coupled tanks system. *International Journal of Robust and Nonlinear Control*, 14(4): 341–353, 2004.

[27] T.B. Blanco, M. Cannon, and B. De Moor. On efficient computation of low-complexity controlled invariant sets for uncertain linear systems. *International Journal of Control*, 83(7):1339–1346, 2010.

[28] J.A. Rossiter, B. Kouvaritakis, and M.J. Rice. A numerically robust state-space approach to stable-predictive control strategies. *Automatica*, 34(1): 65–73, 1998.

[29] M.V. Kothare, V. Balakrishnan, and M. Morari. Robust constrained model predictive control using linear matrix inequalities. *Automatica*, 32(10):1361–1379, 1996.

[30] J. Schuurmans and J.A. Rossiter. Robust predictive control using tight sets of predicted states. *IEE Proceedings Control Theory and Applications*, 147 (1):13–18, 2000.

[31] B. Kouvaritakis, J.A. Rossiter, and J. Schuurmans. Efficient robust predictive control. *IEEE Transactions on Automatic Control*, 45(8):1545–1549, 2000.

[32] B. Kouvaritakis, M. Cannon, and J.A. Rossiter. Who needs QP for linear MPC anyway? *Automatica*, 38(5):879–884, 2002.

[33] H.K. Khalil and J.W. Grizzle. *Nonlinear Systems*. Prentice Hall, Upper Saddle River, NJ, 1996.

[34] M. Cannon. Efficient nonlinear model predictive control algorithms. *Annual Reviews in Control*, 28(2):229–237, 2004.

[35] J. M. Maciejowski. *Predictive Control with Contraints*. Prentice Hall, Essex, England, 2002.

[36] Y.I. Lee, B. Kouvaritakis, and M. Cannon. Constrained receding horizon predictive control for nonlinear systems. *Automatica*, 38(12):2093–2102, 2002.

[37] D.H. van Hessem, C.W. Scherer, and O.H. Bosgra. LMI-based closed-loop economic optimization of stochastic process operation under state and input constraints. In *Proceedings of the 40th IEEE Conference on Decision and Control*, volume 5, pages 4228–4233, 2001.

[38] J.A. Primbs and H.S. Chang. Stochastic receding horizon control of constrained linear systems with state and control multiplicative noise. *IEEE Transactions on Automatic Control*, 54(2):221–230, 2009.

[39] DH van Hessem and OH Bosgra. A full solution to the constrained stochastic closed-loop MPC problem via state and innovations feedback and its receding horizon implementation. In *Proceedings of the 42nd IEEE Conference on Decision and Control*, volume 1, pages 929 – 934, 2003.

[40] P. Li, M. Wendt, and G. Wozny. A probabilistically constrained model predictive controller. *Automatica*, 38(7):1171–1176, 2002.

[41] A.L. Warren and T.E. Marlin. Constrained MPC under closed-loop uncertainty. In *American Control Conference*, volume 5, pages 4607–4612, 2004.

[42] A.L. Warren and T.E. Marlin. Improved output constraint-handling for mpc with disturbance uncertainty. In *American Control Conference*, volume 6, pages 4573–4578, 2006.

[43] M. Cannon, B. Kouvaritakis, and D. Ng. Probabilistic tubes in linear stochastic model predictive control. *Systems and Control Letters*, 58(10-11):747–753, 2009.

[44] M. Cannon, D. Ng, and B. Kouvaritakis. Successive linearization nmpc for a class of stochastic nonlinear systems. In *Nonlinear Model Predictive Control*, volume 384 of *Lecture Notes in Control and Information Sciences*, pages 249–262. Springer, Berlin / Heidelberg, 2009.

[45] W. Langson, I. Chryssochoos, S.V. Raković, and D.Q. Mayne. Robust model predictive control using tubes. *Automatica*, 40(1):125–133, 2004.

[46] D.Q. Mayne, M.M. Seron, and S.V. Rakovic. Robust model predictive control of constrained linear systems with bounded disturbances. *Automatica*, 41(2): 219–224, 2005.

[47] H. Kushner. *Introduction to Stochastic Control*. Holt, Rinehart and Winston New York, 1971.

[48] K.C. Toh, M.J. Todd, and R.H. Tutuncu. SDPT3—a Matlab software package for semidefinite programming. *Optimization Methods and Software*, 11(12): 545–581, 1999.

[49] J. Lofberg. YALMIP: A toolbox for modeling and optimization in MATLAB. In *IEEE International Symposium on Computer Aided Control Systems Design*, pages 284–289, 2004.

[50] S. Boyd and L. Vandenberghe. *Convex Optimization*. Cambridge University Press, Cambridge, 2004.

[51] Y. Wang and S. Boyd. Fast model predictive control using online optimization. *IEEE Transactions on Control Systems Technology*, 18(2):267–278, 2010.

[52] A.G. Wills and W.P. Heath. Barrier function based model predictive control. *Automatica*, 40(8):1415 – 1422, 2004.

[53] A. Hansson. A primal-dual interior-point method for robust optimal control oflinear discrete-time systems. *IEEE Transactions on Automatic Control*, 45 (9):1639–1655, 2000.

[54] M. Shin and J.A. Primbs. A fast algorithm for stochastic model predictive control with probabilistic constraints. In *American Control Conference*, pages 5489–5494, 2010.

[55] F.D. Bianchi, R.J. Mantz, and H. Battista. *Wind Turbine Control Systems*. Springer-Verlag London Limited, London, 2007.

[56] W. Feller. *An introduction to probability theory and its applications*. Wiley, India, 2009.

[57] G.H. Brundtland. *Our Common Future/World Commission on Environment and Development*. Oxford University Press, Oxford, 1987.

[58] N. Kouvaritakis. Prometheus: A tool for the generation of stochastic information for key energy, environment and technology variables. Technical report, ICCS, National Technical University of Athens, Greece, 2000.

[59] N. Kouvaritakis. Methodologies for integrating impact assessment in the field of sustainable development (minima-sud). Technical report, European Commission project EVG1-CT-2002-00082, 2002.

[60] M.S. Lobo, L. Vandenberghe, S. Boyd, and H. Lebret. Applications of second-order cone programming. *Linear Algebra and its Applications*, 284(1-3):193–228, 1998.

[61] B. Kouvaritakis, M. Cannon, and P. Couchman. MPC as a tool for sustainable development integrated policy assessment. *IEEE Transactions on Automatic Control*, 51(1):145–149, 2006.

[62] M. Cannon, B. Kouvaritakis, and G. Huang. Modelling and optimisation for sustainable development policy assessment. *European Journal of Operational Research*, 164(2):475–490, 2005.

[63] L. Ljung. *System Identification: Theory for the User*. Prentice-Hall, Englewood Cliffs, NJ, 1987.

[64] H. Akaike. Fitting autoregressive models for prediction. *Annals of the Institute of Statistical Mathematics*, 21(1):243–247, 1969.

[65] T. Kailath. *Linear Systems*. Prentice-Hall, Englewood Cliffs, NJ, 1980.

[66] N.K. Poulsen, B. Kouvaritakis, and M. Cannon. Constrained predictive control and its application to a coupled-tanks apparatus. *International Journal of Control*, 74(6):552–564, 2001.

[67] M. Cannon, B. Kouvaritakis, S.V. Rakovic, and Q. Cheng. Stochastic tubes in model predictive control with probabilistic constraints. In *American Control Conference*, pages 6274–6279, 2010.